

WEARABLE POWER-ASSISTED PNEUMATIC-BASED KNEE ORTHOSIS

TENG CHUN MAN

**A project report submitted in partial fulfilment of the
requirements for the award of Bachelor of Engineering
(Hons.) Biomedical Engineering**

**Faculty of Engineering and Science
Universiti Tunku Abdul Rahman**

April 2012

DECLARATION

I hereby declare that this project report is based on my original work except for citations and quotations which have been duly acknowledged. I also declare that it has not been previously and concurrently submitted for any other degree or award at UTAR or other institutions.

Signature : _____

Name : _____

ID No. : _____

Date : _____

APPROVAL FOR SUBMISSION

I certify that this project report entitled “**WEARABLE POWER-ASSISTED PNEUMATIC BASED KNEE ORTHOSIS**” was prepared by **TENG CHUN MAN** has met the required standard for submission in partial fulfilment of the requirements for the award of Bachelor of Engineering (Hons.) Biomedical Engineering at Universiti Tunku Abdul Rahman.

Approved by,

Signature : _____

Supervisor: Mr Chong Yu Zheng

Date : _____

The copyright of this report belongs to the author under the terms of the copyright Act 1987 as qualified by Intellectual Property Policy of Universiti Tunku Abdul Rahman. Due acknowledgement shall always be made of the use of any material contained in, or derived from, this report.

©2012 Year, Teng Chun Man. All right reserved.

ACKNOWLEDGEMENTS

I would like to thank everyone who had contributed to the successful completion of this project. I would like to express my gratitude to my research supervisor, Mr. Chong Yu Zheng for his invaluable advice, guidance and his enormous patience throughout the development of the research.

In addition, I would also like to express my gratitude to my loving parent and friends who had helped and given me encouragement especially my parent in financial support.

WEARABLE POWER-ASSISTED PNEUMATIC-BASED KNEE ORTHOSIS

ABSTRACT

Locomotion training has proven to be a highly effective approach in rehabilitation to assist patient in recovering their normal walking patterns. A pneumatically-actuated orthosis will improve gait rehabilitation that is always desirable for exoskeleton by providing a stable, lightweight, accurate and precise power for lower extremities motion. This project presents the design and development of a power-assisted knee orthosis actuated by the pneumatic artificial muscles (PAM). The PAM has additional advantages such as direct connection, easy replacement and safe operation. The power-assisted knee orthosis is intended as a proof-of-concept rehabilitation device for the assessment of the conceptual design, fabrication of the prototype, testing of the power control system including pneumatic system and performing flexion-extension of the knee joint. McKibben Pneumatic Artificial Muscles is selected as the pneumatic actuator and the frame were constructed by aluminium. Fiberglass cast is selected as the fitting and the system is controlled by Peripheral Interface Controller also known as PIC microcontroller. Furthermore, 5/2 way solenoid valve is selected as the air pressure supply controller. The general approach of this project is to develop an inexpensive rehabilitation robotic system consisting of a powered exoskeleton for the lower extremities.

LIST OF PUBLICATION

- | PAPER | TITLE–CONFERENCE |
|--------------|--|
| 1. | Teng, C., Wong, Z., Teh, W., & Chong, Y. Z. (2012). Design and Development of Inexpensive Pneumatically-Powered Assisted Knee-Ankle-Foot Orthosis for Gait Rehabilitation-Preliminary Finding. <i>Engineering and Science</i> , (February), 27-28. |
| 2. | Wong, Z., Teng, C., & Chong, Y. Z. (2012). Power Assisted Pneumatic-Based Knee-Ankle-Foot Orthosis for Rehabilitation – 2012 IEEE-EMBS Conference on Biomedical Engineering (IECBES 2012), 17-18 December 2012. |

TABLE OF CONTENTS

DECLARATION	ii
APPROVAL FOR SUBMISSION	iii
ACKNOWLEDGEMENTS	v
ABSTRACT	vi
TABLE OF CONTENTS	viii
LIST OF TABLES	xi
LIST OF FIGURES	xii
LIST OF SYMBOLS / ABBREVIATIONS	xvii
LIST OF APPENDICES	xix

CHAPTER

1	INTRODUCTION	1
	1.1 Background	1
	1.2 Aims and Objectives	4
2	LITERATURE REVIEW	5
	2.1 Development of Exoskeleton-type Systems	5
	2.1.1 Exoskeleton for Power Augmentation	5
	2.2 Artificial Muscle	8
	2.2.1 Antagonistic Pneumatic Actuators	11
	2.2.2 Pneumatic Muscle Classification	12
	2.3 Mechanical Design	15
	2.3.1 Pneumatic Muscle Actuator Design	17
	2.3.2 Mechanical Design Concept	18

2.4	Control	23
2.4.1	Power control	23
2.4.2	Artificial Pneumatic Muscle Control	24
2.4.3	Control System	29
2.5	Walking Gait Analysis	35
3	METHODOLOGY	37
3.1	Conceptual Designs	37
3.1.1	Pneumatic Artificial Muscle Design	38
3.1.2	Muscle Attachment Shell	40
3.1.3	Knee Joint Design	42
3.1.4	Control System Design	45
3.2	Artificial Muscle	46
4	RESULTS AND DISCUSSIONS	49
4.1	Mechanical Frame	49
4.1.1	Knee Joint of Prototype	50
4.1.2	Material and Locking Mechanism	52
4.1.3	Range of Knee Joint Motion	56
4.1.4	Artificial Muscle	58
4.2	Circuit System	64
4.2.1	Circuit Design	65
4.3	Control System Coding	71
4.4	Pneumatics System	79
4.5	Pneumatics Based Power-Assisted Knee-Ankle-Foot Orthosis	83
4.5.1	Overall Design	83
4.5.2	Overall Circuit and Pneumatic System	84
4.5.3	Walking Gait Cycle	85
5	CONCLUSION AND RECOMMENDATIONS	92
5.1	Conclusion	92
5.2	Recommendations and Future Improvement	93

REFERENCES

94

APPENDICES

97

LIST OF TABLES

TABLE	TITLE	PAGE
1.1	The Comparison Between the Exoskeleton Technology and Its Concept In Biology	2
2.1	History and Achievement of Walking Assistive Exoskeleton	6
2.2	Segment Length Expressed in Percentages of Total Body Height	16
2.3	Segment Radii of Gyration Expressed in Percentages of Segment Lengths	16
1.2	Comparison between Electrical, Pneumatic and Hydraulic power	24
2.4	Accelerometer Types Specification Comparison	30
2.5	Particular for the Volunteers	32
4.1	Muscle length with constant pressure (first data)	58
4.2	Muscle length with constant pressure (second data)	59
4.3	Muscle length with constant pressure (third data)	60
4.4	Characteristic of the inner tube materials	62

LIST OF FIGURES

FIGURE	TITLE	PAGE
1.1	Scheme of the Exoskeleton Human-Machine Intelligence System	3
2.1	Locomot Rehabilitation Exoskeleton	8
2.2	PMA Operation at Constant Load	10
2.3	PMA Operation at Constant Pressure	10
2.4	Human Muscle	11
2.5	Antagonistic Set-up	12
2.6	McKibben Muscle	13
2.7	Pleated Pneumatic Artificial Muscle	14
2.8	PPAM Expanding Diameter Views	15
2.9	Antagonistic Configuration of PPAM with Four Bar Linkage Mechanism	17
2.10	CAD drawing of the Proof-of-concept Active Knee Orthosis	18
2.11	Prototype of Robotic Leg	19
2.12	The Prototype Articulations	20
2.13	Knee Joint Kinematic Model	21
2.14	Knee Articulation Torque Model A - Piston Placed Under the Thighbone Bar	21
2.15	Knee Articulation Torque Model B - Piston Placed Upon the Thighbone Bar	22

2.16	University of Michigan Knee-Ankle-Foot Orthosis	25
2.17	Orthosis Knee Joint Kinetics	26
2.18	Air design for the Pneumatic Actuator	27
2.19	Time Delay between the Operation of the Valve and a Change in the Inner Pressure of the Actuator	28
2.20	Valve Operation scheme for dynamic walking	29
2.21	Knee Joint Flexion-Extension for Volunteers (a), (b) and (c).	33
2.22	Wearable Walking Helper	34
2.23	Measurement of Acceleration of Human Link	34
2.24	Human Walking Gait Cycle	35
2.25	Functional Specification of the Active Orthosis during Gait Cycle	36
3.1	SolidWork Drawing of Pleated Pneumatic Artificial Muscle Flexion	39
3.2	SolidWork Sketching of Pleated Pneumatic Artificial Muscle Extension	39
3.3	SolidWork Sketching of Two-piece Rigid Fiberglass Shells at Thigh	40
3.4	SolidWork Sketching of Two-piece Rigid Fiberglass Shells at Shank with Adjustable Fitting	41
3.5	CAD Drawing of the Proof-of-Concept Active Knee Orthosis; Close-up of the Adjustable Fittings	41
3.6	Pneumatic Muscle Actuated Rotation Modules	42
3.7	Knee Joint Design	43
3.8	Safety Lock for Knee Extension	43
3.9	Flexion (90 °)	44
3.10	Different Views of the Knee Flexion Conceptual Designs	44
3.11	Control System Flow	45

3.12	Materials required for fabricating a MPAM	47
3.13	Steps to fabricate the MPAM	48
4.1	First Prototype	49
4.2	Joint mechanism	50
4.3	Shinbone bar shape (a) “L” shape conceptual design (b) “I” shape prototype	50
4.4	The Knee Joint of the Power-Assisted Knee Orthosis	51
4.5	Mathematical Model of the Frame of Power-Assisted Knee Orthosis	51
4.6	MPAM Connector	53
4.7	Rivet (black circle)	54
4.8	Bolt and Nut	54
4.9	Rivet	54
4.10	Fiberglass Cast	55
4.11	Single Rigid Fiberglass Shell	56
4.12	Graph of Knee Joint Angle versus Muscle Contraction Length	57
4.13	90° flexion of the prototype (sitting position)	57
4.14	flexion of 55 ° walking angle	58
4.15	Graph of Length with actuation versus load (first data)	59
4.16	Graph of Length with actuation versus load (second data)	59
4.17	Graph of Length with actuation versus load for (third data)	60
4.18	Graph of Length without actuation versus load	61
4.19	Festo Air Muscle	62

4.20	Materials consideration for inner tube (a) Silicon tube (b) Balloons (c) Latex gloves (d) Condom	63
4.21	Antagonistic configuration of MPAM	64
4.22	Circuit Connectivity	66
4.23	Real Time Control System Board	66
4.24	Black and Red Buttons Installed to the Bag	67
4.25	PCB Circuit Diagram	67
4.26	Complete Circuit Diagram	68
4.27	Accelerometer ADXL 335	69
4.28	Relay Controlling Circuit Theor	69
4.29	Circuit Running Process	70
4.30	Coding Flow Chart	72
4.31	PIC Setting	73
4.32	Function and Variable	74
4.33	Analogue to Digital Converter (ADC) setting	75
4.34	Configure LCD display	75
4.35	Display Accelerometer ADC value	76
4.36	Flexion-Extension coding	77
4.37	Functions and Delays Examples	78
4.38	Pneumatics connection	79
4.39	Pneumatic artificial muscle (PAM) controlled by solenoid valve	80
4.40	Energized Solenoid Valve	80
4.41	De-energized Solenoid Valve	81
4.42	Single Acting Actuator (MPAM)	82
4.43	Single Acting Actuator	82

4.44	Pneumatics Based Power-Assisted Knee-Ankle-Foot Orthosis	83
4.45	Pneumatics Systems including ankle and foot orthosis	84
4.46	Control System Board	84
4.47	Control System Board	85
4.48	Walking Gait Testing On Biomechanics treadmill	85
4.49	Pneumatics Based Power-Assisted Knee-Ankle-Foot Orthosis during Gait Cycle	86
4.50	Left Limb without Actuation	87
4.51	Right Limb without Actuation	87
4.52	Left Limb with Actuation (first data)	88
4.53	Left Limb with Actuation (second data)	89
4.54	Right Limb with Actuation (first data)	89
4.55	Right Limb with Actuation (second data)	90
4.56	Without Actuation	90
4.57	With Actuation (first data)	91
4.58	With Actuation (second data)	91

LIST OF SYMBOLS / ABBREVIATIONS

F	pulling force
p	gauge pressure
dV	change in volume
dl	change in length
$F_{model A}$	force supplied model A
$F_{model B}$	force supplied model B
Mg	gravity force
θ	knee angular position
h	arm of the torque
O_i	acceleration sensor
a_i	translational acceleration
g/g_i	gravitational acceleration
θ_i	inclination angle
i	x, y, z axis
I_L	load current
V_S	Voltage supply
R_B	base Resistance
psi	pound per square inch
A-SCKAFO	active stance-control knee-ankle-foot-orthosis
CAD	computer-aided design
DAC	digital to analogue converter
DOF	degree of freedom
GRF	ground reaction force
MPAM	McKibben pneumatic artificial muscle
PAM	pneumatic artificial muscle
PCB	printed circuit board

PM	proportional myoelectric
PMFI	proportional myoelectric with flexor inhibition
PMA	pneumatic muscle actuator
PPAM	pleated pneumatic artificial muscle
PWM	pulse width modulator
WPAPBKO	wearable power-assisted pneumatic based knee orthosis

LIST OF APPENDICES

APPENDIX	TITLE	PAGE
A	Gantt Chart	97
B	Festo quotation	98
C	Solidworks Side View without Ankle Joint	99
D	Solidworks 3D drawing Side View with Ankle Joint (in mm)	100
E	Solidworks 3D drawing Top View with Lower Leg MPAM (in mm)	101
F	Solidworks 3D drawing Front View with Ankle and Foot(in mm)	102
G	Solidworks 3D drawing without dimension	103
H	xlcd.c	104
I	xlcd.h	110
J	Original Coding	113
K	PCB board	120

CHAPTER 1

INTRODUCTION

1.1 Background

In the late 20th century, exoskeletons have been rapidly developed especially many novel concepts of man-machine systems have been introduced. The developments of exoskeletons are a great achievement in mechanical and electronic engineering, automation technology, biological and material science (Yang, C.-j. et al., 2008). Due to the bottleneck of the artificial intelligence and the limitation of the automatic robotic system, the exoskeleton has the advantages in using human intelligence to control the power of robotic.

The exoskeleton is controlled and wearable device or machine that increases the speed, strength and endurance of the operator (Matthias, H., 2007). In military area, exoskeleton assists a soldier lift and carries heavier loads, run faster and jumps higher (Yang, C.-j. et al., 2008). It helps a soldier to fight better with protected armour and well equipped with more weapons and more strength than a normal people have. According to Matthias, H., exoskeleton is to increase the physical performance of the soldier wearing such as:

- Increase payload: more fire power, supplies, and heavier armour increasing soldier surviving chance of a direct hit or explosion.
- Increase speed and range: enhanced ground reconnaissance and battle space dominance.
- Increase strength: larger calibre weapons and obstacle clearance.

Table 1.1: The Comparison Between the Exoskeleton Technology and Its Concept In Biology (Yang, C.-j. et al., 2008)

Function	The biological exoskeleton	The exoskeleton technology	Application
Support	Supporting the body of the invertebrates	Supporting physically disabled patient or walking assistance	Rehabilitation robotics or power amplifier
Enhancement	Enhancing the power of animals	Strengthening the human operator	Assistance equipments
Protection	Protecting the animal's body	Protecting the human operator	Automatic armour for soldier, rescue devices or safe manipulation for the radioactive materials in nuclear plant
Sensing and data fusion	Obtaining the information, acting as the sensorium	Interface of human operator and the environment and making data fusion with information obtained by the human operator	Telerobotics, VR

In non-military areas, the exoskeleton can be used in medical application such as rehabilitation and handicap support system. For example, those aged or disable people whose lower extremities have locomotors deficiencies due to several reasons: accident, paralysis and etc. Although the disable or aged people can used a wheelchair to move around but the wheelchair has its limitation where barriers such as bumps and steps restrict the area that these people have access to (Matthias, H., 2007). Therefore, a wearable lower extremities exoskeleton can enhance their leg muscular strength to enable them to move and walk as a normal people. Table 1.1 illustrates the exoskeleton technologies and its concept in biology.

The wearable power-assisted pneumatic based knee orthosis is an exoskeleton system and a kind of human-machine system operated by human. The pneumatic based meaning the power system is developed by mechanical power which used compressed air to generate power to the system. It is designed as an external mechanical support system whose joints correspond to human knee joints to enhance or support the human in lower extremities movement. It combines the human intelligence and the machine power to enhance the intelligence of the machine and the power of human operator (Yang, C.-j. et al., 2008).

The combination of human-machine system involves information exchanging so human and the exoskeletons are coupled together. If necessary, the exoskeleton can take the duty of data fusion, data processing and even assisted human operator with decision such as an obstacle avoidance system (Yang, C.-j. et al., 2008). Figure 1.1 illustrates the typical scheme of the exoskeleton system. According to Yang, C.-j. et al. (2008), in the control architecture, human operator is the commander of the system and also a part of the control loop. In the loop, human operator mainly makes decisions and the exoskeleton implement the tasks. But, the feedback information received by operator and exoskeleton will keeps interchanging bilaterally between each other. This is to optimize the control target.

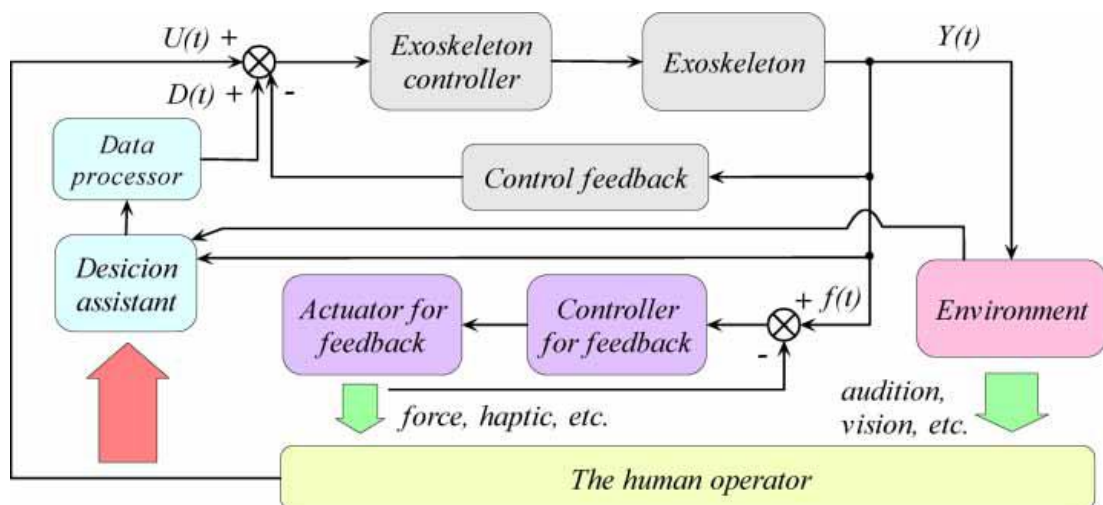


Figure 1.1: Scheme of the Exoskeleton Human-Machine Intelligence System

(Yang, C.-j. et al., 2008)

1.2 Aims and Objectives

The aims of the wearable power-assisted pneumatic-based knee orthosis are:

- To assist patient in rehabilitation.
- To determine the mechanical performance of the wearable power-assisted pneumatic-based knee orthosis.

The objectives of the project are:

- To study the biomechanics of lower extremities and types of artificial muscle.
- To investigate the best sensor for angle detection and stability.
- To design a wearable power-assisted pneumatic-based knee orthosis that is able to help human to stand and walk further.
- To develop a low cost wearable power-assisted pneumatic-based knee orthosis to aid patient with lower extremities problem.

CHAPTER 2

LITERATURE REVIEW

2.1 Development of Exoskeleton-type Systems

In the early stage, an exoskeleton-type system for master-arm robot teleoperation was invented. In the 1990s, the developments of the force reflect and haptical feedbacks were widely employed in the exoskeleton-type systems for bilateral teleoperation but human operator preferred doing the work directly instead of through the exoskeleton device so the performance of telerobotic is improved. In the new stage, exoskeleton is introduced into many fields including power amplifier, rehabilitation and etc. Nowadays, the exoskeleton technology is heading toward a new phase with special purposes, dedication, and high integration. (C-J Yang et al., 2008) In this project, the master-arm robot teleoperation exoskeleton is not concerned while the power amplifier for rehabilitation is the main target.

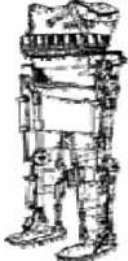
2.1.1 Exoskeleton for Power Augmentation

Body weight supporting and power amplification are the two main objectives of the new stage of exoskeleton for human operator. Power amplifier exoskeleton objective is to assist human operator to carry or finish the heavy loads task. Besides that, power amplifier exoskeleton for lower extremities is to help human to walk and further improves to running and even jumping at higher degree than a normal human.

Table 2.1 illustrate the history and the achievement of the walking assistive exoskeletons from the last century until recent years.

The Locomot designed by Hocomo AG, Switzerland was a bilateral robotic orthosis that was used in conjunction with a body-weight support system to control patient leg movement in the saggital plane (Yang, C.-j, et al., 2008). In Figure 2.1, the Locomot has shown the training gait style according to the bio-feedback of patient.

Table 2.1: History and Achievement of Walking Assistive Exoskeleton

Exoskeleton-type	Year	Description
	1948	The exoskeleton-type system with motor actuators designed by Professor Bernstein. (Yang, C.-j, et al., 2008)
	1960	Hardyman system, designed by GE company. The soldier can drive it by hydraulic system to strengthen him and load more weapons. (Yang, C.-j, et al., 2008)
	1970	Designed with 87kg. (Yang, C.-j, et al., 2008)
	1971	Developed by Professor Vukobratovic. It is used to assist patients for walking. (Yang, C.-j, et al., 2008)



1990 Gehl life system. (Yang, C.-j, et al., 2008)



2001 RoboKnee developed by Yobotics, Inc with computer, amplifiers, and batteries in a backpack. It did provide user to perform knee bends almost indefinitely. (Matthias, 2007)



2004 Berkeley Lower Extremity Exoskeleton (BLEEX) is developed to have three degree at the ankle and hip, and one degree at the knee. It is employed with a high-tech compact Hydraulic Power Unit, hydraulically actuated to allow flexion and extension of the hip and knee joints while dorsiflexion and plantarflexion of the ankle joints. The drawback of BLEEX is the user seemed hampered and unnatural during walking, backpack looks bulky and makes the whole system rather unbalanced. (Matthias, 2007)



2005 AKROD-v2 developed by Northeastern University consists of a robotic knee brace that is portable and programmable. (Matthias, 2007)



2007 NTU's assistive Device with footpad design has been developed and tested for walking and stair-climbing. (Matthias, 2007)



2008 HAL-5 system developed by Professor Yoshiyuki from Tsukuba University was utilised to realize the waling aid for the gait disorder person with the help of sensors such as angle sensors, myoelectrical sensors, floor sensor and etc. It had hybrid control systems which consist of the autonomous controller such as posture control and comfortable power assist controller based on biological feedback and predictive feed forward. (Kawamoto, H., et al., 2009)



Figure 2.1: Locomot Rehabilitation Exoskeleton (Yang, C.-j, et al., 2008)

According to Yang, C.-j, et al. (2008), a wearable power-assisted device based on a curved pneumatic muscle actuator (PMA) was designed which it can be directly put on because of its lightweight and soft texture. A lightweight design is always desirable for exoskeleton so it can be easily wear and walk naturally without affecting the human operator. The PMA has additional advantages such as direct connection, easy replacement and safe operation (Wetenschappen, F. T., 1999).

2.2 Artificial Muscle

There are several types of pneumatic actuators such as:

- Cylinders
- Bellows
- Pneumatic engine

- Pneumatic stepper motor
- Pneumatic muscle actuator

Wetenschappen, F. T. (1999) who proved that PMA is extremely light weight as their core element is but a membrane that can transfer the same amount of energy as cylinder since they operate at the same pressure ranges and volume. Besides that, Frank, D. also proved that PMA can be made very strong with force ranging up to several thousand Newtons. Hence, PMA is chosen. According to Wetenschappen, F. T. (1999), the force is not only dependent on pressure but also of inflation (Wetenschappen, F. T., 1999). The membrane will bulge outward when the compressed air is supplied can cause the PMA in contraction mode. On the other hands, when the air is sucked out, the PMA will be in dilation mode. PMA usually operate at an overpressure where generating and supplying compressed air is easier to accomplish (Wetenschappen, F. T., 1999). Charging an overpressure PMA with pressurized gas enables it to move a load, discharging it, conversely make it yield to a load (Wetenschappen, F. T., 1999).

The artificial muscles have specific properties that are of special interest in the field of legged robots (“*Muscle*,” 2011):

- High torque, high power-to-weight ratio
- Muscle natural compliance
- Actuator can be positioned at the joint without complex gearing mechanism
- Adaptable passive behaviour suited for energy storage
- Shock absorbance during impact

According to Wetenschappen, F. T. (1999), an experiment was carried out to indicate the relationship of the pressure and mass affects the pulling force of the PMA. At the beginning state for a constant mass, when there is no pressure supply to the PMA, the volume is minimal, V_{\min} , and PMA length is maximal, l_{\max} as shown in Figure 2.2. If the PMA is pressurized to p_1 , PMA starts to bulge as pressure increases, volume increases and its length becomes shorter at the same develop a pulling force. The mass will thus be lifted until generated force is equal to Mg (Wetenschappen, F. T., 1999). As for the Figure 2.3 shown the PMA is under constant pressure, it will

shorten if its load is decreased and contract which it develops no force and its enclosed volume is maximal (Wetenschappen, F. T., 1999).

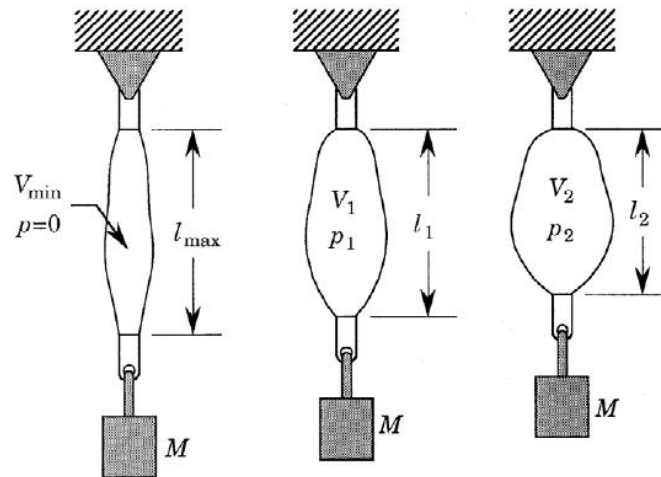


Figure 2.2: PMA Operation at Constant Load (Frank, D., 1999)

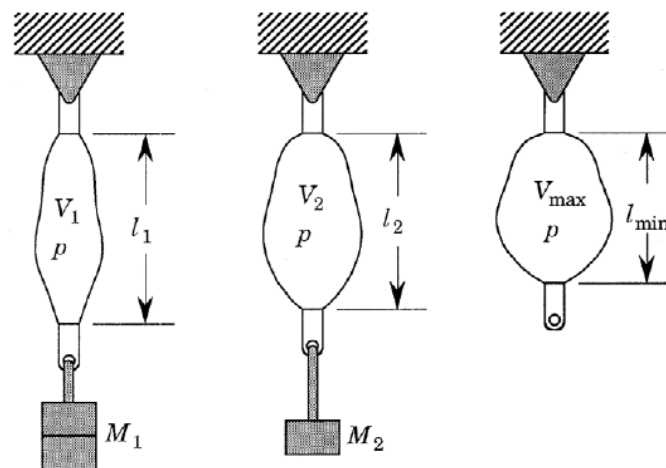


Figure 2.3: PMA Operation at Constant Pressure (Frank, D., 1999)

The relationship of the pressure, volume and mass can be expressed based on the formula below. Consider one muscle at gauge pressure p has an infinitesimal mass dm of gas forced into it during time interval dt and thus the membrane's volume increases by dV . A net amount of work of pdV crosses the boundary and under the same dt , the actuator's length change by dl (<0 for shortening). F in the formula denotes the load force required to pull the mass or the pulling force. (Wetenschappen, F. T., 1999)

$$F = -p \frac{dV}{dl} \quad (1.1)$$

where

F = pulling force

p = gauge pressure

dV = change of volume

dl = change of length

2.2.1 Antagonistic Pneumatic Actuators

The antagonistic artificial muscle set-up is similar to human skeletal muscle generates the movement of a certain part of the body. For every muscle that generates movement of a body part, there is another muscle that generates an opposite movement (Deaconescu, A., & Deaconescu, T., 2009). The muscle which generates opposite movement is called antagonistic muscles. As one muscle contracts, the other (opposite movement) will relax and vice versa as shown in Figure 2.4.



Figure 2.4: Human Muscle (Deaconescu, A., & Deaconescu, T., 2009)

Pneumatic muscle actuators need to be coupled in order to generate a bidirectional motion which one for each direction (Wetenschappen, F. T., 1999 and Beyl, P. et al., 2007). As one of the muscle actuator moves the load, the other will act as a brake to stop the load at its desire location dependent on the length of the PMA

(Wetenschappen, F. T., 1999). In order to move the load in the opposite direction, the muscle has to change its function and this generally referred to antagonistic set-up. The antagonistic can be used for rotational motion as shown in Figure 2.5.

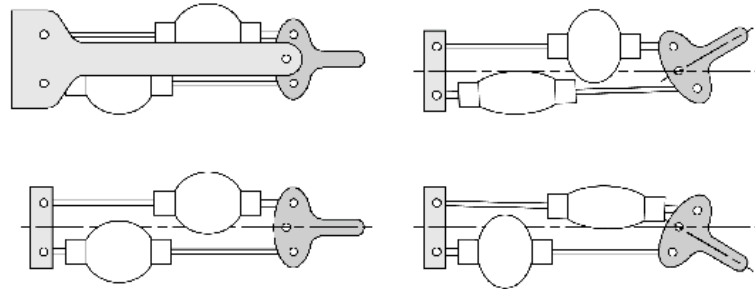


Figure 2.5: Antagonistic Set-up (Wetenschappen, F. T., 1999)

The equilibrium position of the effectors driven by antagonistic couple will be determined by the ratio of both the muscle gauge pressures due to the generated force of each muscle is proportional to the applied pressure (Wetenschappen, F. T., 1999).

2.2.2 Pneumatic Muscle Classification

The pneumatic muscle is classified to braided muscle (McKibben Muscle), pleated pneumatic artificial muscle, netted muscle and embedded muscle. The project focuses on two types of pneumatic muscle: the McKibben muscle and the Pleated Pneumatic Artificial Muscle (PPAM). The McKibben muscle was the most frequently used and the PPAM was recently developed as an improvement with regards to the drawback of the McKibben design (Wetenschappen, F. T., 1999).

The difference between the netted muscle and the McKibben muscle is the density of the network surrounding the membrane, a net being a mesh with relatively large holes and McKibben being tightly woven (Wetenschappen, F. T., 1999). Therefore, the netted muscle can only withstand low pressures. Among all the embedded muscle types in the review of Wetenschappen, F. T. (1999), it can be concluded that the embedded muscle has complex design, gauge pressures have to be

limited to low value, generated force was low, hard to built and etc. Thus, the embedded is not considered in this project.

2.2.2.1 McKibben Muscle

This type of artificial muscle is made of a tube and its sleeving connected at the both ends to fitting which function as to transfer fiber tension and serve as gas closure (Wetenschappen, F. T., 1999). Typical materials used are latex and silicone rubber and Nylon fibers (Wetenschappen, F. T., 1999). Figure 2.6 clearly explains the operation and structure of the McKibben Muscle.

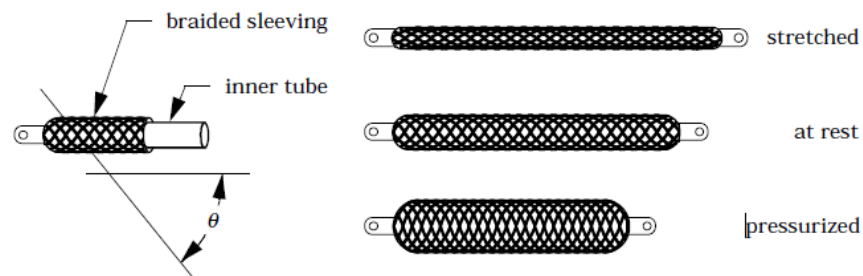


Figure 2.6: McKibben Muscle (Frank, D., 1999)

According to the Wetenschappen, F. T., (1999), the typical value of force is found to be 650N at rest length, 300N at 15% contraction and 0N at 30% contraction all at pressures of 300kPa. Typical operating gauge pressure range of McKibben Muscles is 100-500kPa (maximum allowable gauge pressure determined by the strength of the tube). The higher the pressure, the more energy can be transferred but pressure too high, the tube will burst. As for the power to weight ratio, the value is range from 1.5kW/kg at 200kPa and 3kW/kg at 400kPa (Wetenschappen, F. T., 1999). But, another author in the review of Wetenschappen, F. T., (1999) cites a value of 5kW/kg and even 10kW/kg. The typical value of the McKibben muscle's weight is about 50g at initial length of 34cm and initial diameter of 1.4cm (Wetenschappen, F. T., 1999).

The major advantages of McKibben muscle are its simple design, ease of assembly and low cost. The major disadvantages are its inherently dry friction that leads to hysteresis and threshold pressure that leads to accurate position control is difficult to achieve. Besides that, the friction temperature will affect the muscle operation. Additionally, the disadvantages are the limited displacement and the energy needed to deform the rubber membrane, thus lowering the output force. (Wetenschappen, F. T., 1999 and Deaconescu, A., & Deaconescu, T., 2009)

2.2.2.2 Pleated Pneumatic Artificial Muscle (PPAM)

The PPAM membrane has a number of pleats in the axial direction and when it expands, it unfolds the pleated membrane. Because of this, no friction is involved which it is the improvement of the McKibben muscle. In the absence of friction, there will no hysteresis (Wetenschappen, F. T., 1999). Moreover, there is no energy required for the membrane to expand as membrane stresses are kept negligibly small and decrease with an increasing number of folds (Wetenschappen, F. T., 1999). The energy is required when membrane bulges. This is a very small amount as can be deduced from low value of threshold pressure (Wetenschappen, F. T., 1999).



Figure 2.7: Pleated Pneumatic Artificial Muscle (Wetenschappen, F. T., 1999)

Wetenschappen, F. T., (1999) stated the characteristic of the PPAM depend on the ratio of full length to minimum diameter, on the strain behaviour of membrane's material on the contraction rate and on the applied pressure. A thick

muscle contract less than thin but generate higher forces at low contraction rates (Wetenschappen, F. T., 1999). The PPAM's membrane is made of a para-aramid fiber unidirectional fabric and end fittings are made of aluminium (Wetenschappen, F. T., 1999). Its total weight is about 60g and maximum contraction of this muscle was experimentally found by Wetenschappen, F. T., (1999) to be 41.5%. Furthermore, the pressure was limited to 300kPa and maximum force was limited to about 3500N in order not to damage the actuator. Due to the absence of the hysteresis, position accuracy was better than 0.1° for a motion range of 60° .

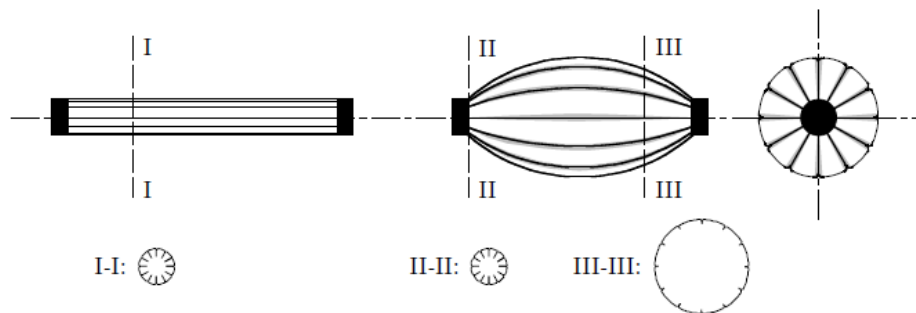


Figure 2.8: PPAM Expanding Diameter Views (Frank, D., 1999)

Based on Wetenschappen, F. T., (1999), Deaconescu, A., & Deaconescu, T., (2009), Beyl P. et al., (2007) and “*Muscle*,” (2009), the pleated pneumatic artificial muscle (PPAM) would be the best option of the artificial muscle for this project. The consideration is based on the design and material selection for both the membrane and end fitting. Besides that, the characteristic of the artificial muscle also taken into consideration. Furthermore, the PPAM used are connected bidirectional whereby the muscles are in antagonistic set-up as shown in Figure 2.5.

2.3 Mechanical Design

The design specification of power-assisted knee orthosis should include the following conditions that are based on Beyl, P. et al., (2007):

- Sufficient knee joint torque to achieve physiological walking gait pattern
- Support user body weight and morphologies
- Easily adaptable to the anatomy of the user

- Allow large range of variation of foot, shank and thigh link lengths
- Lightweight, compact, ergonomic and provide sufficient comfort
- Ensure a safe interaction

The design will be tailored to the requirement of the author whose the weight is about 55kg to 60kg. The length of the design parts will be based on the length of the anatomy of the author. The knee joint range of motion of 90° in flexion is sufficient in normal overground walking. Besides that, the 90° flexion assistance in sit-to-stand motion that designed to be easily strapped to the user while seated rather than strapped to the user in standing position.

Suppose the length of the design parts have to reach the requirement of Table 2.2 but due to the limited subject, the prototype will be tailored to the author. Table 2.2 depicts the average body length of males and females in percentage to the height of both the males and females (Hall, S.J., 2007). Table 2.3 depicts the average segment radii of gyration expressed in percentages of segment lengths (Hall, S.J., 2007).

Table 2.2: Segment Length Expressed in Percentages of Total Body Height (Hall, S.J., 2007)

Segment	Males	Females
THIGH	23.2	24.9
LOWER LEG	24.7	25.7

Table 2.3: Segment Radii of Gyration Expressed in Percentages of Segment Lengths (Hall, S.J., 2007)

SEGMENT	Males		Females	
	PROXIMAL	DISTAL	PROXIMAL	DISTAL
THIGH	54.0	65.3	53.5	65.8
LOWER LEG	52.9	64.2	51.4	65.7

2.3.1 Pneumatic Muscle Actuator Design

The pleated pneumatic artificial muscle (PPAM) is designed as a single acting force actuator. In order to obtain a bidirectional rotative actuator, two single acting force actuators are required in an antagonistic configuration. According to Beyl, P. et al., (2007), the design has a constant lever arm length and the actuators operate along a fixed axis which favours simple and compact design. A direct connection through fixed levers can solve the nonlinear force contraction (Beyl, P. et al., 2007).

Beyl, P. et al., (2007) proposed a configuration based on a four bar linkage mechanism gives the advantages of good torque matching and compact design. Figure 2.9 depicts the bidirectional rotative actuator powered by PPAMs in an antagonistic configuration with four bar linkage. Two bar linkage instead of four bar linkage has been designed and the lever arms and PPAMs of the design will be utilized Beyl, P. et al., (2007) design.

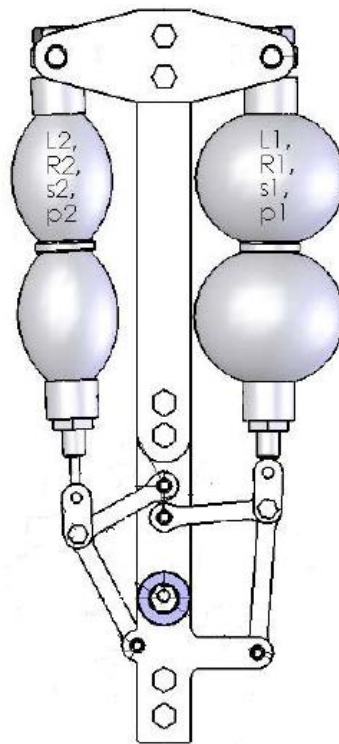


Figure 2.9: Antagonistic Configuration of PPAM with Four Bar Linkage Mechanism (Beyl, P. et al., 2007)

2.3.2 Mechanical Design Concept

According to Beyl, P. et al., (2007), the PPAMs are attached unilateral frame, consisting of upper and lower leg sidebars interconnected by a hinge at the knee. A strap-on footplate is connected by to the sidebar of the lower leg by means of a hinge at the ankle joint which added to carry weight of the orthosis and prevent it from sliding down the user's leg (Beyl, P. et al., 2007). Both the length of the sidebar and the location of the hinge are made adjustable (Beyl, P. et al., 2007). The footplate also allows rotation at the metatarsalphalangeal joint during roll-over of the foot to preserve normal walking conditions as much as possible (Beyl, P. et al., 2007).

Beyl, P. et al., (2007) designed the fittings for both the thigh and the shank with two-piece rigid thermoplastic shells with a foam inlay and Velcro straps. These meet the requirement of easily fit and adaptable fit to the user lower extremities. The position and orientation of each shell are simultaneously adjustable in the sagittal plane by means of an integrated slider mechanism (Beyl, P. et al., 2007). Clamp elements are used for the lateral distance and inclination of the shells with respect to the frame (Beyl, P. et al., 2007). Therefore, adjustability should be sufficient to align the orthosis and to achieve a good fit in a quick manner (Beyl, P. et al., 2007).

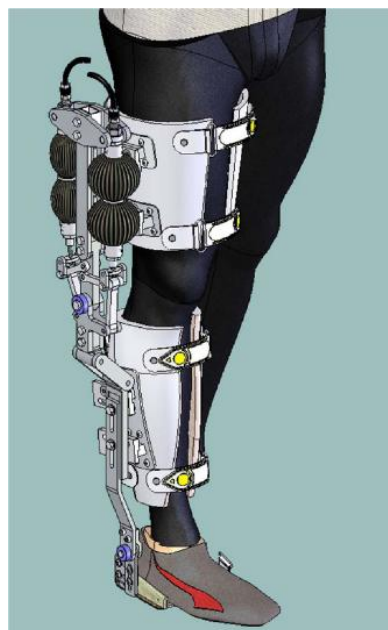


Figure 2.10: CAD drawing of the Proof-of-concept Active Knee Orthosis (Beyl, P. et al., 2007)

Based on Muscato, G., & Spampinato, G. (2007) in the journal paper titled kinematic model and control architecture for a human inspired five DOF robotic leg, the mechanical structure of the robotic inferior limb is made up of four links, corresponding to the pelvis, thighbone, shinbone and foot jointed by five degree of freedom (DOF). The knee joint is moved by one rotational degree freedom while the ankle joint is implemented by two rotational degrees of freedom each one through two universal joints (Muscato, G., & Spampinato, G., 2007). The pelvis or hip joint is not concerned in this project while the knee joint involves thighbone and shinbone is the main concerned.

The mechanical structure of the robotic leg is actuated by five pneumatic pistons, two of which move the ankle articulation, the third moves the knee joint, whereas the last two move the hip articulation which is not my focus (Muscato, G., & Spampinato, G., 2007). Figure 2.11 illustrates the prototype of the robotic leg.



Figure 2.11: Prototype of Robotic Leg (Muscato, G., & Spampinato, G., 2007)

Although the journal paper is a robotic leg instead of a wearable power assisted knee orthosis, but some of the mechanical design of the knee joint by Muscato, G., & Spampinato, G. (2007) is considered. In Figure 2.12 depicts the mechanical structures of the articulations. The black squares shown in Figure 2.12

are the design of the knee joint where the knee movement is controlled by a pneumatic actuator that connected to the lower robotic leg.

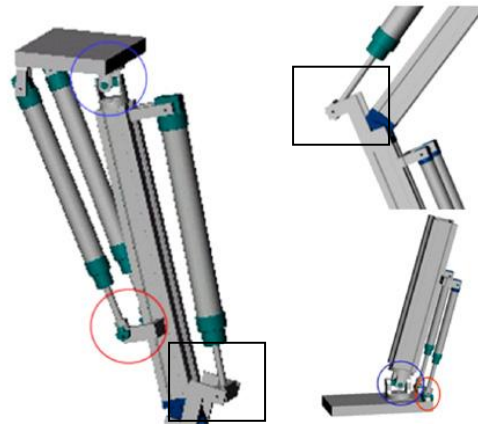


Figure 2.12: The Prototype Articulations (Muscato, G., & Spampinato, G., 2007)

For safety reasons, Beyl, P. et al., (2007) designed the four bar linkage mechanism to prevent hyperextension of the knee and flexion angles exceeding 90° . The active knee orthosis will be tethered to an external pressurized air supply system, including fast switching valves (Beyl, P. et al., 2007). For Muscato, G., & Spampinato, G., (2007), the flexion and extension movements runs within a wide range including 0° in extension until 150° in flexion with respect to the thighbone longitudinal axis.

The knee articulation has only one DOF and thus is actuated by only one pneumatic piston in Muscato, G., & Spampinato, G. (2007) journal paper. So, in order to determine the pistons extension ranges, the kinematic relation between the piston extension and the angular position is computed. The knee kinematic model is shown in figure 2.13 where a segment represents the pneumatic piston and the knee angular position is indicated by the θ angle (Muscato, G., & Spampinato, G., 2007). An accurate analysis of the kinematic relations between a and θ , allows to estimate the piston excursion range corresponding to the θ working range of degrees that is the maximum range that the knee joint mechanical structure is able to provide (Muscato, G., & Spampinato, G., 2007).

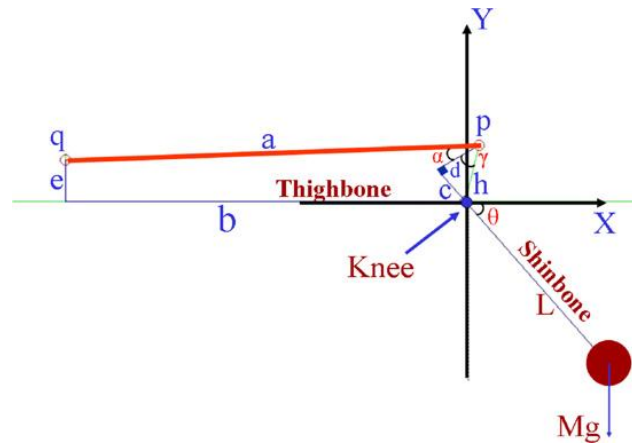


Figure 2.15: Knee Articulation Torque Model B - Piston Placed Upon the Thighbone Bar (Muscato, G., & Spampinato, G., 2007)

Muscato, G., & Spampinato, G. (2007) stated that the maximum torque occurs when the knee angular position θ is about 40° and for a simple torque balance, the relation between F and the knee angular position θ is expressed for both the knee articulation models.

$$F_{model A} = \frac{MgL \cos(\theta)}{h \sin(\beta)} \quad (2.1)$$

where

$F_{model A}$ = force supplied

Mg = gravity force

θ = knee angular position

h = arm of the torque

$$F_{model B} = \frac{MgL \cos(\theta)}{h \sin(\alpha + \gamma)} \quad (2.2)$$

where

$F_{model B}$ = force supplied

Mg = gravity force

θ = knee angular position

h = arm of the torque

Based on the Beyl, P. et al., (2007) and Muscato, G., & Spampinato, G. (2007) studied, I have utilized the design of the PPAMs and lever arm of Beyl, P. et al., (2007) and the knee joint design of Muscato, G., & Spampinato, G. (2007) as shown in figure 2.12. The PPAMs are used instead of the pneumatic piston and the knee joint design is applied to a wearable power-assisted knee orthosis where the PPAM is placed upon the thighbone bar. As mentioned by Beyl, P. et al., (2007), the design is a four bar linkage mechanism but my design will only consist of two bar linkage where each PPAM with one linkage bar.

2.4 Control

Beyl, P. et al., (2009) proposed that the data-acquisition is performed by National Instruments PCI-6229 data-acquisition board at a sampling rate of 500Hz, whereas the pressure control is done by Kolvenbach KPS ¾-00 pressure regulating valves. They also proposed that the knee joint angles are measured by means of Avagotech AEDEA 3300-TE1 high resolution increment encoders and each of the PPAM is equipped with a gauge pressure sensor. They stated that in order to provide direct, more accurate force measurements the coupling element between each PPAM and the joint is equipped with a calibrated full bridge strain gauge circuit.

2.4.1 Power control

Pneumatic power actuator is applied in the power assisted knee orthosis because of the sufficient power-to-weight ratio for a human-machine system. Although the electrical servo motor is also suitable for the power assisted knee orthosis but the servo motor is more expensive than the pneumatic muscle actuator, therefore it has against the objective to develop a low cost human-machine exoskeleton. Hydraulic power has high power-to-weight ratio or high torque which developed for heavy load machine. Therefore, hydraulic power is not suitable to assist human in movement. Hydraulic can be developed in human-machine system as carry heavy loads system.

Table 2.4: Comparison between Electrical, Pneumatic and Hydraulic power

Electrical		Pneumatic		Hydraulic	
Expensive		Inexpensive		Expensive in long run	
Low	power-to-weight ratio	Low	power-to-weight ratio	High	power-to-weight ratio
High	precision and accuracy	Low accuracy		High accuracy	
Good for all size of robot		Sufficient for exoskeleton system		Good for large robot and heavy payload	

Electric drives need a speed reduction because of their high revolution speeds and low value of torque. Such gearing introduces unwanted phenomena in the system, such as backlash and extra inertia. Hence, pneumatic muscle actuator (PMA) can be directly connected to the structure they power, they can easily fit because they are small and value of speed and force are in the range of requirement. (Wetenschappen, F. T., 1999)

2.4.2 Artificial Pneumatic Muscle Control

Sawicki G.S. & Ferris D.P. (2009) implemented a physiologically-inspired controller that incorporated the user's own surface electromyography to dictate the timing and magnitude of artificial muscle force. They chose to control each artificial pneumatic muscle with an electromyography signal generated by a biological muscle with analogous mechanical action. Artificial extensors were controlled by biological extensors while artificial flexors were controlled by biological flexors. As more specific to the knee, they used vastus lateralis to control the two artificial knee extensors and medial hamstrings to control the two artificial knee flexors.



Figure 2.16: University of Michigan Knee-Ankle-Foot Orthosis (Sawicki, G. S., & Ferris, D. P. 2009)

Two proportional myoelectric control modes using a real-time computer interface were programmed where first allowed co-activation of artificial extensor and flexor muscles (proportional myoelectric, PM) and the second prevented co-activation by inhibiting flexor activation when the antagonist extensor was active (proportional myoelectric with flexor inhibition, PMFI) (Sawicki, G. S., & Ferris, D. P. 2009). In both cases, Sawicki, G.S. & Ferris, D.P. (2009) amplified, high pass filtered, full wave rectified, low pass filtered and applied a threshold and gain to convert the raw voltage commanding the pneumatic hardware. The time between the control signal onset and initial rise of artificial muscle tension (50ms) of the device was comparable to response times of human muscle (Sawicki, G.S. & Ferris, D.P., 2009).

For PM during walking, the knee artificial flexors and extensors co-activated stiffening the joint and delivered a small net flexor torque over the entire stride. As for the PMFI, timing of the knee orthosis torque was more similar to normal walking when compared to PM. The mechanical power delivered by the orthosis knee joint was greater with the PMFI compared to the PM. However, the orthosis knee is was poor at absorbing mechanical energy; it absorbed significantly less mechanical energy than biological knee muscle-tendon during normal walking. (Sawicki, G.S. & Ferris, D.P., 2009)

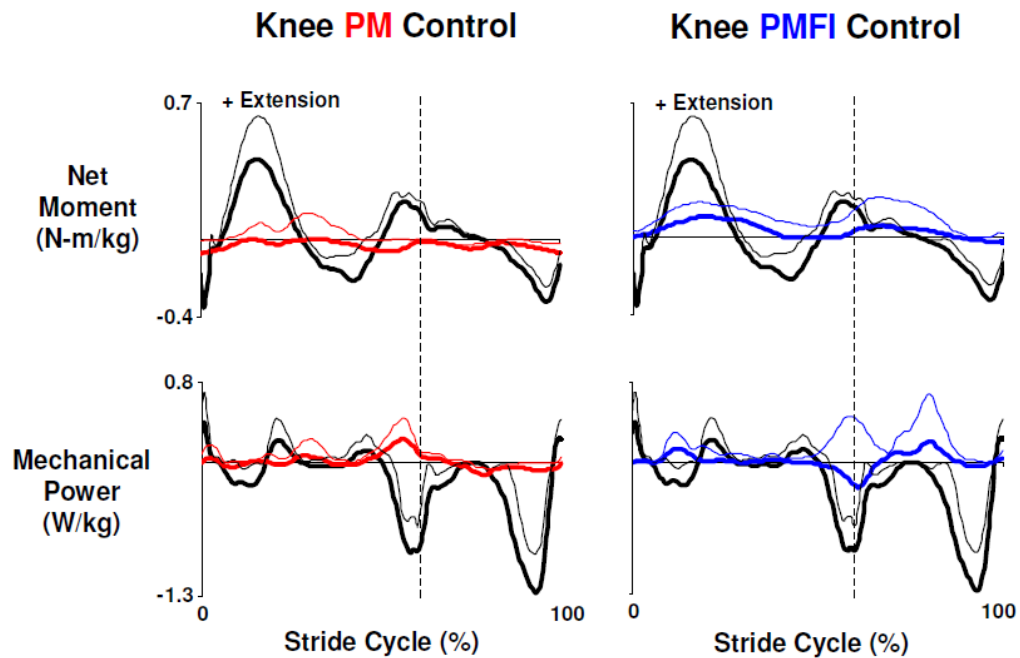


Figure 2.17: Orthosis Knee Joint Kinetics (Sawicki, G. S., & Ferris, D. P., 2009)

In Figure 2.17 depicts that the data traces are mean (solid lines) + 1 SD (thin lines) from the left leg of three subjects who walked overground at 1.25 m/s with a knee-ankle-foot orthosis powered in two control modes. In the left column, data from powered trials with direct proportional myoelectric control (PM, red) for net torque (N-m/kg) (top) generated by knee joint artificial muscles and the resulting mechanical power (W/kg) (bottom) is compared with the net ankle muscle-tendon moment (N-m/kg) and mechanical power (W/kg) recorded during walking without the orthosis (black). The right column shows similar data for powered trials using proportional myoelectric control with a flexor inhibition algorithm (PMFI, blue). Stride cycles begin (0%) and end (100%) at left heel strike. Dotted vertical lines mark the stance swing transition at ~60% of the stride cycle. Knee extensor torque/moment is positive. Positive mechanical power indicates energy generation and negative mechanical power indicates energy absorption. (Sawicki, G.S. & Ferris, D.P., 2009)

Takuma, T. & Hosoda, K. (2006) proposed that they used 3-port solenoid on/off valves as the pneumatic actuator controller. They used 3-port solenoid on/off valves used having a closed center position so that they could preserve the amount of

air by closing the valve. Their pneumatic actuators are McKibben instead of the PPAM. Figure 2.18 shows the air circuit used for controlling the pneumatic actuator.

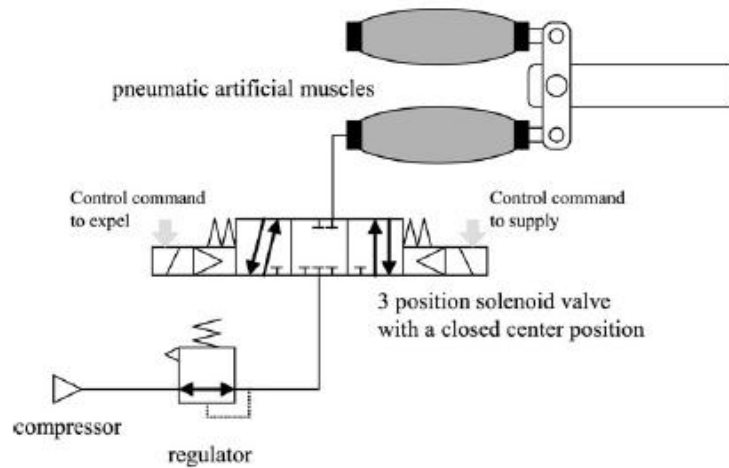


Figure 2.18: Air design for the Pneumatic Actuator (Takuma, T. & Hosoda, K., 2006)

Since Takuma, T. & Hosoda, K. (2006) used solenoid valves, the controller becomes extremely simple with only two bits are required to control an actuator (on or off supply/expel valves). Although the controller becomes simple but there is a time delay between the operation of the valve and a change in the inner pressure of the muscle as shown in figure 2.19. The supply valve is opened at 1 second and the expel valve is opened at 3 seconds which the delay is more than 0.4 seconds. At the same time, Takuma, T. & Hosoda, K. (2006) have utilized the delay for changing the compliance of the actuator by regulating the opening duration of the supply or expel valves. They also mentioned that Pulse width modulation (PWM) is used to regulate the movement of pneumatic actuators with on/off valves and the pressure could be modulated for achieving more precise control of the joint motion, although involve additional control cost. Unfortunately, they do not use PWM but they intend to investigate its use in their future studies.

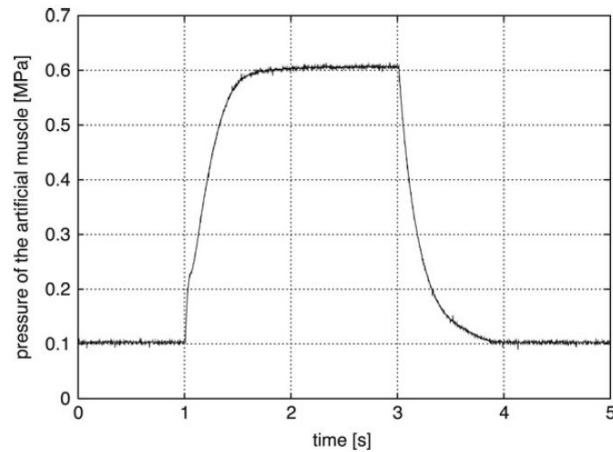


Figure 2.19: Time Delay between the Operation of the Valve and a Change in the Inner Pressure of the Actuator (Hosoda K. et al., 2008)

Furthermore, Takuma, T. & Hosoda, K. (2006) proposed a valve operation scheme for dynamic walking as shown in figure 2.20 which is almost the same as the one proposed by T. Takuma & K. Hosoda (2006) with the exception of the ankle valve operation. The knee and the ankle extensor muscles of the swing leg are filled with a certain amount of air at the beginning of the walking trial and are not operated but rather remain closed during their experiment (Takuma, T. & Hosoda, K., 2006). The muscles of the stance leg are not operated well (Takuma, T. & Hosoda, K., 2006). The Valve operation is initiated by the touch signal from the sensor embedded on the sole and after the signal, the ankle flexor is activated and remains fixed for T_s to kick off the ground (Takuma, T. & Hosoda, K., 2006). In order to provide the propulsion force, the hip extensor is activated for T_w while air is expelled from the flexor (Takuma, T. & Hosoda, K., 2006). After $(T_w + T_b)$, air is expelled from the knee flexor so that the swing leg clears the ground (Takuma, T. & Hosoda, K., 2006).

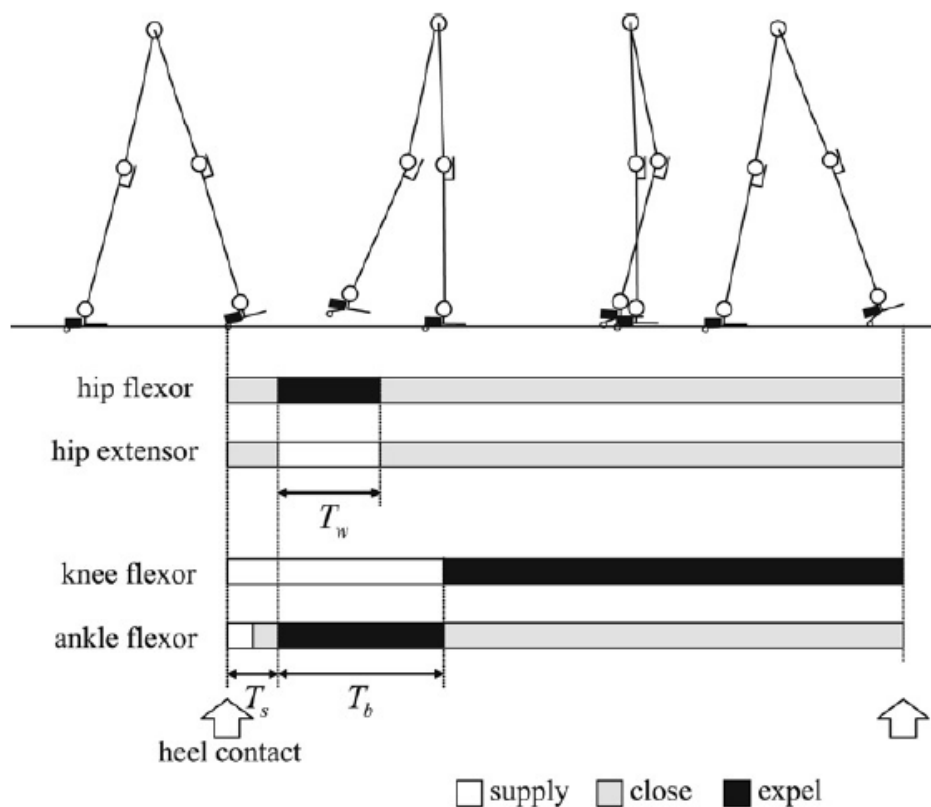


Figure 2.20: Valve Operation scheme for dynamic walking (Takuma, T. & Hosoda, K., 2006)

2.4.3 Control System

There are many types of sensor for movement classification and balance control evaluation in the market such as Hall Effect sensor, accelerometer and etc. Based on Hirata Y. et al. (2009) and Yang, C.-C. & Hsu, Y.-L. (2010), the accelerometer would be the best choice for the project. The sensor placement is important to obtain an optimal result. The accelerometer can be located in the collar area, rear of upper arm, forearm, waist, thigh, shin and top of the foot (Yang, C.-C., & Hsu, Y.-L., 2010). These locations have relatively larger continuous surface and low movement and flexibility (Yang, C.-C., & Hsu, Y.-L., 2010).

Ankle-attached accelerometers can reflect gait-related features during locomotion or walking. Steps, travel distance, velocity and energy expenditure can be estimated by an ankle-worn accelerometer. Besides that, the sensors can be easily

fit. Therefore, it can be directly attached to the skin or with some form of indirect attachment by using straps, pant belts or other accessories. (Yang C-C & Hsu Y-L, 2010)

According to Yang, C.-C. & Hsu, Y.-L. (2010), human postures can be distinguished according to the magnitude of acceleration signals along sensitive axes from only one accelerometer worn. Furthermore, two accelerometers can be attached to the torso and thigh to distinguish standing and sitting postures from static activities. Acceleration signals can be used to determine walking in ambulatory movement. Walking can be identified by frequency-domain analysis and it is characterized by a variance of over 0.02 g in vertical acceleration and frequency peak within 1-3Hz in the signal spectrum. Discrete wavelet transform is used to distinguish walking on a level ground and walking on stairway. Moreover, accelerometry data can be used to identify heel strike, gait cycle frequency, stride symmetry and regularity. (Yang, C.-C., & Hsu, Y.-L., 2010)

Table 2.5: Accelerometer Types Specification Comparison (Yang, C.-C., & Hsu, Y.-L., 2010)

	AMP331	StepWatch	activPAL	IDEAA
Size (mm)	71.3x24x37.5	75x50x20	53x35x7	70x54x17
Weight (g)	50	38	20	59
Accelerometer type	na	na	pizoresistive	pizelectric
Accelerometer axis	1 uni-axis and 1 dual-axis	2	1	2
Sensor placement	Ankle	Ankle	Thigh	Chest, Thigh, Feet
Sampling rate	na	128Hz	10Hz (8 bit)	32Hz
Sensitivity range	na	na	2 g	5 g
Battery type	na	750mAh Lithium	3V li-polymer rechargeable	1 1.5V AA
Data transmission	916MHz RF (USB wireless)	USB (docking station)	USB (docking station)	USB

adapter)				
Data storage capacity	na	2 months	na	7 days
Reported parameters	Steps, cadence, walking speed, stride length, distance, EE	Steps gait characteristics	Sedentary and upright time, steps, stepping time, cadence, sit-to-stand activities, MET, PAL, kCal	Activity types, gait types, EE

According to Takeda, R. et al. (2009), the acceleration sensors can be used as inclination sensors. The sensor units are placed on the lower limb segments of the volunteers, both thigh and both shanks. The length and inclination of each segment was used to calculate the joint positions of both left and right hips, both knee and both ankles during walking. A tri-axial acceleration sensor is used as an inclination sensor as it able to measure the gravitational acceleration and the output of an acceleration sensor O_i .

$$O_i = a_i - g_i \quad (2.3)$$

where

O_i = acceleration sensor

a_i = translational acceleration

g_i = gravitational acceleration

The translational acceleration, a_i and gravitational acceleration, g_i are measured along the i axis ($i=x,y,z$) of the acceleration sensor (Takeda, R. et al., 2009). If the acceleration sensor is static, the a_i is zero, means the g_i is the only output. Thus, the angle of inclination for the three axes of an acceleration sensor against the gravitational acceleration direction can be expressed as following.

$$\theta_i = \cos^{-1} \frac{O_i}{g} \quad (2.4)$$

where

θ_i = inclination angle

O_i = acceleration sensor

g = gravitational acceleration

Besides that, the gravitational acceleration can be expressed as following.

$$g = \sqrt{O_x^2 + O_y^2 + O_z^2} \quad (2.5)$$

where

g = gravitational acceleration

O_x = acceleration sensor (x-axis)

O_y = acceleration sensor (y-axis)

O_z = acceleration sensor (z-axis)

Takeda, R. et al. (2009) have done some experiment on the knee flexion-extension by using the acceleration sensor and they have chose three different characteristic of volunteers as their subjects. Table 2.5 is the particular of the volunteers.

Table 2.6: Particular for the Volunteers (Takeda, R. et al., 2009)

Volunteer	Gender	Age	Height (cm)	Weight (kg)	Past injuries
(a)	Male	23	180	67	none
(b)	Male	28	173	73	none
(c)	Male	23	170	56	none

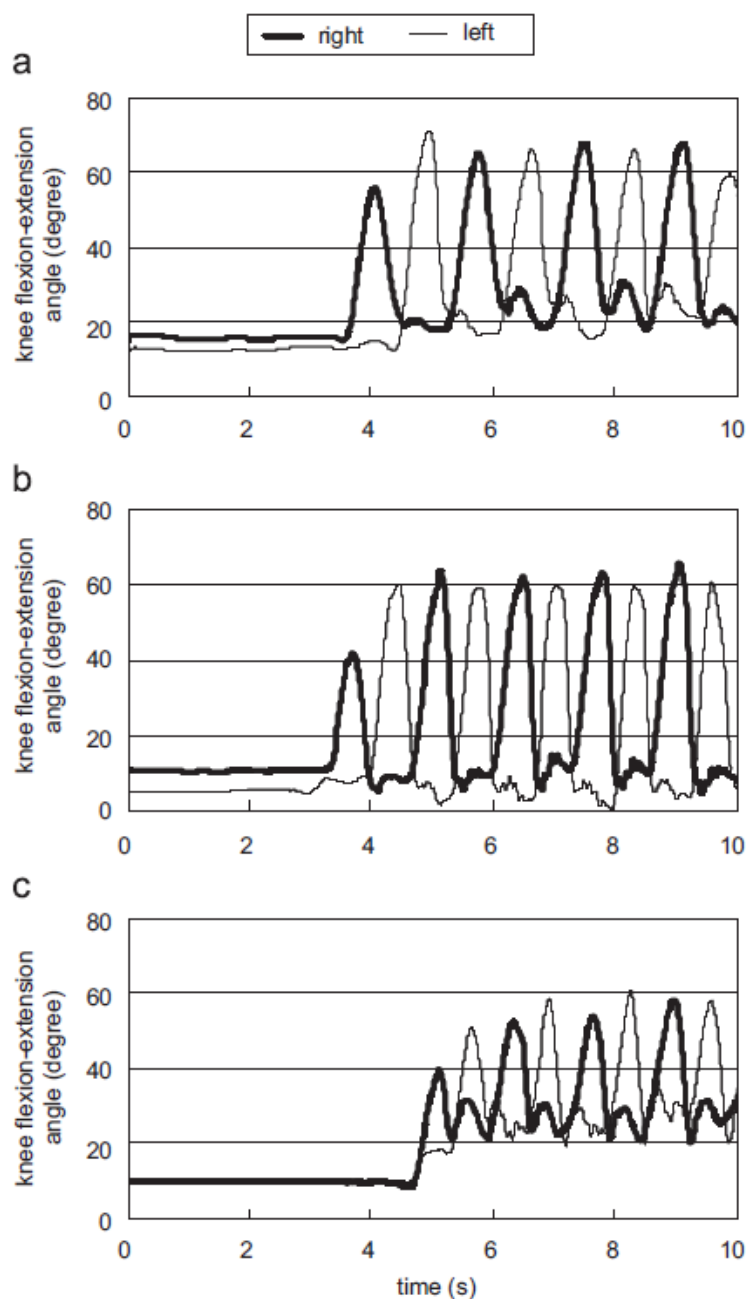


Figure 2.21: Knee Joint Flexion-Extension for Volunteers (a), (b) and (c).

(Takeda, R. et al., 2009)

In figure 2.21, the vertical axis represents the angles in degrees and the horizontal axis represents the time in seconds (Takeda, R. et al., 2009). The 0° is the joint angle during standing, negative values represent flexion and positive value represent extension (Takeda, R. et al., 2009). The fat lines indicate the joint angles for right leg and the thin lines indicate the joint angles for the left leg (Takeda, R. et al., 2009).

Figure 2.22 illustrates the wearable walking helper with accelerometer. The system have three potentiometer to measure the rotation angle of each joint, two force sensors attached to shoe sole to measure ground reaction force (GRF) and a 3-axis accelerometer to measure inclination of the link (Hirata, Y. et al., 2009).

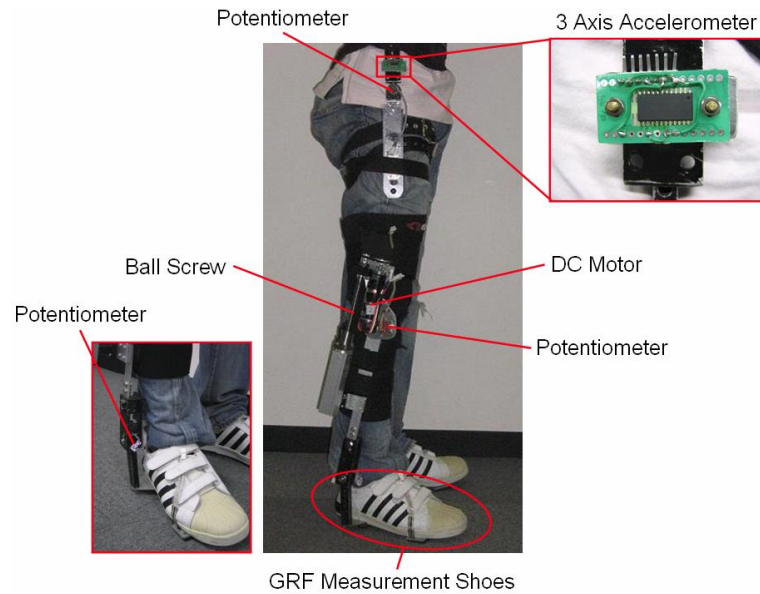


Figure 2.22: Wearable Walking Helper (Hirata, Y. et al., 2009)

Hirata, Y. et al. (2009) have introduced a method to measure the inclination of the link with an accelerometer and they have verified the effectiveness of the method by preliminary experiments. In their preliminary experiment, they have proved that by using accelerometer, the system could support not only the stance phase but also the swing phase of the gait appropriately.

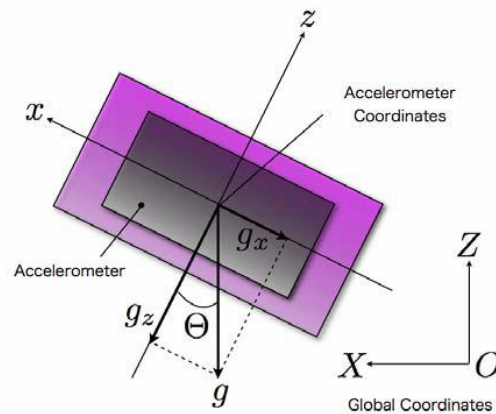


Figure 2.23: Measurement of Acceleration of Human Link (Hirata, Y. et al., 2009)

As shown in Figure 2.23, the gravitational acceleration $g[m/s^2]$ is imposed along the vertical direction (Hirata, Y. et al., 2009). The system was able to measure the gravitational acceleration decomposed in three directions under the condition of no dynamic acceleration with the help of 3-axis accelerometer (Hirata, Y. et al., 2009). In order to measure the inclination of the human link, the x - z plane of the accelerometer coordinate system corresponds to the X - Z plane of the global coordinate as shown in the figure 2.23 (Hirata, Y. et al., 2009). Furthermore, the system can calculate the inclination of the accelerometer with the following equation where θ is inclination of the accelerometer respect to the vertical direction. g_x and g_z are gravitational accelerations in the direction of x axis and z axis (Hirata, Y. et al., 2009).

$$\theta = \tan^{-1} \left(\frac{g_x}{g_z} \right) \quad (2.6)$$

where

θ = inclination of the accelerometer

g_x = gravitational acceleration (x axis)

g_z = gravitational acceleration (z axis)

2.5 Walking Gait Analysis

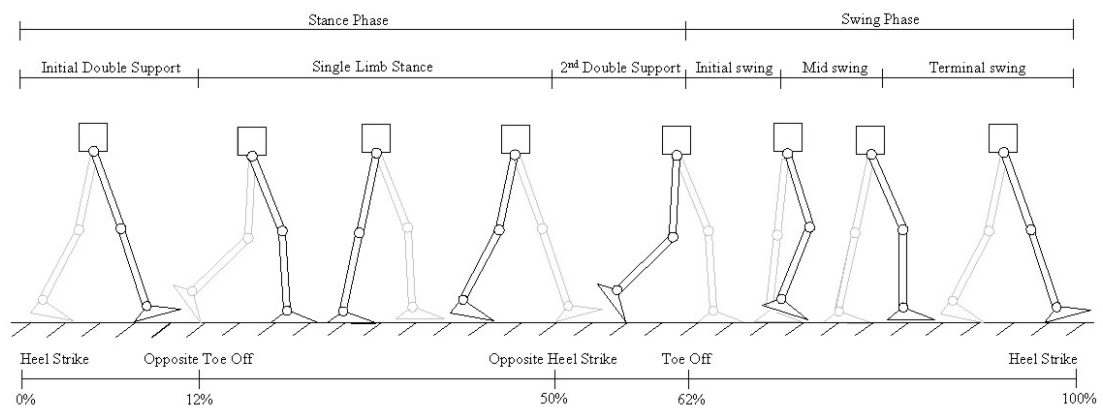


Figure 2.24: Human Walking Gait Cycle (Dollar, A. M., & Herr, H., 2007)

Figure 2.24 is a simplified diagram of human walking gait and note that the timing of the labelled events during the gait cycle is approximate and varies across individuals and condition (Dollar, A. M., & Herr, H., 2007). The percentages showing the contacts events are given at their approximate location in the cycle. The human walking gait cycle is represented as starting 0% and ending 100% at the point of heel strike on the same foot, with heel strike on the adjacent foot occurring at approximately 62% of gait cycle (Dollar, A. M., & Herr, H., 2007).

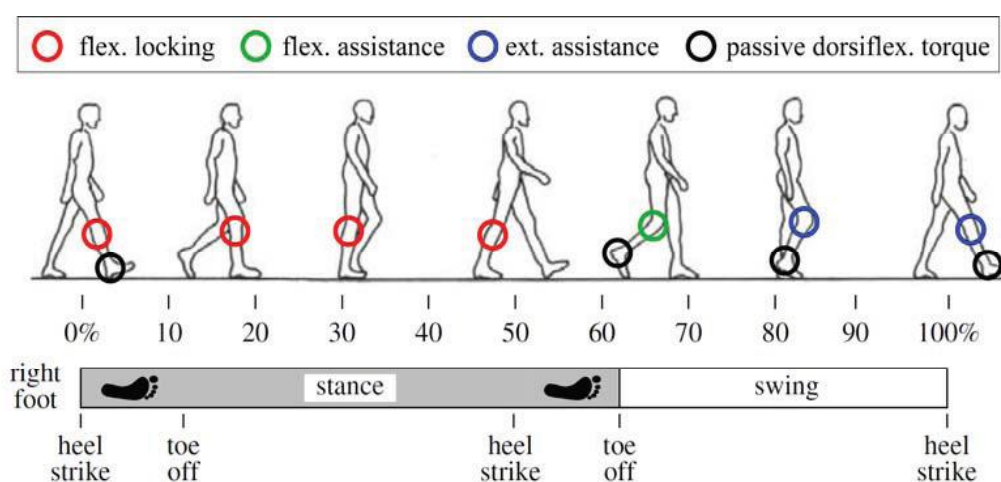


Figure 2.25: Functional Specification of the Active Orthosis during Gait Cycle

(Font-llagunes, J. M. et al., 2011)

Dollar, A. M., & Herr, H. (2007) and Font-llagunes, J. M. et al. (2011) are stated that heel strike on the adjacent foot occurring at approximately 62% of gait cycle as shown in both the figure 2.24 and 2.25. Figure 2.25 shows the gait cycle and the specified functions of the active stance-control knee-ankle-foot-orthosis (A-SCKAFO) at the knee and ankle joints (Font-llagunes, J. M. et al., 2011).

Based on Font-llagunes, J. M. et al. (2011), they have proposed A-SCKAFO with several sensors in both the knee and ankle for its autonomous control. The orthosis has to include plantar sensors on the insoles to detect foot-ground contact and also the period within the stance phase. Angular sensors at both joints needed to detect the gait phase and used as inputs of the actuation control system.

CHAPTER 3

METHODOLOGY

3.1 Conceptual Designs

The design idea is mainly come from two papers entitled mechanical design of an active knee orthosis for gait rehabilitation and kinematical model and control architecture for a human inspired five DOF robotic leg by Beyl, P. et al. (2007) and Muscato, G., & Spampinato, G. (2006) respectively. the idea of Beyl, P. et al. (2007) has been adapted in their mechanical design concept regarding the pneumatic artificial muscle design with four bar linkage. Besides that, for the fitting, IBeyl, P. et al. (2007) has been utilised design where they used two-piece rigid thermoplastic shells with a foam inlay and Velecro straps for both at the thigh and the shank. The idea of design for the shells is attached to the thigh and shank are adjustable according to the comfortable of the user and this idea is also adapted from Beyl, P. et al. (2007).

Furthermore, Muscato, G., & Spampinato, G. (2006) have contributed the knee joint concept. With the help of the design concept from Muscato, G., & Spampinato, G. (2006), the design can has more flexibility at the knee joint where flexion of 90 ° is possible.

3.1.1 Pneumatic Artificial Muscle Design

Among all the pneumatic artificial muscle, the pleated pneumatic artificial muscle (PPAM) has been chosen as the artificial muscle because of its specification as discussed in 2.2.2.2. Firstly, the material of the PPAM is the priority and the material must be able to pleat and air resistance, thus para-aramid fiber would be the best for PPAM as proven by Wetenschappen, F. T. (1999). Secondly, the bars that hold the PPAM and the end fitting of the PPAM should be built with aluminium to have a light weight pneumatic artificial muscles. If a single PPAM is not able to make a large flexion of 90°, two PPAMs connected in series as shown in the design of Beyl, P. et al. (2007) would be efficient.

Figure 3.1 depicts single PPAM design at each upon and under thighbone bar. The PPAM placed upon the thighbone bar is connected to upon of shinbone bar while the PPAM placed under the thighbone bar is connected to under of shinbone bar. Figure 3.1 shows the flexion of 90° where the PPAM placed under the thighbone bar is contracted while PPAM placed upon the thighbone bar is relaxed and they are antagonistic set-up. Yellow colour indicates the PPAM, grey colour indicates the end fitting bar of PPAM and black colour bar is fixed to the thighbone bar but flexibly attached to the PPAM.

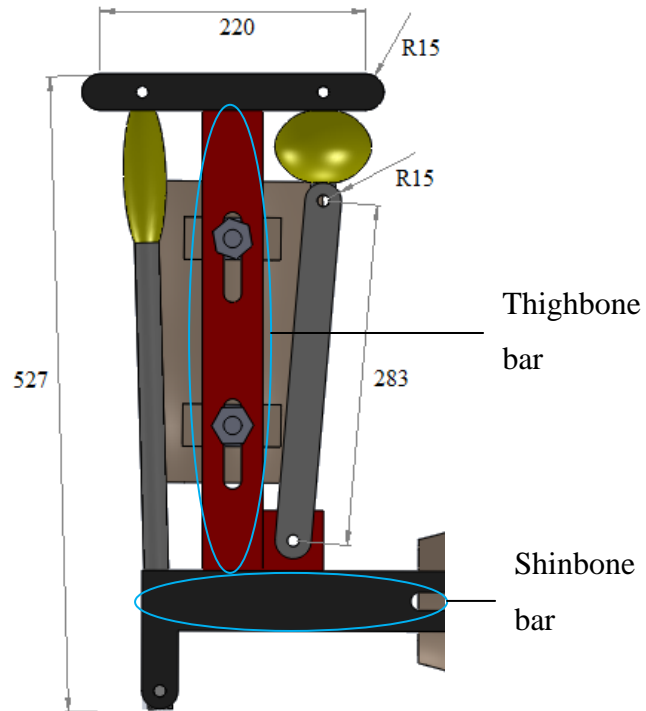


Figure 3.1: SolidWork Drawing of Pleated Pneumatic Artificial Muscle Flexion

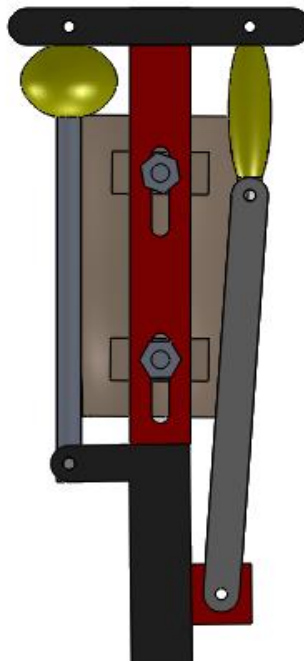


Figure 3.2: SolidWork Sketching of Pleated Pneumatic Artificial Muscle Extension

As shown in Figure 3.2, the design is in extension whereby the PPAM function in the opposite way than that in Figure 3.1. Both the figures depict the

working function of the PPAMs to generate the flexion-extension movement of the design concept. The connectors between both the PPAMs and the shinbone bar are moveable so they could freely change their position to fit the movement. The connectors between both the PPAMs and the thighbone bar also moveable to allow freely change of the PPAM position.

3.1.2 Muscle Attachment Shell

For the fitting, two-piece rigid fiberglass shells with a foam inlay and Velcro straps or belts have been chosen for both at the thigh and the shank. Fiberglass is chosen because of the high durability, hard, lightweight, adaptable fit and low cost compared to the thermoplastic. Velcro strap or belt is to tightly join both the fiberglass shell together. They also hold and support the weight of the thigh and shank.

Figure 3.4 illustrate the design of two-piece rigid fiberglass shells and the Velcro straps or belts will be placed at the gaps of the two-piece rigid fiberglass shells as shown in Figure 2.10 designed by Beyl, P. et al. (2007).

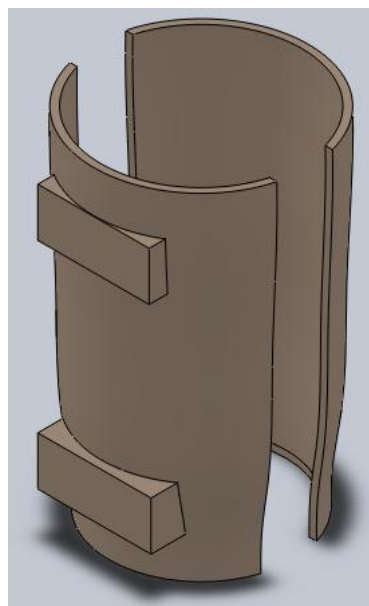


Figure 3.3: SolidWork Sketching of Two-piece Rigid Fiberglass Shells at Thigh

The position and orientation of each shell are adjustable by means of an integrated slider mechanism. In Figure 3.5 shows the two-piece fiberglass shells at shank with adjustable fitting and the two-piece fiberglass shells at thigh also applied the same slider mechanism. A clamp element will be implemented to both the thighbone and shinbone bar to each of the aluminium plate built at the shell. The idea is similar as proposed by the beyl, P. et al. (2007) in Figure 3.5. In this way, adjustability should be sufficient enough to align the orthosis and to achieve a good fit and good support for the orthosis.

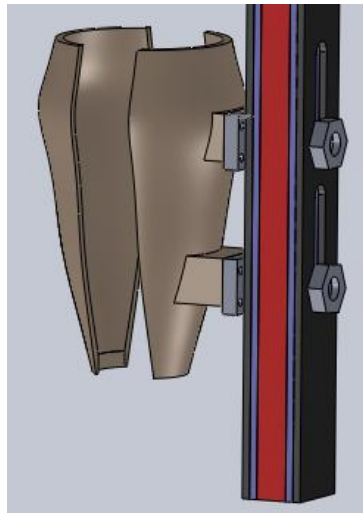


Figure 3.4: SolidWork Sketching of Two-piece Rigid Fiberglass Shells at Shank with Adjustable Fitting

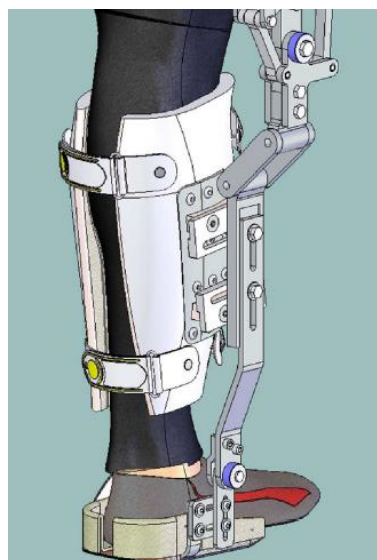


Figure 3.5: CAD Drawing of the Proof-of-Concept Active Knee Orthosis; Close-up of the Adjustable Fittings (Beyl, P. et al., 2007)

3.1.3 Knee Joint Design

The first idea of the knee joint design was based on a pulley and wires which is similar to Figure 3.6 designed by Deaconescu, A., & Deaconescu, T. (2009). Although the idea of pulley can work but the flexion mechanism is not optimal where only 60° to 70° of bending is performed. Besides, although the wires applied at the pulley can reach a 90° flexion but the wire tension has to be considered and thus will be complicated.

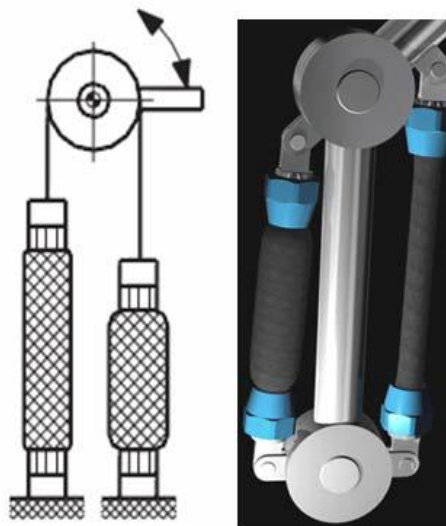


Figure 3.6: Pneumatic Muscle Actuated Rotation Modules

(Deaconescu, A., & Deaconescu, T., 2009)

Based on Muscato, G., & Spampinato, G. (2006) journal paper, the idea has been adapted for the knee joint design as shown in Figure 2.12 where the pulley and wire can be eliminated from the design. The robot design proposed by Muscato, G., & Spampinato, G. (2006) is able to have more than 90° flexion without wires and thus the design is benefit for the design to have a more degree of flexion.

Figure 3.7 depicts knee joint design with the capability of 90° flexion and 0° extension. The figure on the left side is the full set of my design where it is in extension mode. The blue colour and red colour bars are connected as the joint. The black colour bar is the outer bar to facilitate the knee joint extension movement by connected to the PPAM (grey). The red colour bar is the inner bar to act as the support bar and to facilitate the knee joint flexion by connected to the PPAM (grey).

The inner shinbone bar is designed in an “L” shape to limit the knee flexion of 90° as shown in Figure 3.9. The 90° flexion is limited when the inner thighbone bar is collided with the “L” shape inner shinbone bar and stops the flexion. The figure on the left side is the full set of the design where it is in flexion mode.

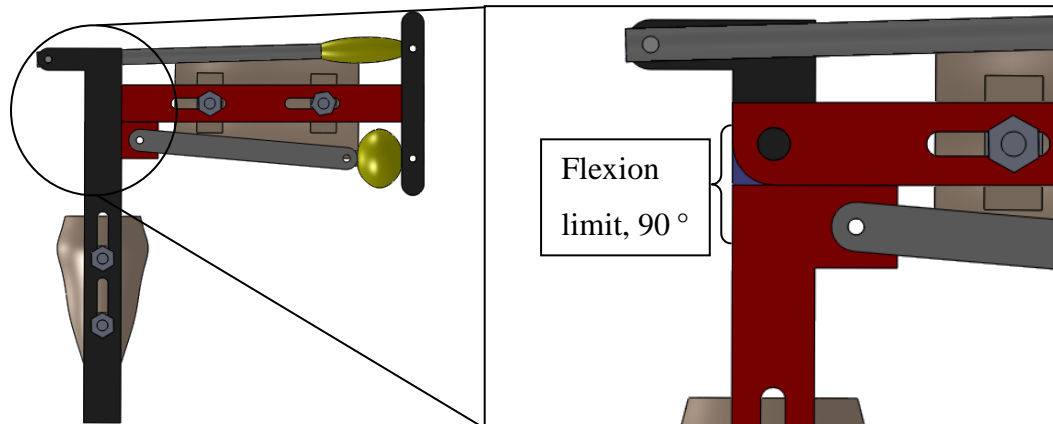


Figure 3.9: Flexion (90°)

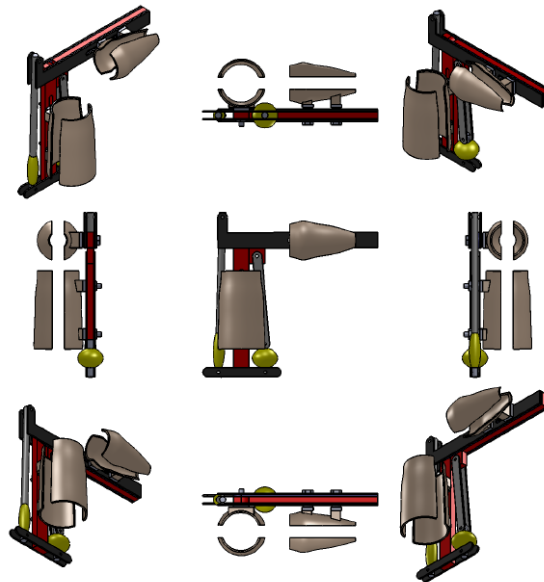


Figure 3.10: Different Views of the Knee Flexion Conceptual Designs

As shown in figure 3.10 is the different views of my wearable power-assisted pneumatic based knee orthosis conceptual design in flexion mode.

3.1.4 Control System Design

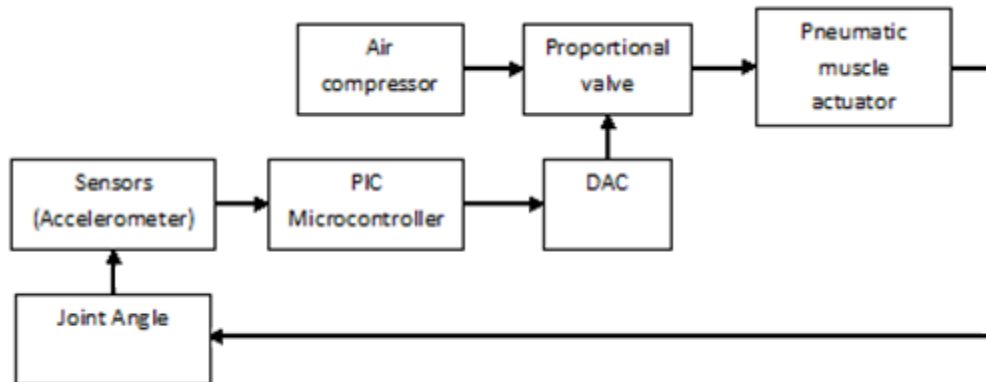


Figure 3.11: Control System Flow

During the walking gait cycle, the initial walking movement of the wearable power-assisted pneumatic based knee orthosis (WPAPBKO) have to trigger by the user by moving the leg with only a small range of joint angle degree. In this way, the user can initiate the WPAPBKO with just a little movement of the leg. After the WPAPBKO has been triggered, the walking motion will be generated automatically and thus assisting the user in walking.

When the system sensed a joint at the desire angle by an accelerometer, the PIC microcontroller will process the signal. Pulse width modulation (PWM) can be used to regulate the movement of pneumatic actuators with on/off valves and the pressure could be modulated for achieving more precise control of the joint motion. Therefore, the PIC microcontroller should have a built in PWM to process the signal.

The proportional valve proposed by Hosoda K. et al., a 3-position solenoid valve with a closed center position. When the pressurized air is supplied to the proportional valve that controlled by the PIC microcontroller, the pneumatic artificial muscle in this case is PPAMs initiated according to the output signal of the PIC microcontroller. After the PPAMs are initiated, the sensor will continue sensing the joint ankle and thus a feedback is generated to continue the process. Therefore, a walking gait cycle of the WPAPBKO is produced.

Different views of the conceptual designs are created using Solidworks and included at the appendix C to G. Appendix C to F are the dimensional views of the conceptual design and the appendix G is 3D view of the design. The appendix of the conceptual designs was modified due to the replacement of pleated pneumatic artificial muscle with McKibben pneumatic artificial muscle.

3.2 Artificial Muscle

Section 3.1.1 discussed the type of artificial muscle selected which is the pleated pneumatic artificial muscle (PPAM). Due to some circumstances, the pleated pneumatic artificial muscle was decided to replace with McKibben PAM. Although the artificial muscle can be purchased from the Festo industry company but the price to customize the desire length of artificial muscle was extremely expensive.

The inner tube of the MPAM is made of condom (Durex[®], “extra safe”) and the muscle end capping is fabricated by CNC turning machine. The size and contour of the end capping will determine the size of the MPAM consequently contributed to a variable of forces the MPAM could exert upon pressurization. The suitable material to fabricate the muscle end capping is aluminium because of its lightweight characteristic.

Materials required for single piece of MPAM:

1. Condom (Durex[®] extra safe)
2. Cotton
3. Braided nylon sleeve
4. White tape
5. Hose clamp
6. Custom made muscle end capping



Figure 3.12: Materials required for fabricating a MPAM

Procedures to fabricate MPAM:

1. End capping was fabricated by CNC turning machine.
2. End capping was drilled to assemble the “L” shape tube connector.
3. White tape was wrapped around the end capping to prevent loosening when connected with the inner tube.
4. Two condoms were used as the inner tube of the artificial muscle.
5. At the end of the two condoms was cut to make a hole for the end capping.
6. One of the ends of the two condoms was wrapped tightly to the end capping by using white tape.
7. The cotton was used to cover the condom and prevent the condom from friction with the braided nylon sleeve.
8. After the cotton layer was done, the cotton was covered with the outer layer of braided nylon sleeve.
9. Then, two hose clamps were inserted outside the braided nylon sleeve.
10. Steps 3 to 5 were repeated for the other end of condom.
11. When the condom’s ends were wrapped tightly to the end capping, the hose clamps was moved to both the end capping.
12. Last, both the hose clamps were tightened up to the braided nylon sleeve, cotton and the condom.

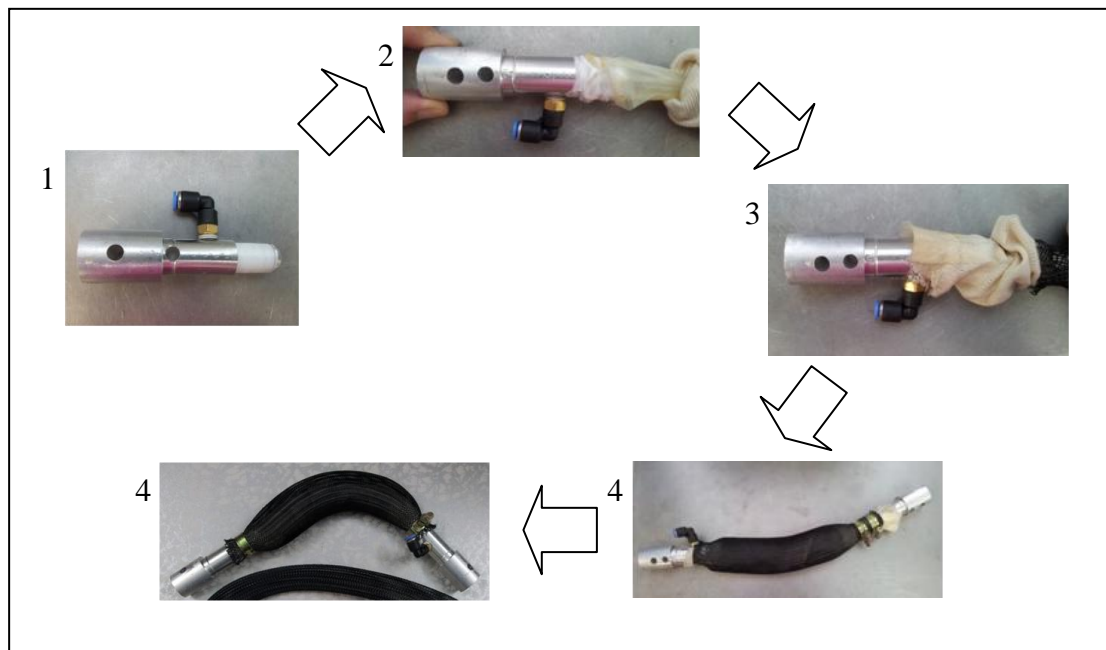


Figure 3.13: Steps to fabricate the MPAM

Precaution steps:

1. The double layer of condoms must wrap to the end capping independently each at one time.
2. The cotton must able to cover the entire condom including during extension of the artificial muscle to avoid interaction between condom and braided nylon sleeve.
3. Avoid twisting the inner tube (condoms) in order to have an optimum performance.
4. The exact length of braided nylon sleeve is important to determine the maximum extension.

CHAPTER 4

RESULTS AND DISCUSSIONS

4.1 Mechanical Frame

From the mechanical design concept, the first prototype of the pneumatic based power-assisted knee orthosis, powered by McKibben Pneumatic Artificial Muscle (MPAM) was constructed (Figure 4.1). When constructing the prototype, the frame was separated into three categories to ease the fabrication, the three categories are:

1. Upper leg,
2. Lower leg and
3. Foot



Figure 4.1: First Prototype

4.1.1 Knee Joint of Prototype

Figure 4.2 depicts the mechanism of the knee joint of the frame between the shinbone bar and the thighbone bar. The size of the hollow bar is 1 inch \times 2 inch. As for the performance of the joint mechanism, the smoothness of the joint motion is unexpected as it is as smooth as the pulley system or the gear system. The prototype in Figure 4.3 was similar to the conceptual design except for the “L” shape of shinbone bar. The shinbone bar was fabricated in “I” shape (Black Circle) rather than “L”. This is because “I” shape is comprehensive to limit the maximum flexion angle of 90 ° as discussed in section 3.1.3.

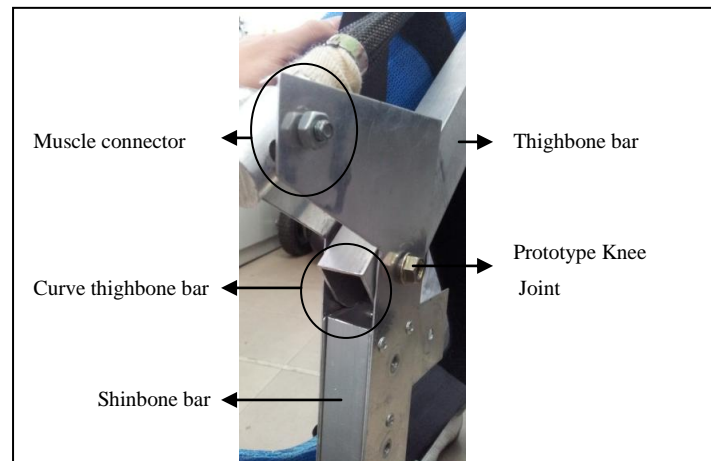


Figure 4.2: Joint mechanism

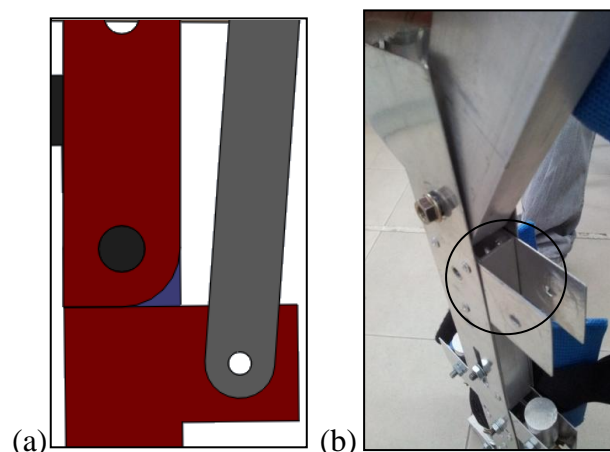


Figure 4.3: Shinbone bar shape (a) “L” shape conceptual design (b) “I” shape prototype

The relationship between inclination angle of each joint and MPAMs' displacement can be expressed in a formula using trigonometry method. For example, in order to determine the relationship between the knee joint and the MPAM to create flexion at the knee joint, each parameter is defined as shown in Figures 4.4 and 4.5. By using trigonometry method the relationship between inclination angle of knee joint, θ and the respective MPAM's length, x can be written as

$$\theta = 180^\circ - \tan^{-1} \frac{w}{v} - \cos^{-1} \frac{v^2 + w^2 + y^2 + z^2 - x^2}{2(v^2 + w^2)(y^2 + z^2)} - \tan^{-1} \frac{y}{z} \quad (4.1)$$

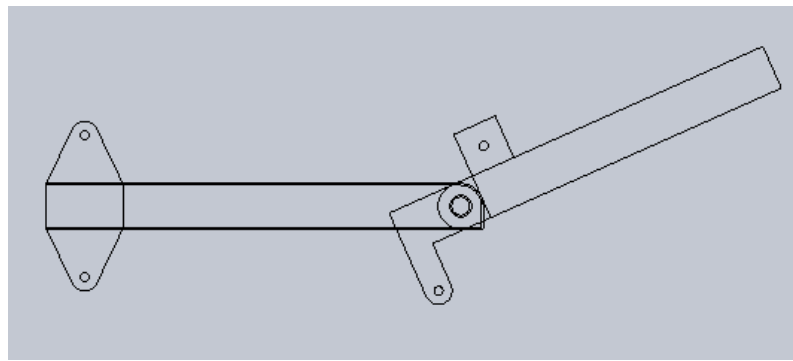


Figure 4.4: The Knee Joint of the Power-Assisted Knee Orthosis

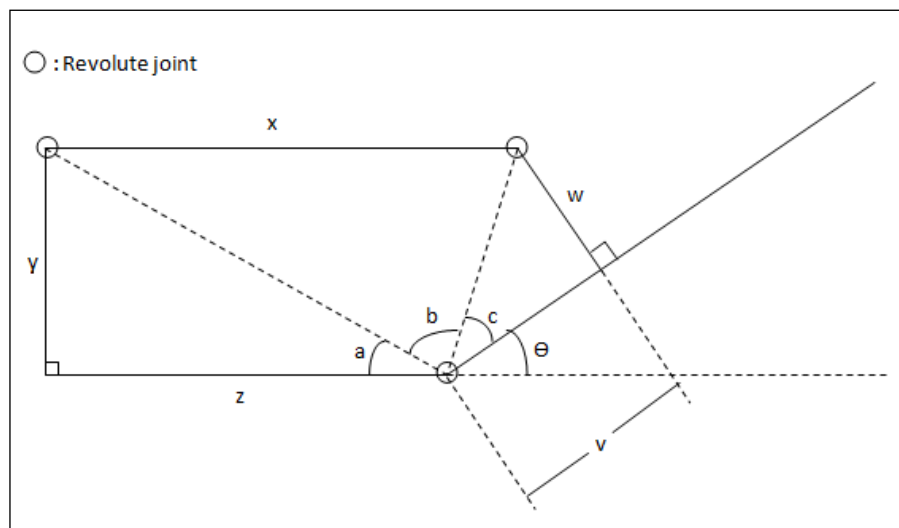


Figure 4.5: Mathematical Model of the Frame of Power-Assisted Knee Orthosis

The real time prototype of knee joint can be fabricated to perform sitting position when the system is not running. Although the sitting position is not the main concern at the current stage but the design of the prototype is fabricated to have the

ability to perform sitting position. A sitting position is required to ease the wearing of the prototype and comfortable of the user especially to the patient with weakness of lower extremities.

When the system is ready to run, standing position is required as the system will perform standing position initially to withstand the user weight before a walking gait is performed. Therefore, for sit-to-stand theory, the knee joint of the prototype must have sufficient flexibility to perform a sitting position of 90° to standing position of 0° . Besides that, the extension of the prototype's knee joint is limited to 0° as mentioned in section 3.1.3 to prevent hyperextension of the human knee joint.

If the prototype can be fully fabricated by mechanical machine, there will be no limitation as discussed as below.

1. The thighbone bar is fabricated manually by hand instead of machine, thus, the quadrant is not a perfect curve to make a smooth and strong knee joint system but it still can run sufficiently.
2. The size of the joint mechanism utilized in the prototype as shown in figure 4.2 is customized manually. Therefore, there might be a gap or error in the orientation that will affects the optimal performance.
3. Besides affecting the performance, unwanted sounds might occurs due to the friction between aluminium bar and the metal joint.

4.1.2 Material and Locking Mechanism

Aluminium plate of 1mm thickness is sufficient to withstand the pulling force of the artificial muscle. Two aluminium plates were connected at each side of the shinbone bar with an artificial muscle as shown in Figure 4.6. The shape of the aluminium plate was a handmade product by using simple aluminium cutter gadget. If the aluminium plate is fabricated by using an automated machine, sharp edges would be excluded as designed in the conceptual designs.



Figure 4.6: MPAM Connector

Aluminium material was used to construct the prototype including the muscle end capping. The reason the aluminium is selected is its lightweight characteristic and these meet the power-assisted orthosis design requirement to perform a normal walking gait. The subject selected is 1.75m in height, 0.45m long of upper leg and 0.48m of lower leg. The prototype was constructed to be modular to ease and fit the user in various height of 1.65m to 1.75m.

Bolt and nut mechanism was first applied to the prototype as shown in the Figure 4.6 but unfortunately, they increase the weight of the prototype. To overcome this limitation, bolt and nut mechanism was replaced with rivet. Figure 4.8 depicts the rivet was applied to the prototype and when the weight of bolt and nut was replaced by rivet, the weight reduced from 2.7kg to 2.6kg.

Rivet mechanism is replaced to the prototype after the bolt and nut mechanism was applied for a period of time as shown in Figure 4.7. Bolt and nut apparently contributed more weight to the prototype and loosened when the system is running. To overcome this problem, rivet is considered and has been applied to the prototype for some testing under a period of time. As a result, rivet performance is as convincing as the bolt and nut mechanism with the benefits of less weight contribution and no disconnection when the system is running.

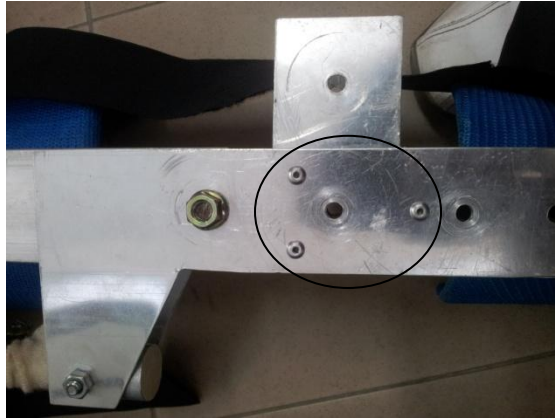


Figure 4.7: Rivet (black circle)



Figure 4.8: Bolt and Nut



Figure 4.9: Rivet

Fiberglass cast is a lighter, synthetic alternative to the more traditional plaster cast. Hence, fiberglass cast is selected to be the shell or fitting of the prototype. It

was created by padding the desire part of the extremities required in this project with cotton, followed by wrapping several layers of knitted fiberglass bandages impregnated with a water-soluble, quick-setting of resin. The following were the quick procedures to create the fibreglass cast shell:

1. The material was moved into a well ventilated room.
2. The desire part was covered with clothing and latex gloves were put on to protect from the toxic resin fumes.
3. The fiberglass cloth was padded and wrapped several layers to the desire part covered with clothing impregnated with water.
4. The fiberglass was dried for about 15 minutes until it is no longer tacky to the touch.
5. Steps 1 through 4 were repeated for different desire part of extremities.

The fiberglass is lighter and more durable compared to the plaster, so fiberglass has become the preferred type of casting.



Figure 4.10: Fiberglass Cast (“miro-polycast”, 2007)

Section 3.1.2 proposed two rigid fiberglass cast shells as the fitting to be attached to the user and they were designed to be adjustable to comfortably fit to the user. However, in the current design only single rigid fiberglass cast shell was applied as shown in Figure 4.11 rather than two rigid fiberglass cast shells. Nevertheless, the result was the same as single cast shell was able to provide comfortable fit to user as well. After testing on single rigid fiberglass cast shell by tightens up with a Velcro strap, the result was excellent to support the subject.



Figure 4.11: Single Rigid Fiberglass Shell

Besides the shell is adjustable, the height of the prototype was also fabricated to be adjustable. This means that the user has the flexibility in adjusting the height of the prototype according to the user height as the prototype range of height allowable is 165 cm to 175 cm. Maximum height of 175 cm was set according to the subject testing height to ease the testing and troubleshooting procedure. Comfort of the user is always the first priority to be concerned in this project. Both the adjustable shells and height of the prototype are to ensure the comfort and safety level of the user or subject testing.

4.1.3 Range of Knee Joint Motion

Figure 4.12 illustrates that the contraction length of the muscle is directly proportional to the knee joint angle of the prototype. Figure 4.13 proved that the prototype and MPAM were able to perform flexion of 90° even in a sitting position. The higher the muscle contraction yields a higher knee joint angle. A knee joint angle that is beyond the walking angle is not considered, but the prototype has proven that a higher degree of contraction is functional.

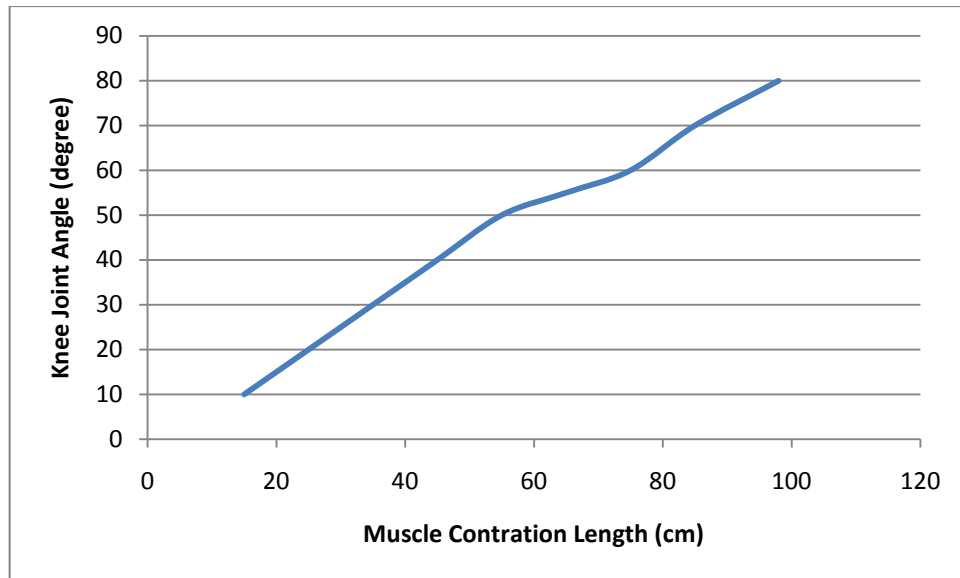


Figure 4.12: Graph of Knee Joint Angle versus Muscle Contraction Length



Figure 4.13: 90° flexion of the prototype (sitting position)

4.1.3.1 Range of Motion

In this project, walking required knee flexion angle of about 30° to 50° therefore, maximum allowable flexion angle of 55° has been set for the safety purpose although the MPAM able to provide more than 55° of flexion. The artificial muscle contraction length that allows the 55° flexion angle is 65mm (515mm to 450mm).

The MPAM able to generation contraction length of 98mm (maximum) for 80° flexion and further evaluation will be discussed in section 4.2.2. Maximum 80° flexion at the knee joint is unnecessary for walking gait hence 55° of flexion is set as maximum walking flexion instead of 80°. Figure 4.14 depicts the flexion of 55° walking angle.



Figure 4.14: flexion of 55 ° walking angle

4.1.4 Artificial Muscle

Tables 4.1, 4.2 and 4.3 illustrated the readings of the MPAM at different state such as original length (without load), length without actuation (with load) and length with actuation (with load) under the constant pressure of 20 psi and variable of load.

Figures 4.15, 4.16 and 4.17 depict the graphical data of the readings recorded according to the Tables 4.1, 4.2 and 4.3 respectively. R^2 value was calculated for each of the graph and correlation coefficient, R , was calculated.

Table 4.1: Muscle length with constant pressure (first data)

MPAM (Condoms)			
Load (kg)	Original Length (mm)	Length without actuation (mm)	Length with actuation (mm)
1.0	410	510	418
2.0	410	520	425
3.0	410	530	432
3.5	410	530	440
4.0	410	530	440
Constant Pressure = 20psi			

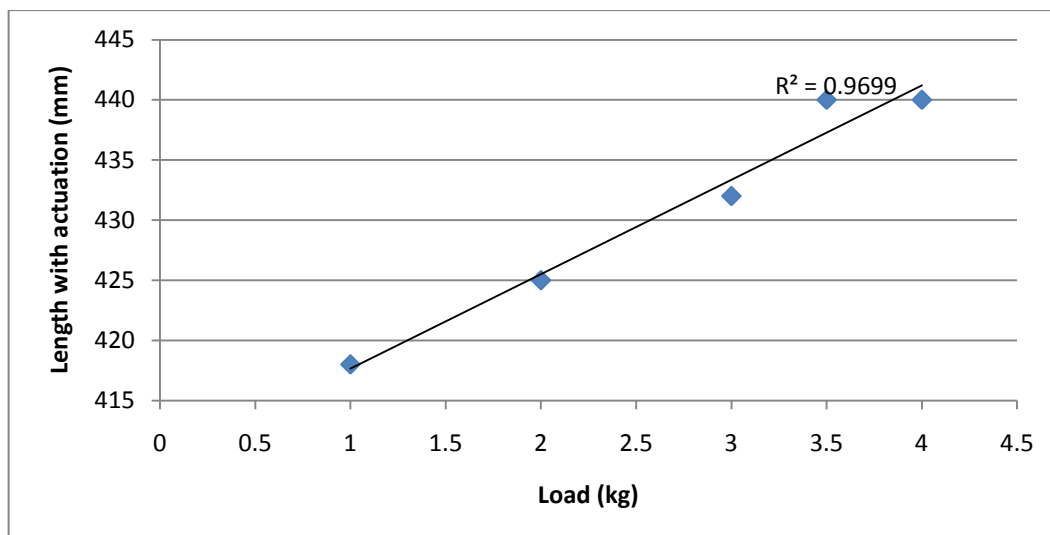


Figure 4.15: Graph of Length with actuation versus load (first data)

Table 4.2: Muscle length with constant pressure (second data)

MPAM (Condoms)			
Load (kg)	Original Length (mm)	Length without actuation (mm)	Length with actuation (mm)
1.0	410	510	417
2.0	410	520	425
3.0	410	530	434
3.5	410	530	439
4.0	410	530	440
Constant Pressure = 20psi			

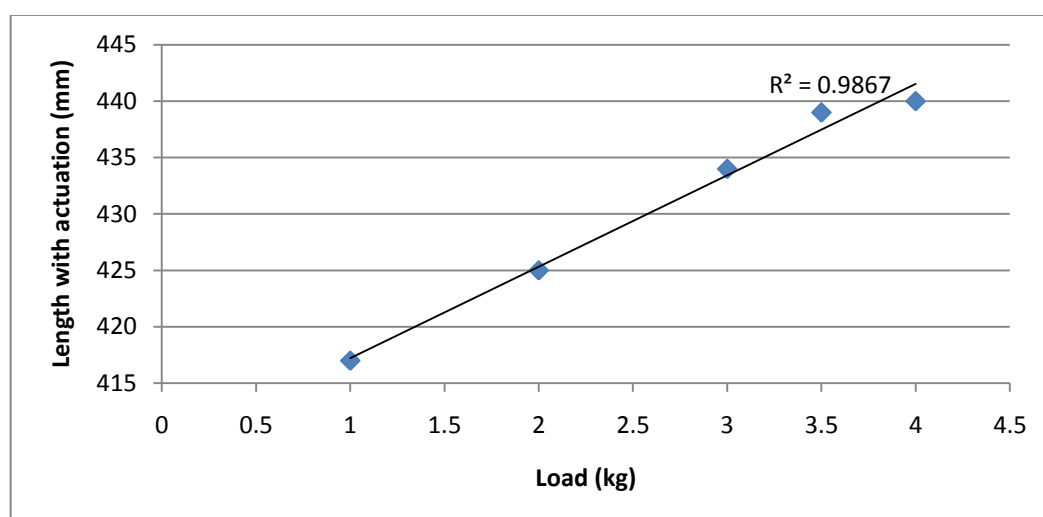
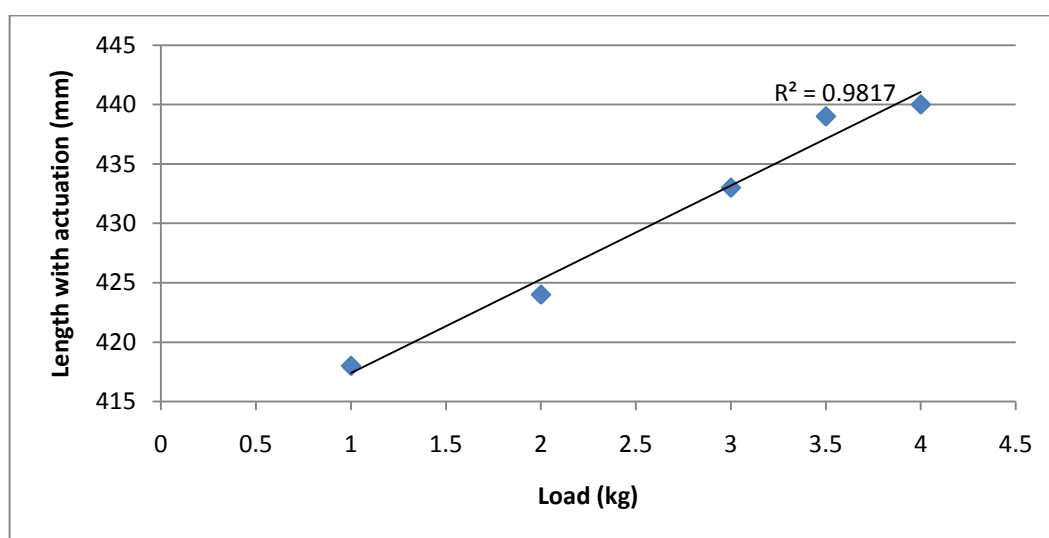


Figure 4.16: Graph of Length with actuation versus load (second data)

Table 4.3: Muscle length with constant pressure (third data)

MPAM (Condoms)			
Load (kg)	Original Length (mm)	Length without actuation (mm)	Length with actuation (mm)
1.0	410	510	418
2.0	410	520	424
3.0	410	530	433
3.5	410	530	439
4.0	410	530	440
Constant Pressure = 20psi			

**Figure 4.17: Graph of Length with actuation versus load for (third data)**

For the length without actuation, the values for loads of 1kg to 4kg are the same for the three data recorded. As shown in Figure 4.18, the elasticity of the MPAM is very high and stable. When the load is at 3kg, the length of MPAM is at 530mm and remains constant as the load increased to 3.5kg and 4kg. The reason 4kg is the maximum load setting in the experiment is due to the total weight to be exerted to the prototype is below 4kg.

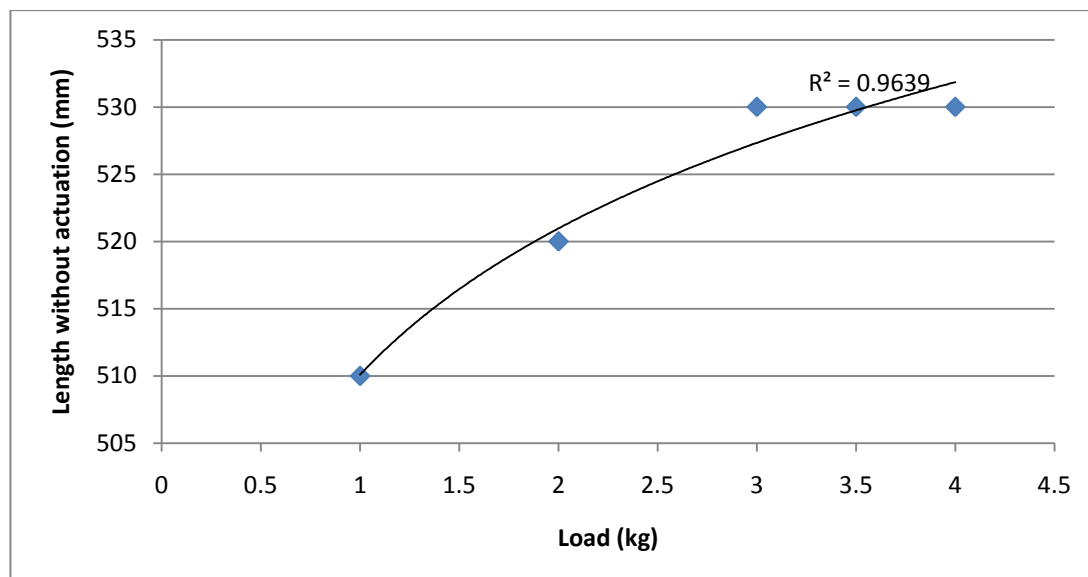


Figure 4.18: Graph of Length without actuation versus load

Unfortunately, the process of fabricating the PPAM is complicated and the desire size of Kevlar fiber material is difficult to obtain. Besides that, the readily PPAM is considered low demand in the market, thus, it will be expensive and difficult to purchase. PPAM requires precise technology to have an equal quantity and size of the pleated material. Unfortunately, lacking of this technology affects the construction of a high performance PPAM.

Instead of continue discovering the process of fabricating the PPAM, alternative option such as air muscle or MPAM has been decided. In term of performance, PPAM is more excellent but the MPAM is considered sufficient to provide extension-flexion of the knee joint. The benefit of using the MPAM is its simple construction by using readily available material throughout the market and the most important is its cost of fabricating is low (RM15++ per piece). Although the air muscle in industrial market is available to be purchased such as air muscle by FESTO but the price is unreasonable (RM1330.20) for this project as shown in appendix. The advantages of ordering from FESTO are its material characteristic, custom made size, and save time to fabricating the MPAM.



Figure 4.19: Festo Air Muscle (Schneider, R.T., 2002)

As a result, MPAM is chosen mainly due to its cost, simple and easy to fabricate. Before fabricates the MPAM, some of the materials are taking into consideration for the inner tube such as silicon/latex tube, balloon, latex glove and condom. Table 4.4 describes the characteristic of the inner tube materials. The inner tube is important to decide the contraction length of the artificial muscle.

Table 4.4: Characteristic of the inner tube materials

	Silicon/latex tube	Balloon	Latex glove	Condom
Pressure	>100psi	<10psi	20-80psi	20-80psi
Length	Depends	220mm	75mm	>220mm
Diameter	Depends	5mm	40mm	52.5mm

Silicon/latex tube and balloon are the first to be disqualified due to the pressure required does not fulfil the requirement. Although high pressure is efficient to sustain more weight and provide more forces but waste energy in term of providing unnecessary high force to a system required only intermediate force. For the balloon, low pressure unable to promote contraction of artificial muscle and even sustain the weight of prototype is a problem.

Latex glove and condom almost shared similar characteristic except the length characteristic. High contraction rate of artificial muscle is required to present high degree of flexion to the knee joint. The longer the artificial muscle, the higher

the contractions rate. Therefore, latex glove is eliminated. Figure 4.20 depicts the materials consideration for inner tube.



Figure 4.20: Materials consideration for inner tube (a) Silicon tube (b) Balloons (c) Latex gloves (d) Condom

4.1.4.1 Synchronise

Prior to the actual dimensioning of the actuation mechanism, a suitable actuator configuration is important to be selected. In order to obtain a bidirectional rotative actuator system, two single-acting actuators are required to configure in an antagonistic configuration. Figure 4.21 depicts the mechanical design of a bidirectional rotative actuator powered by MPAMs in an antagonistic configuration. Both the MPAMs are connected by a hinge joint with its axis in O . A_i and B_i are rotors to allow the freedom of rotation during muscle contraction and relaxation in order to have a smooth knee joint movement. X_i represents the length of the MPAM.

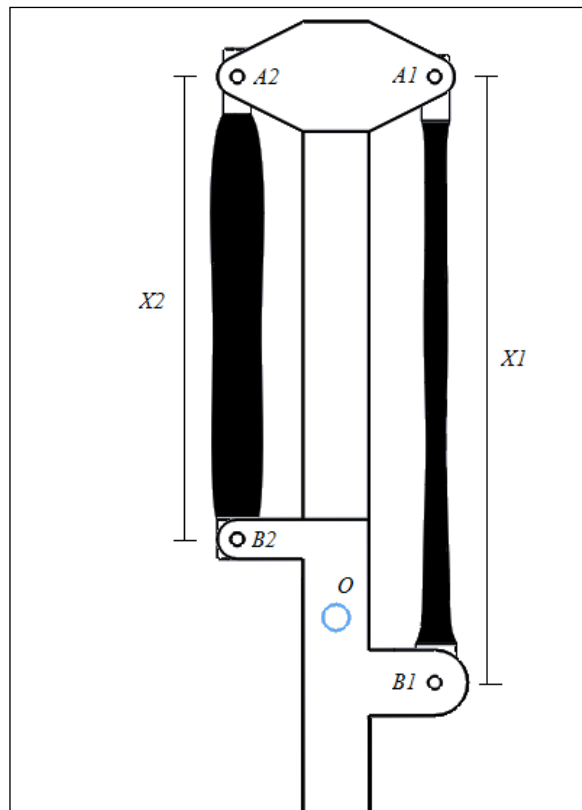


Figure 4.21: Antagonistic configuration of MPAM

As the results shown in Figure 4.15, Figure 4.16 and Figure 4.17, the R^2 reading for the three graphs are close to “1” and the correlation coefficients are 0.9848, 0.9933 and 0.9908 respectively. The closer the correlation coefficient to “1”, the better the result is for the MPAM performance. A perfect fit of correlation coefficients gives a coefficient of “1”. Figure 4.18 depicts the maximum elasticity of MPAM stops at 530mm from 3kg to 4kg. This mean that the MPAM has great sustainability to the weight of the load and one of the reasons is because of the braided nylon sleeve acts as a limiter to the inner tube of condom elasticity (expanding and releasing).

4.2 Circuit System

Circuit development in this stage of project is simply to generate a normal walking gait with the attachment of the frame to the subject. The sensor is to detect the hip joint initial movement. For example, when the hip tends to move, the muscle will

generate little contraction or signal and alter the hip position. EMG and accelerometer were the first sensors to be considered. EMG required contacts to the subject hence might affect the comfort of subject. Therefore, accelerometer was first to implement in this study.

4.2.1 Circuit Design

Two 12 volt batteries were used to power up the SK40C board, printed circuit board (PCB) and solenoid valves. One of the 12V battery was to supply to both the SK40C and PCB while the solenoid valve was supplied by the series connection of 12V batteries (total=24V). Figure 4.22 shows the simplify circuit of the main control system.

The PCB consists of DC power jack, two relay, two voltage regulator, two transistors, two diodes, two resistors and Molex. SK40C components such as led and buttons (sw0, sw1, reset) have been utilized to act as indicator and input respectively. The buttons at the SK40C functions as troubleshooting purpose. Figure 4.23 depicts the combination of PCB and SKC40C with others application to create a real time control system. Figure 4.24 shows the buttons, black and red, installed to the bag for the ease of the user to trigger the circuit. Black is to start and red is to stop.

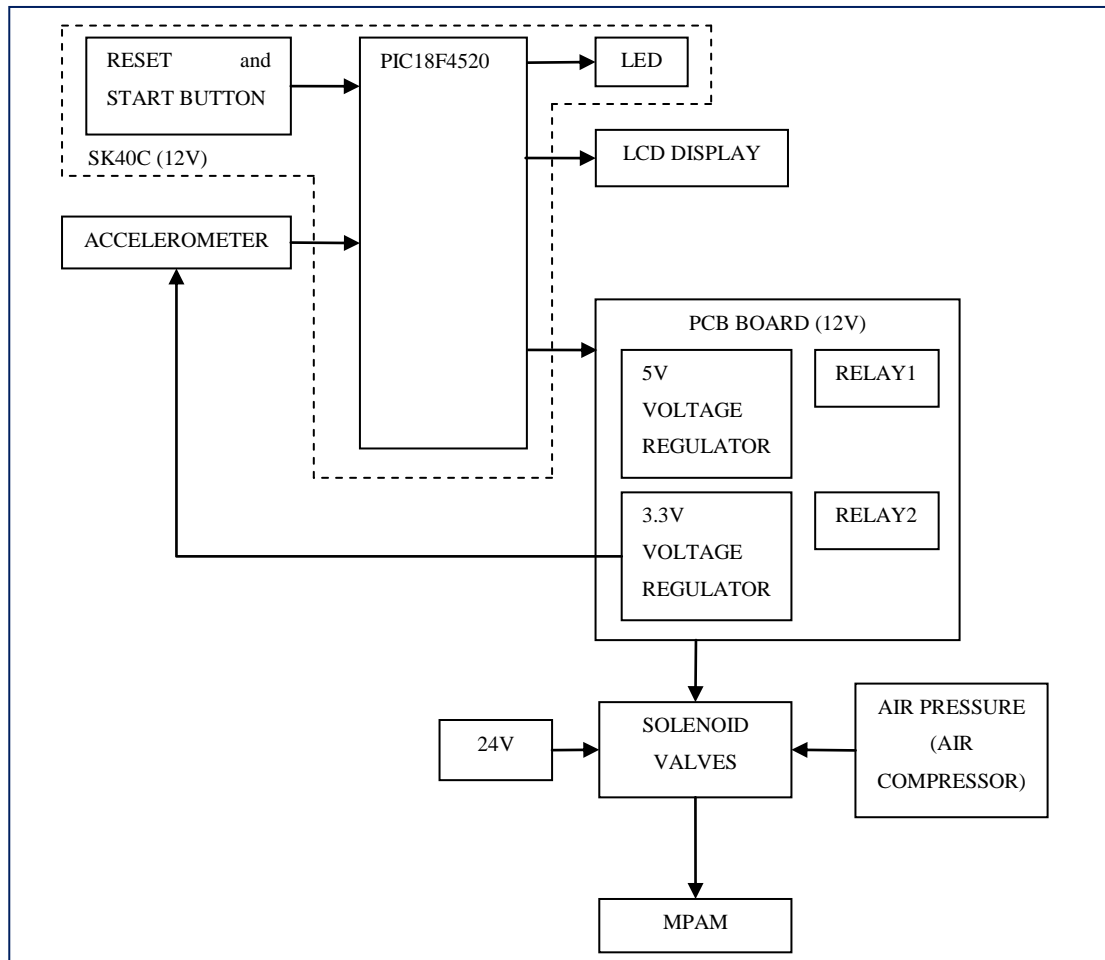


Figure 4.22: Circuit Connectivity

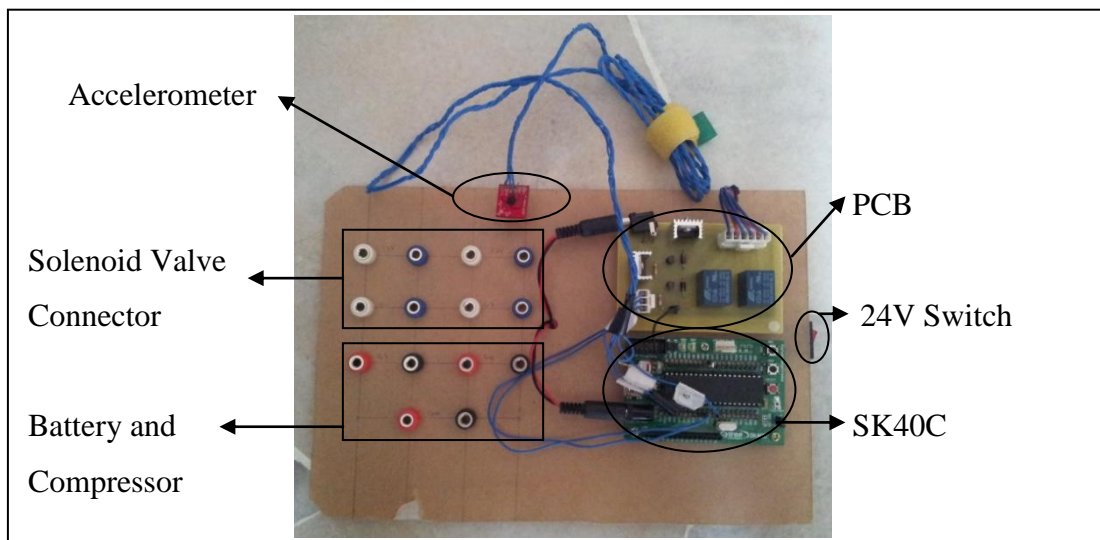


Figure 4.23: Real Time Control System Board



Figure 4.24: Black and Red Buttons Installed to the Bag

Eagle software was used to design the PCB of relays as indicated in figure 4.25 and to sketch the complete circuit consists of PIC18F4520, LCD display, accelerometer and PCB of relays as depicted in Figure 4.26. In order to reduce the complicated connection, buttons, 20MHz crystal and capacitors were not included. PIC microcontroller and the LCD display were constructed within a single board which is SK40C whereas the accelerometer was connected between the PCB and SK40C.

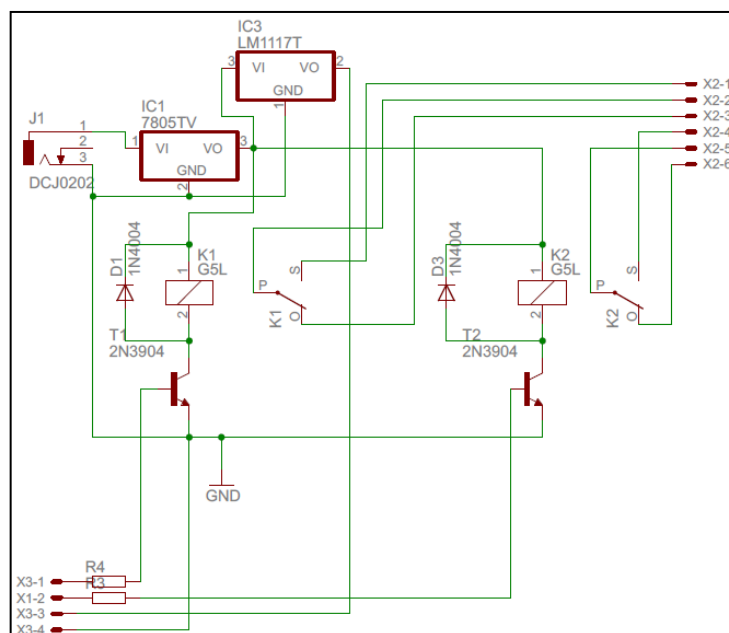


Figure 4.25: PCB Circuit Diagram

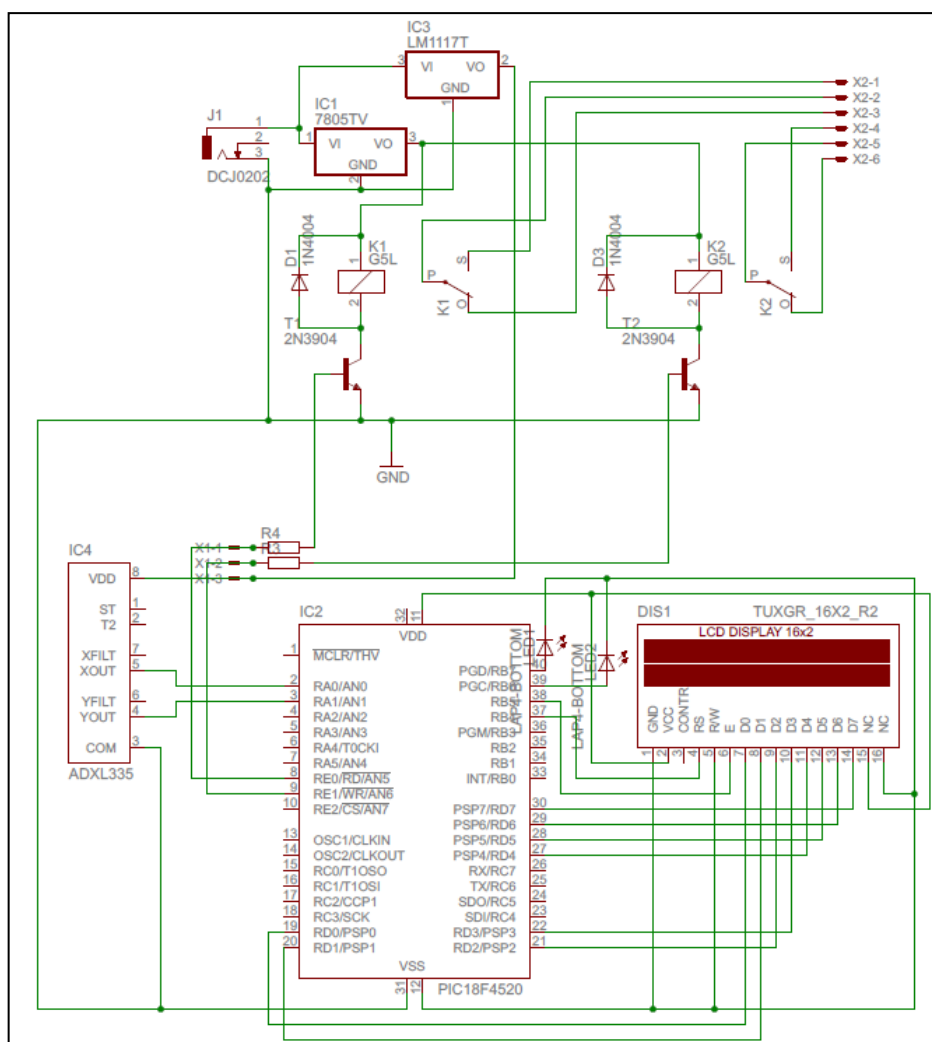


Figure 4.26: Complete Circuit Diagram

Before the system is ready to start, the frame has to be attached to the subject and comfortably connected to the subject in order to perform a stable normal walking gait. When the push start button is being triggered, the motherboard is ready to receive signal from accelerometer. The accelerometer as shown in Figure 4.27 will provide the x and y axis analogue signals whenever there is a walking motion being initiated by subject.

Accelerometer is attached to the top of the frame which is considered at the hip of the subject. Whenever there is a movement detected at the hip by the accelerometer, the reference point of x-y axes of the accelerometer will vary the voltage depending on the degree of rotation of the accelerometer. The signals from the accelerometer will be supplied to the input of PIC for processing according to the

variation of voltage. The x axis signal is sent to the pin RA0 and y axis signal is sent to the pin RA1.

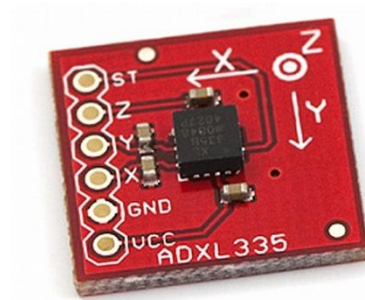


Figure 4.27: Accelerometer ADXL 335 (“ADXL 335 sensor”, 2011)

With the analogue signal from accelerometer, the PIC microcontroller would not be able to read and process it. Hence, ADC in the PIC microcontroller will convert the analogue signal to digital form to be further processed in order to provide the desired output. The ADC coding was modified and based on the PIC18F family library source (MPLAB[®] C18 C COMPILER LIBRARIES). The digital output source will act as the input to the relay as shown in the Figure 4.28.

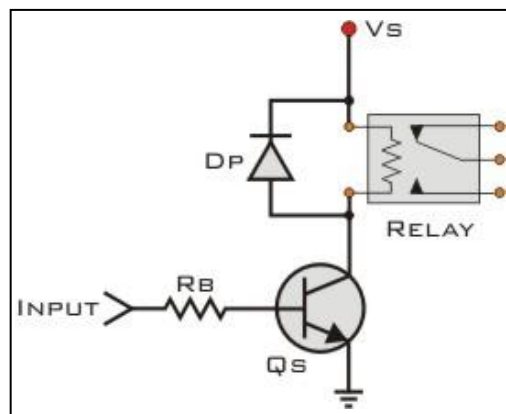


Figure 4.28: Relay Controlling Circuit Theory (Lazaridis, G., 2009)

The output of PIC is required to operate a relay with 100 Ohm coil. The supply voltage is 5V and the maximum current input is 5mA. By using the formula below, calculation of the R_B required.

$$I_L = \frac{V_S}{R_L} \quad (4.2)$$

$$h_{FE} > 5 \times \frac{I_L}{I_{INPUT}} \quad (4.3)$$

$$R_B = 0.2 \times R_L \times h_{FE} \quad (4.4)$$

The I_L and h_{FE} are calculated as below,

$$I_L = \frac{V_S}{R_L} = \frac{5}{100} = 50mA$$

$$h_{FE} > 5 \times \frac{I_L}{I_{INPUT}}$$

$$h_{FE} > 5 \times \frac{50}{5} > 50$$

$$R_B = 0.2 \times 100 \times 50 = 1000 \text{ Ohm}$$

Therefore, the resistor value of R_B is 1k Ohm by using transistor 2N3904 and diode 1N4001.

The relay will act as the switch of 24V supply to the two solenoid valves where one is connected to normal closed of relay and another one is connected to normal open. Hence, the MPAMs will operate in antagonistic that controlled by the relay switch in either normal close or normal open. Figure 4.29 shows the simplify version of the process.

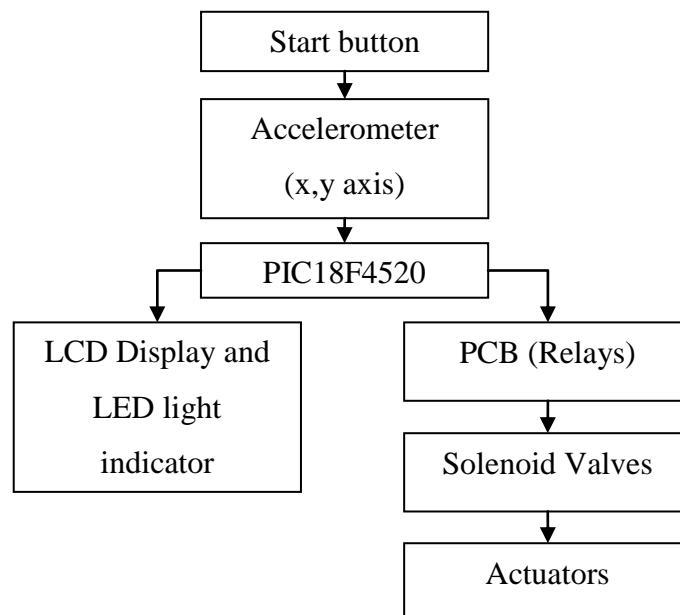


Figure 4.29: Circuit Running Process

4.3 Control System Coding

The MPLAB software coding is written in C programming language instead of the assembly programming language. As discussed in section 4.3, the coding for walking gait is required. Hence, antagonistic of MPAMs is required to generate flexion-extension of the knee joint by programming the output to the solenoid valve with perfect timing.

Figure 4.30 depicts the coding flow chart. Figures 4.31 to 4.32 are PIC18F4520 C programming language by using MPLAB software. PICKIT 2 was utilized in order to program the coding into the PIC. The PIC has built-in ADC technology thus the accelerometer analogue input was converted to digital form by the PIC without an external ADC. In order to trigger the ADC, some configurations have to be included and the coding applied to this system is based on the library of PIC18F as shown in Figure 4.34. The description of the coding is included after each coding.

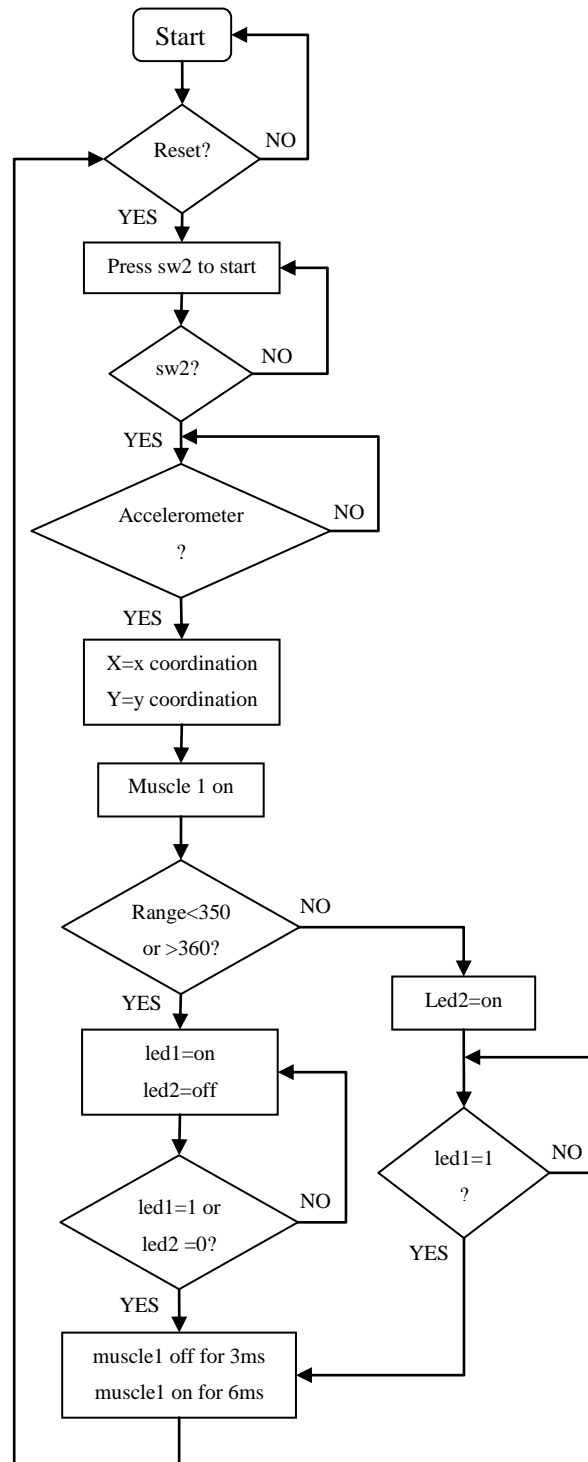


Figure 4.30: Coding Flow Chart

```

#include <p18f4520.h>
#include <adc.h>
#include "xlcd.h"
#include "delays.h"
#include <timers.h>           // Timer library functions
#include <math.h>             // C Library for math operations
#include <stdlib.h>           // C Library
#include <stdio.h>            // C Library
#include <string.h>           // C Library

#pragma config OSC = HS           // HS oscillator,
#pragma config FCMEN = OFF       // Fail-Safe Clock Monitor disabled
#pragma config IESO = OFF        // Oscillator Switchover mode disabled
#pragma config PWRT = OFF        // PWRT disabled
#pragma config BOREN = OFF       // Brown-out Reset disabled in hardware and software
#pragma config WDT = OFF         // WDT disabled (control is placed on the SWDTEN bit)
#pragma config MCLRE = ON        // MCLR pin enabled; RE3 input pin disabled
#pragma config PBAEN = OFF       // PORTB<4:0> pins are configured as digital I/O on Reset
#pragma config CCP2MX = PORTBE   // CCP2 input/output is multiplexed with RC1
#pragma config LVP = OFF         // Single-Supply ICSP disabled
#pragma config XINST = OFF       // Extended Instruction Set

#define led1    LATBbits.LATB6    //led1 as output port RB6
#define led2    LATBbits.LATB7    //led2 as output port RB7
#define muscle1 LATCbits.LATC0    // muscle1 as output port RC0
#define sw1     PORTBbits.RB0     //sw1 as input port RB0
#define sw2     PORTBbits.RB1     //sw2 as input port RB1
#define x_axis  PORTAbits.RA0     //x_axis as input port RA0
#define y_axis  PORTAbits.RA1     //y_axis as input port RA1

```

Figure 4.31: PIC Setting

```

//-----
//      DECLARE FUNCTION
//-----
void Delay_1msX (unsigned int milliseconds);
void Delay_100msX (unsigned int msec);
int      adc_readch0();
int      adc_readch1();

//-----
// VARIABLE
//-----
unsigned int i, j, t;
unsigned char dataString1[5];
unsigned char dataString2[5];
int readch0;
int readch1;
int e_ch0;
int e_ch1;
unsigned int
        bin = 0,           //temp buffer variable for ADC value for BCD conversion process
        binADC0 = 0,      //buffer variable for showing direct ADC value on LCD
        binADC1 = 0,

//BCD coversion variables
        ch0d0 = 0,
        ch0d1 = 0,
        ch0d2 = 0,
        ch1d0 = 0,
        ch1d1 = 0,
        ch1d2 = 0;

```

Figure 4.32: Function and Variable

```

//set I/O input output
TRISB = 0b00000011;      //Configure PORTB I/O direction
TRISD = 0b00000000;      //Configure PORTD I/O direction
TRISC = 0b11111100;      //Configure PORTB I/O direction
TRISE = 0b00000000;      //Configure PORTB I/O direction

PORTB = 0;                //Clearing port
PORTD = 0;                //Clearing port
PORTC = 0;                //Clearing port
PORTE = 0;                //Clearing port

TRISA = 0b11111111;      //Configure PORTD I/O direction

// See ADC configuration on PIC18F4520's datasheet
OpenADC( ADC_FOSC_32
        & ADC_RIGHT_JUST
        & ADC_16_TAD,ADC_CH0
        & ADC_INT_OFF
        & ADC_VREFPLUS_VDD
        & ADC_VREFMINUS_VSS, 13 );

```

Figure 4.33: Analogue to Digital Converter (ADC) setting

Furthermore, the LCD configuration shown in Figure 4.34 has to include two external files, `xlcd.c` and `xlcd.h`, which are the general configuration setting of LCD display. The sample codes are provided in the appendix.

```

//-----
// Configure External LCD
//-----

OpenXLCD( EIGHT_BIT & LINES_5X7 );
ClearXLCD();                //Clear display
SetCurXLCD(0);             //set cursor at line 1
putsXLCD("Press sw2");      //Display at line 1
SetCurXLCD(20);           //set cursor at line 2
putsXLCD("to start");       //Display at line 2

```

Figure 4.34: Configure LCD display

```

if(!sw2)                                     //sw2 to run
{
    while(!sw2) led2=1;                       //Debounce sw2, Turn on led2
    led2=0;                                   //Turn off led2
    Delay_100msX(1);                          //Delay 100ms
    ClearXLCD();                              //Clear LCD
    SetCurXLCD(0);                            //Set cursor at line 1
    putsXLCD("X=");                            //”X=” at line 1
    SetCurXLCD(20);                           //Set cursor at line 2
    putsXLCD("Y=");                            //”Y=” at line 2

    while(1)
    {
        adc_readch0();                         //Function
        adc_readch1();                         //Function
        e_ch0 = readch0;                       //assign value
        resultch0 = e_ch0;                     //assign value
        e_ch1 = readch1;                       //assign value
        resultch1 = e_ch1;                     //assign value
        binADC0 = resultch0;                   //assigning ADC value to buffer variable

        //convert ADC value to BCD
        ch0d2 = binADC0 % 10;
        ch0d1 = (binADC0 / 10) % 10;
        ch0d0 = (binADC0 / 100) % 10;

        //convert BCD digit numbers to ASCII text characters for LCD
        ch0d0 += '0';
        ch0d1 += '0';
        ch0d2 += '0';

        //SendLCD(0x80,0); //activate LCD line 1
        SetCurXLCD(3);

        //print the ADC value on LCD
        putcXLCD(ch0d0);
        putcXLCD(ch0d1);
        putcXLCD(ch0d2);
    }
}

```

Figure 4.35: Display Accelerometer ADC value

The delay times were set as 1ms and 100ms. There is only one delay in Figure 4.37 but in the complete coding, there are two delays for the ease of programming. For example, if 100ms is required, the following coding is used.

```
Delay_100msX(1);
```

If 200ms is required, the following coding is used by just adding the value in the “()”.

```
Delay_100msX(2);
```

```

//-----
// OUTPUT TO RELAY
//-----
muscle1 = 1;      //initial state is set for extension of knee
resultled1 = resultch1;
    //Accelerometer position range when hip joint moves forward
    if (resultled1 < 350 | resultled1 > 360)
    {
        led1 = 1;      //led1 on within the range
        led2 = 0;      //led2 off within the range
        if (led1==1 | led2==0)
        {
            muscle1 = 0;      //flexion of knee
            Delay_100msX(3); //flexion for 300ms
            muscle1 = 1;      // extension of knee
            Delay_100msX(6); // extension for 600ms
        }//end if
    }//end if
else
{
    led2 = 1;      //led2 on when out of the range while led1 still on
    if(led1==1)
    {
        muscle1 = 0;      //flexion of knee
        Delay_100msX(3); //flexion for 300ms
        muscle1 = 1;      // extension of knee
        Delay_100msX(6); // extension for 600ms
    }//end if
} //end else
} //end while

else if(!sw1)      //sw1 to stop
{
    while(!sw2) led2=1;      //Debounce sw2, Turn on led2
    led2=0;      //Turn off led2
    muscle1 = 1;      //when stop button trigger, set for extension of knee

} //end else if
} //end if
} //end of while

CloseADC();      // Disable A/D Converter

} //End of main

```

Figure 4.36: Flexion-Extension coding

```

//-----
// FUNCTION
//-----
int adc_readch0()
{
    SetChanADC(ADC_CH0);    // Set channel for adc ADC_CH0
    // Delay10KTCYx = Delay in multiples of 10,000 instruction cycles.
    //unsigned char (8 bit value) Delay for 500/4 milliseconds with 40 MHz clock
    //Using a 40 MHz external oscillator, it means 40 MHz / 4 --> 10^-7 = cycle time.
    //Then in the PIC18F4520's datasheet page 129
    //delay function duration (in second) = 10 * cycle time * value between the brackets
    ConvertADC();           // Start Conversion
    while( BusyADC() );     // Wait for completion
    readch0 = ReadADC();    // Read result
    return(readch0);       // This function returns "adc_value" which is the adc result
}
//-----
// DELAY
//-----
//delay 100ms
void Delay_100msX (unsigned int msec)
{
    t=0;
    while(t<msec)
    {
        Delay10KTCYx(119);
        Delay1KTCYx(9);
        Delay10TCYx(96);
        t++;
    }
}
//End of Delay_100msX

```

Figure 4.37: Functions and Delays Examples

4.4 Pneumatics System

The solenoid valve was controlled by the relay switch at the PCB where the signal was from the PIC to the input of relay. The relay switch was the input source and act as a switch to turn on or off the supply of 24V to the solenoid valve. The solenoid valve required voltage of 24V in order to energize and alter the form of air pressure supply. Figure 4.38 shows the connection of knee pneumatic system.

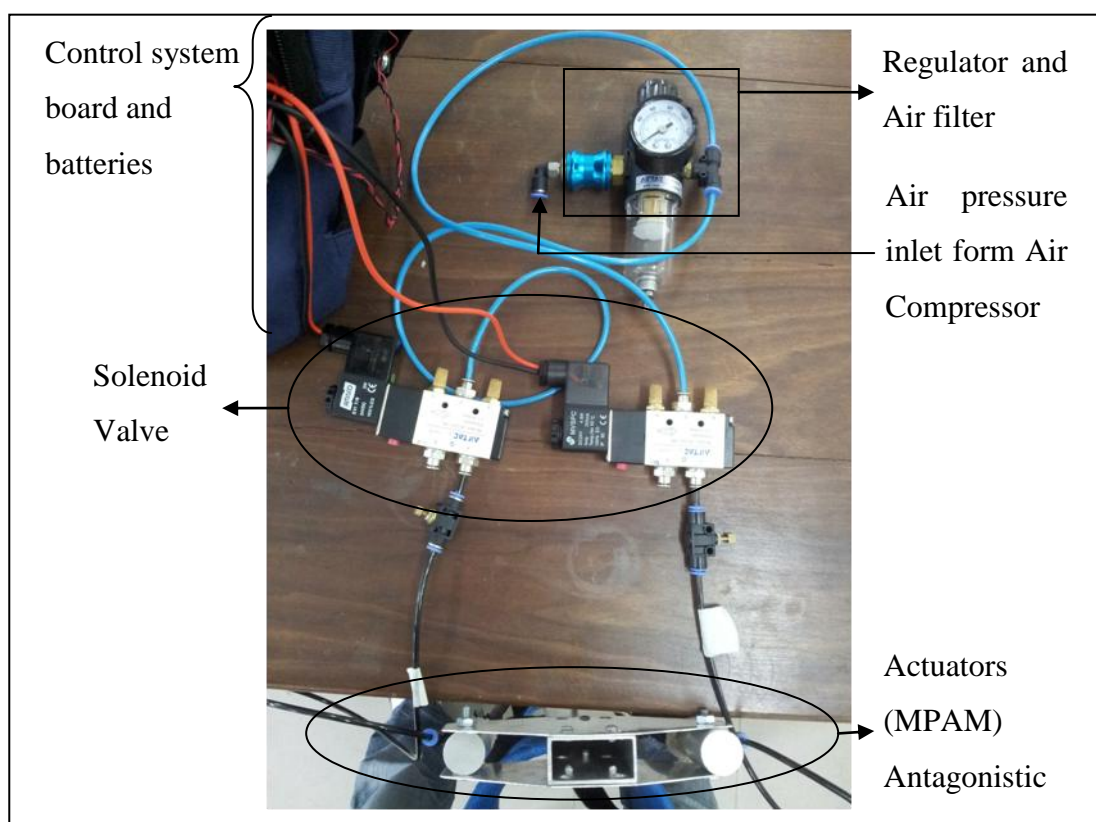


Figure 4.38: Pneumatics connection

Figure 4.39 shows the state of each solenoid valve controlling each pneumatic artificial muscle (PAM) in my project. When the solenoid valve was energized, the single acting PAM was contracted and flexion of knee joint occurs. As the relay switch was in normal open, there was no voltage being supplied to energize the solenoid valve.

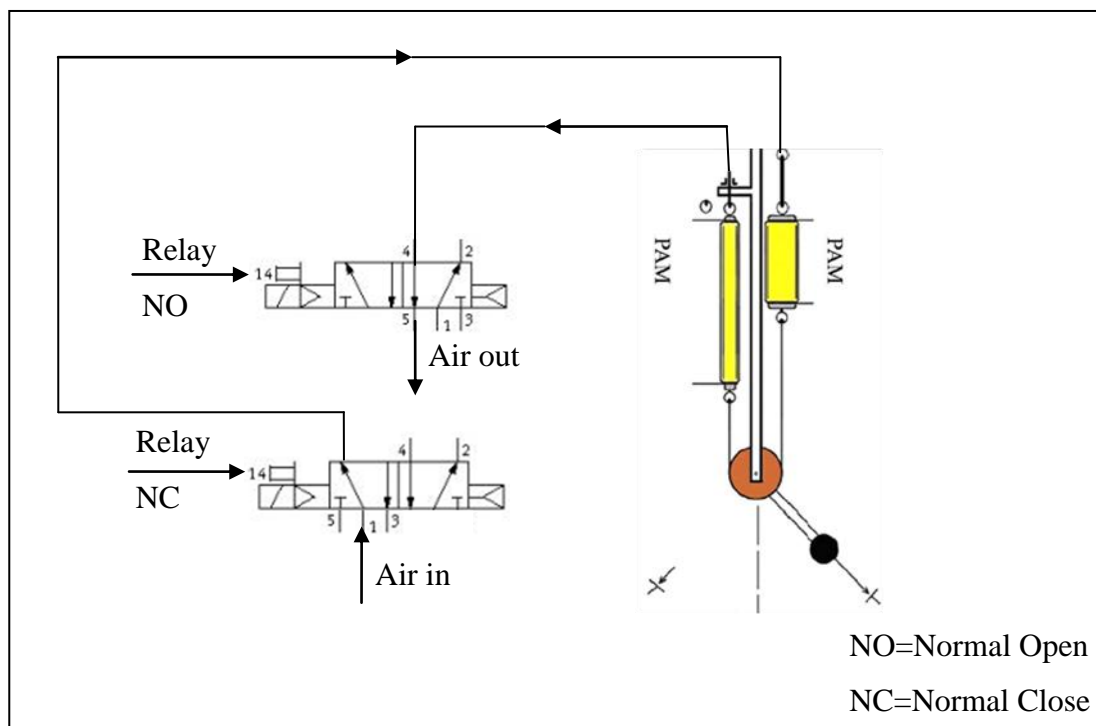


Figure 4.39: Pneumatic artificial muscle (PAM) controlled by solenoid valve

When the solenoid operator is energized as shown in Figure 4.40, the solenoid coil creates a magnetic field surrounding the plunger assembly and plunger. The plunger is lifted off by the magnetic field and thus supply air provides an internal pilot pressure that is directed to the pilot piston that shifts the spool and compresses the main spring. This shifting directs the flow of supply air from inlet P to cylinder port A while cylinder port B is connected to exhaust port R2. (“Solenoid valve”)

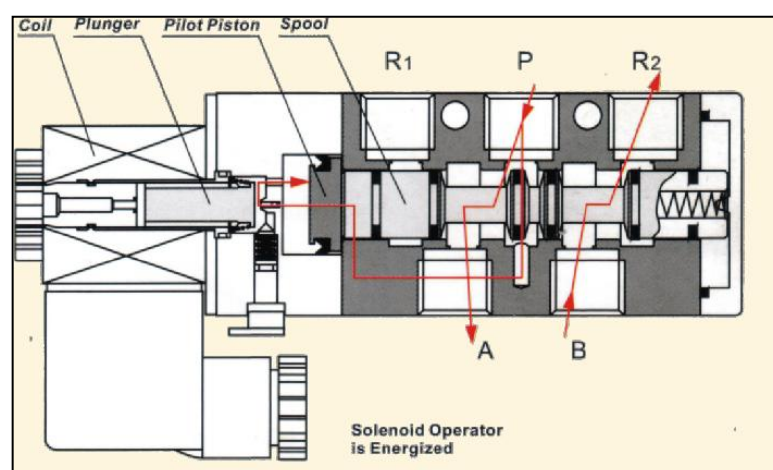


Figure 4.40: Energized Solenoid Valve (“Solenoid Valve”, 2012)

When the solenoid coil is de-energized as shown in Figure 4.41, a spring on the plunger will return the plunger to its seat, blocking internal pilot air and open a vent port. This vent port will allow the air on the spool's pilot piston to escape. And the main spring will return the spool to its normal position, in this position, the spool directs flow of supply air from inlet port P to cylinder port B while cylinder port A is connected to exhaust port R1. ("Solenoid Valve", 2012)

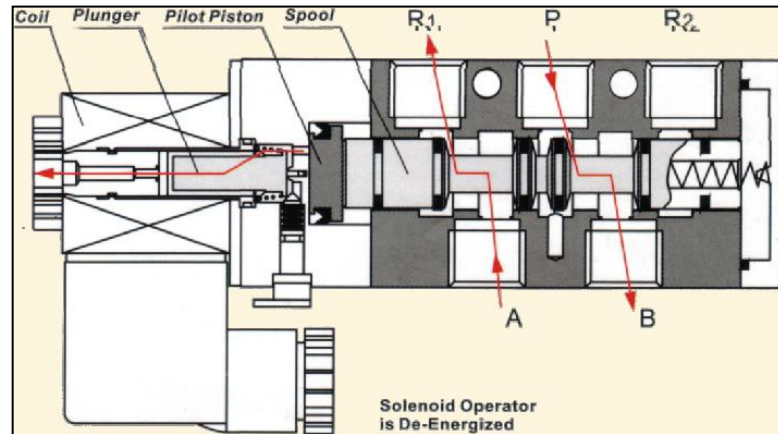


Figure 4.41: De-energized Solenoid Valve ("Solenoid Valve", 2012)

The main reason of 5/2 way solenoid valve is used rather than 3/2 way solenoid valve is because the market availability. According to the dealer, 3/2 way solenoid valve has the same cost as the 5/2 way solenoid and unfortunately, 5/2 way solenoid valve can be applied as 3/2 way solenoid valve while 3/2 way solenoid valve unable to function as 5/2 way solenoid valve. Although 3/2 way solenoid valve is enough for the project study but due to availability and cost efficiency, 5/2 way solenoid valve is selected. Figure 4.42 depicts the single acting MPAM that is connected to the 5/2 way solenoid valve for the source of air pressure.



Figure 4.42: Single Acting Actuator (MPAM)

McKibben Pneumatic artificial muscle (MPAM) acts as a single acting actuator. Single acting actuator in this case uses air power for movement in one direction and spring for its return but MPAM does not required spring for its return. MPAM will only expand when air pressure is supplied while MPAM release the air for its return. Figure 4.43 shows the single acting cylinder.



Figure 4.43: Single Acting Actuator

4.5 Pneumatics Based Power-Assisted Knee-Ankle-Foot Orthosis

4.5.1 Overall Design

The combination of knee, ankle and foot orthosis powered by McKibben Pneumatics Artificial Muscle is shown in Figure 4.44. By combining the knee and ankle pneumatics orthosis, a complete left leg of the prototype is tested with the subject of 175cm in height and weight of 55kg. Besides the prototype is attached to the subject, the control system board and accessories are included in a bag and to be carried with the subject. The accessories are two batteries, four solenoid valves, an air regulator and tubing connecting the pneumatic systems.

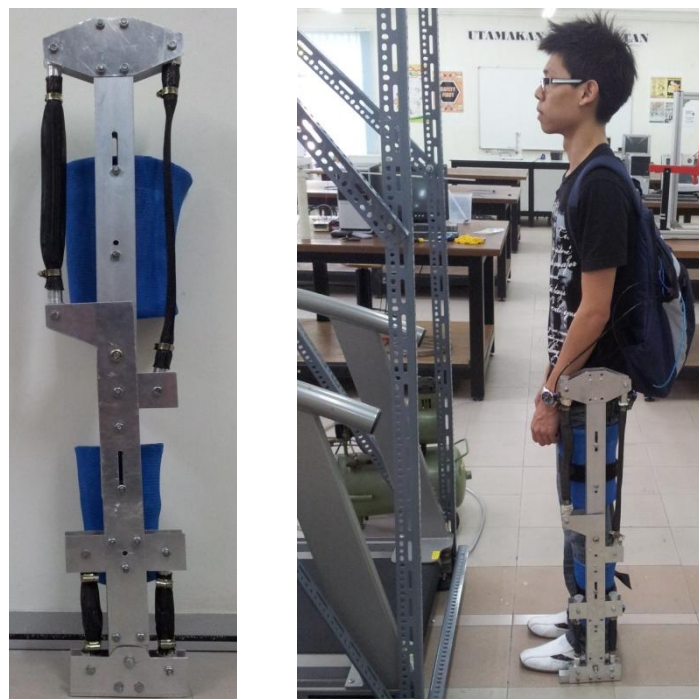


Figure 4.44: Pneumatics Based Power-Assisted Knee-Ankle-Foot Orthosis

After the entire system is attached to the subject, the total weight is 62kg without including the portable air compressor. The frame as shown in left side of the Figure 4.44 is only 3kg and most of the weight are due to the weight of batteries and solenoid valves. Portable air compressor is not included because the pressure provided is not sufficient and budget problem affects the purchasing of efficient air compressor.

4.5.2 Overall Circuit and Pneumatic System

Figure 4.45 depicts the complete pneumatics system connection of pneumatic based power-assisted knee-ankle-foot orthosis. The connection of solenoid valves to the control system board is shown in Figure 4.46. The 24V solenoid valve will be energized when a switch is turn on to prevent overheated of the solenoid valve and for the safety purpose as large voltage is used. Figure 4.47 depicts the complete circuitry of pneumatic and electric systems. The pneumatic and electric systems will be inserted to the bag.

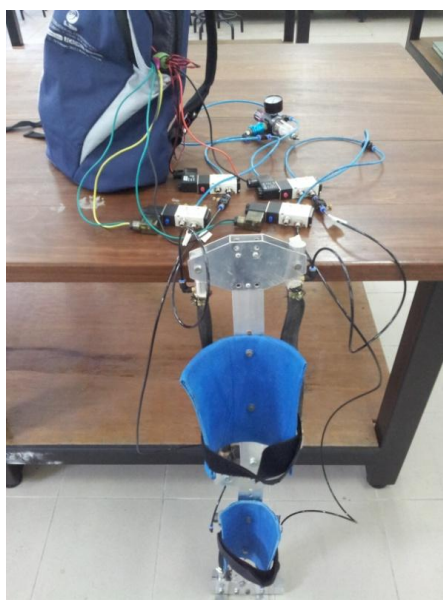


Figure 4.45: Pneumatics Systems including ankle and foot orthosis

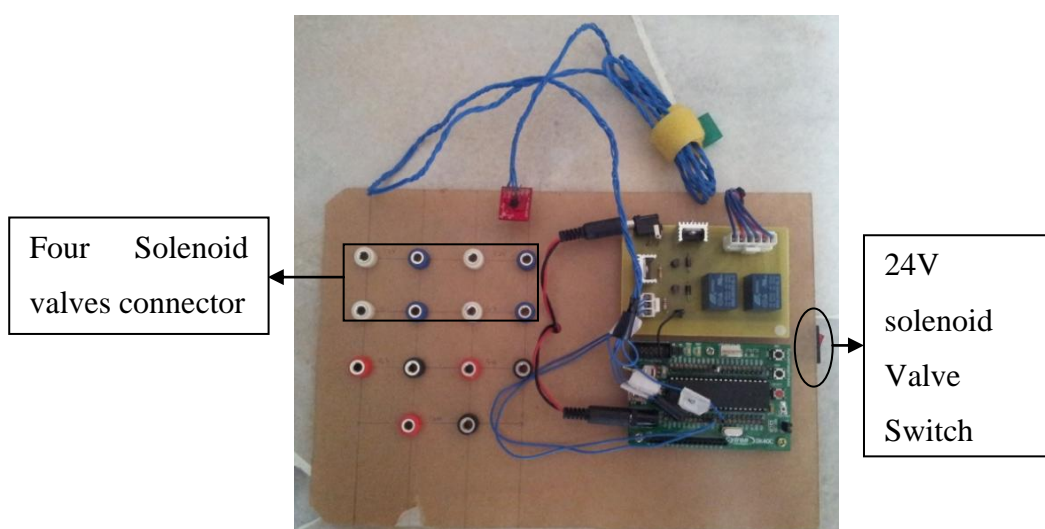


Figure 4.46: Control System Board

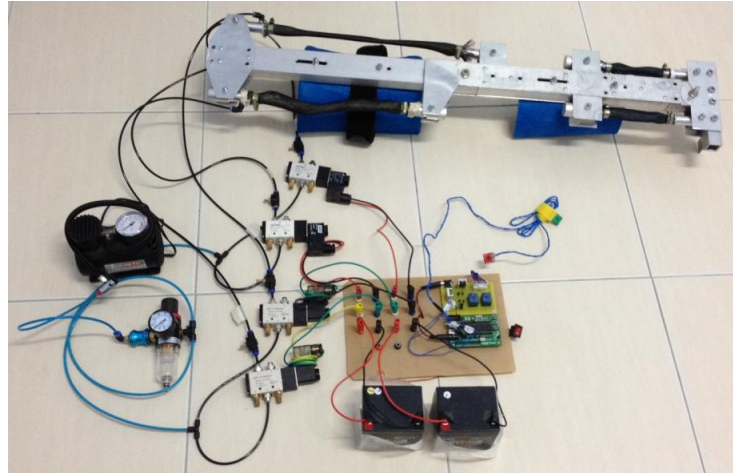


Figure 4.47: Control System Board

4.5.3 Walking Gait Cycle

A walking gait cycle of the combination of knee, ankle and foot orthosis powered by McKibben Pneumatics Artificial Muscle was accomplished based on Figure 2.25. The pneumatics based power-assisted knee-ankle-foot orthosis of walking gait study was carried out on a biomechanics treadmill as shown in Figure 4.48. As a result, vertical ground reaction forces (VGRF) of left and right legs were obtained. Figure 4.49 depicts the walking gait with the complete prototype of left leg.

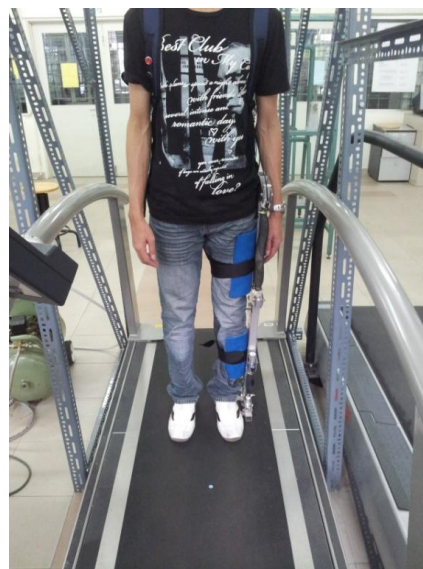


Figure 4.48: Walking Gait Testing On Biomechanics treadmill



Figure 4.49: Pneumatics Based Power-Assisted Knee-Ankle-Foot Orthosis during Gait Cycle

There are two types of results obtained for determining the normal walking gait cycle which are walking without the MPAM actuation and walking with the MPAM actuation. Both the results of walking gait cycle are performed with the prototype being attached to the subject (175cm height and 55kg weight). Figure 4.50 and Figure 4.51 show the left leg and right leg without MPAM actuation respectively. Figures 4.52 to 4.55 indicate the walking with actuations of left leg and right leg.

The walking VGRF data exhibits two noticeable peaks. According to Tongen, A., & Wunderlich, R. E., the first peak corresponds to the period just after the heel touches the force plate and the center of gravity is travelling down toward the ground, resulting in an increased reaction force from the ground in the vertical direction.

According to Tongen, A., & Wunderlich, R. E., the second peak corresponds to the toe pushing of the force plate, applying a force into the ground which is matched by an increase in the ground reaction force. The dip in the middle of these

peaks occurs when the center of gravity is rising away from the ground, thus decreasing the force of the body on the ground and therefore decreasing the reaction force the ground is exerting on the body in the vertical direction.

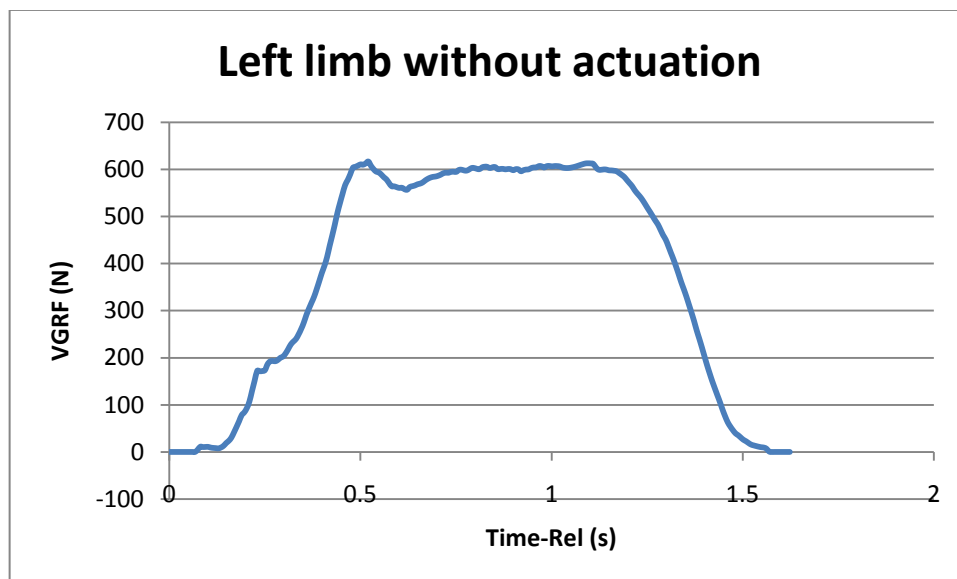


Figure 4.50: Left Limb without Actuation

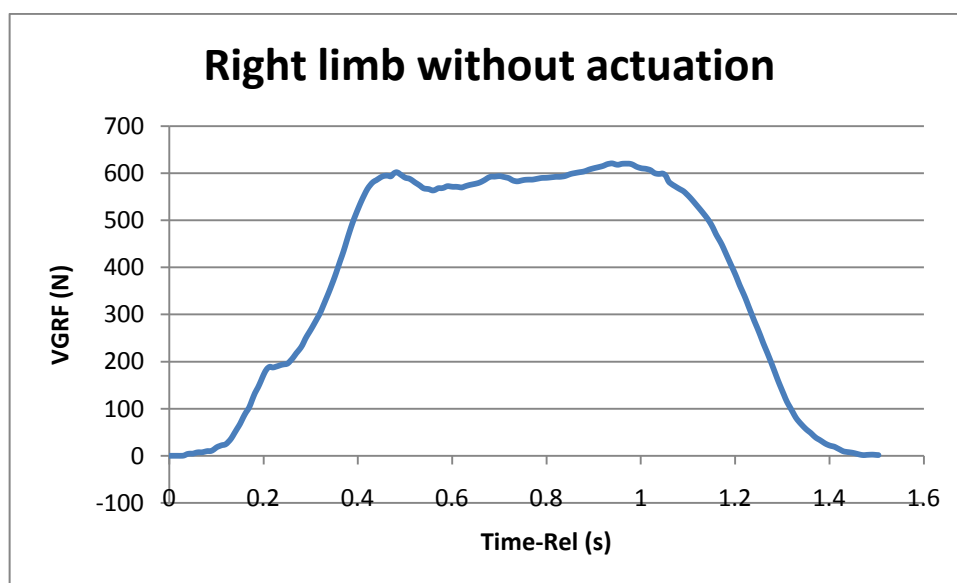


Figure 4.51: Right Limb without Actuation

Without the actuation of MPAM, the walking gait cycle is stable for both the left and right leg except the left leg has slightly higher vertical ground reaction force due to the additional weight of prototype at the left leg.

When there is MPAM actuation, the first and second data obtained for left leg have almost the same pattern of graph. By comparing them to Figure 4.50, there is a difference between the times of 0s to 0.5s. This might due to the force plate unable to detect the foot design of the frame before the heel fully touches the force plate. At the time, the heel is fully touches the force plate, first peak is generated and the graph shows a sudden increased of VGRF at 0.5s.

Besides that, the data shows higher VGRF during walking gait cycle at the left leg which about 630N of VGRF. This shows that the weight of the frame at the left leg will affects the VGRF of walking gait.

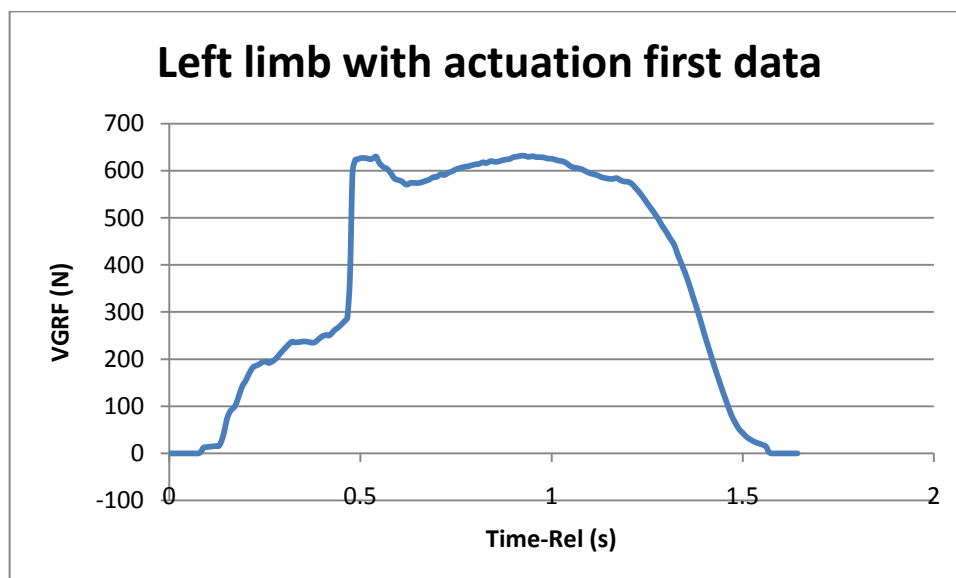


Figure 4.52: Left Limb with Actuation (first data)

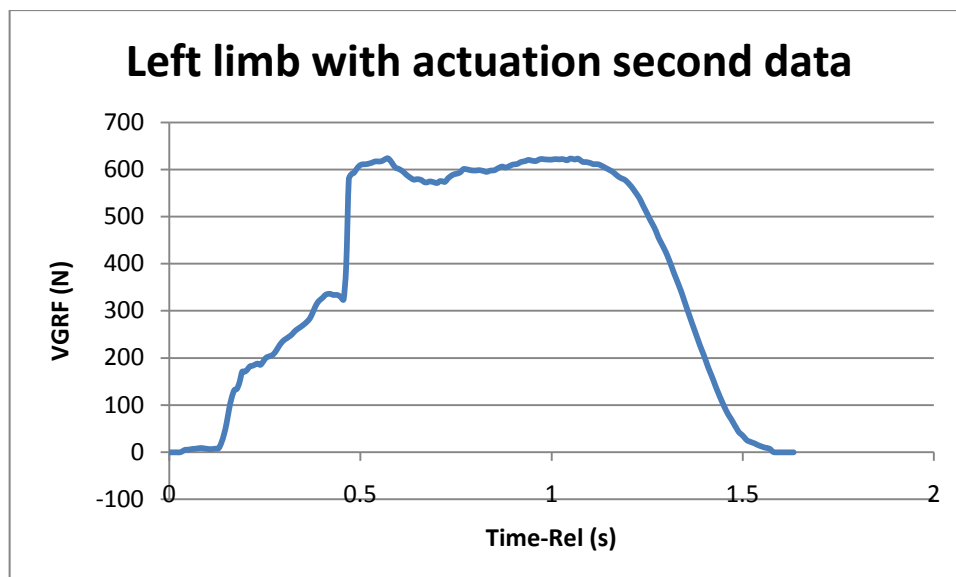


Figure 4.53: Left Limb with Actuation (second data)

Figure 4.54 and Figure 4.55 depict the right leg with actuation. The results obtained show that the two graphs do not share the similarity of walking gait cycle. During the walking gait testing on the biomechanics treadmill, there is a time where the subject was balancing his body to prevent falling. Hence, this might be the reason of abnormal right leg walking gait is obtained.

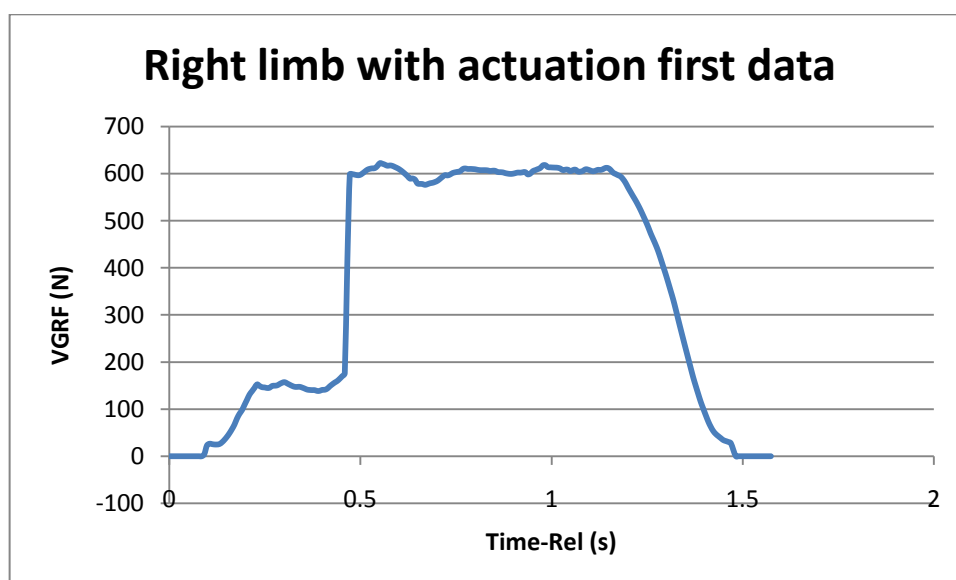


Figure 4.54: Right Limb with Actuation (first data)

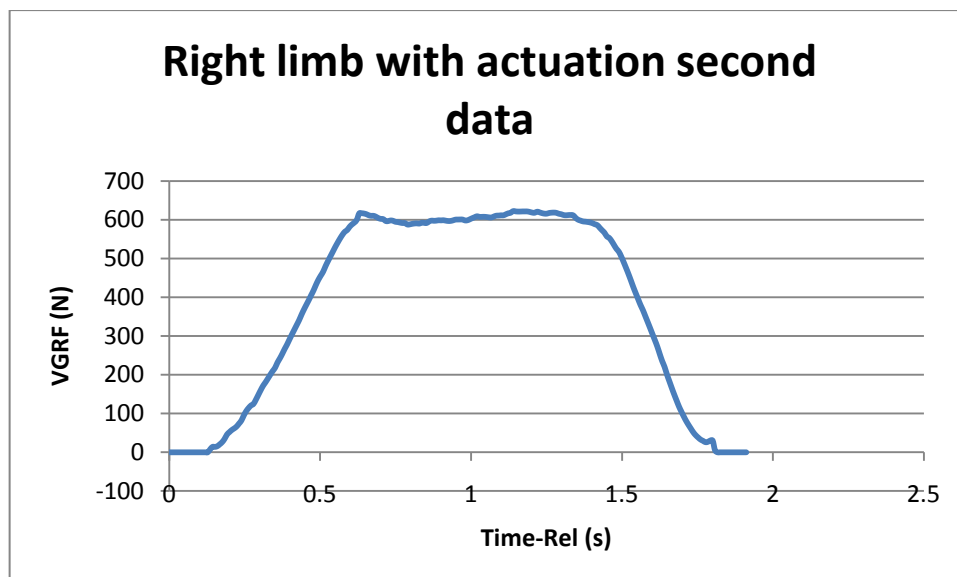


Figure 4.55: Right Limb with Actuation (second data)

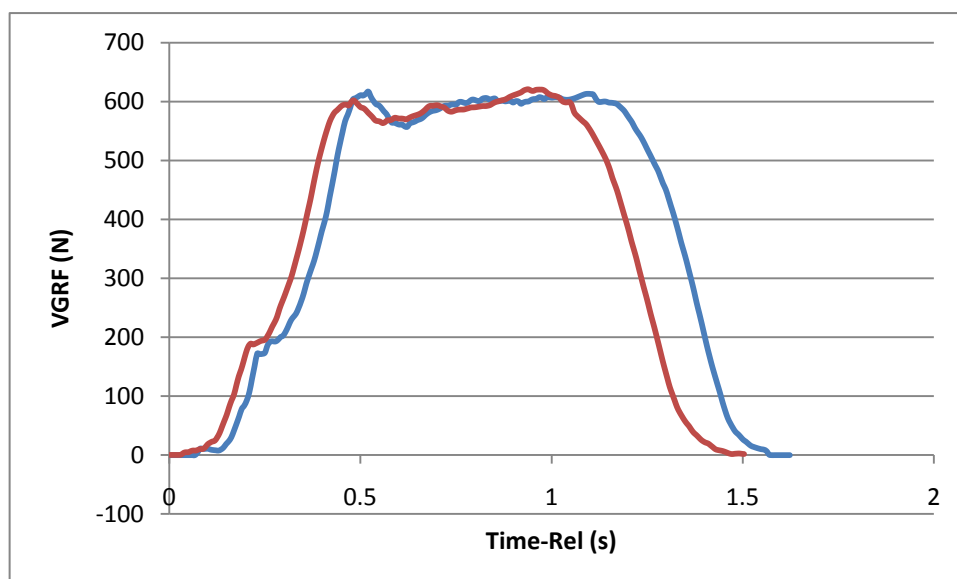


Figure 4.56: Without Actuation

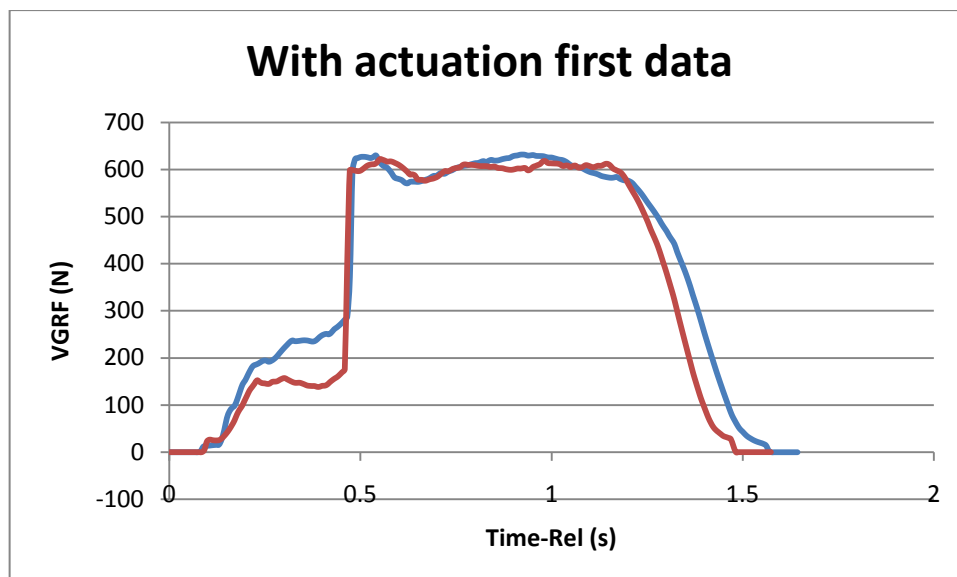


Figure 4.57: With Actuation (first data)

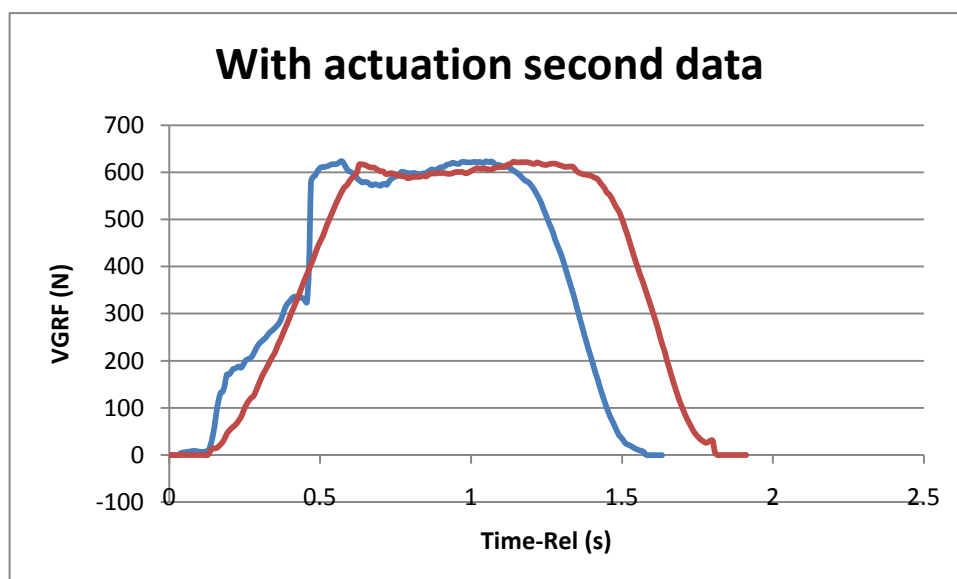


Figure 4.58: With Actuation (second data)

CHAPTER 5

CONCLUSION AND RECOMMENDATIONS

5.1 Conclusion

A wearable prototype of pneumatic based power-assisted knee orthosis using McKibben pneumatic artificial muscle is successfully designed, fabricated and tested. The MPAM is constructed and tested in several conditions. On the other hand, the pneumatic based power-assisted knee orthosis can be easily fitted to the user comfortably and has met the main design requirement.

Furthermore, the frame and the fittings of the power assisted knee orthosis are modular to fit the height of the user within the range of 1.65m to 1.75m. Finally, a normal walking gait can be performed by the user while wearing the prototype with the actuation from MPAMs. Biomechanics of the lower extremities and types of artificial muscle have been studied before the entire prototype is built. Sensors for motion detection and control system have been investigated to accomplish the system in performing walking gait cycle.

The estimation cost of this project is RM1000 including the ankle and foot power-assisted orthosis. By comparing to the market rehabilitation robotic application, this combination projects of pneumatic based power-assisted knee-ankle-foot orthosis has successfully developed a low cost of rehabilitation device.

5.2 Recommendations and Future Improvement

The next stage of the prototype will be the improvement of the control system, circuit design and software programming. EMG can be applied to detect the intention movement by the user and potentiometer can be applied to record the motion angle data for study purpose. Labview study would be one of the options to increase the development of the system. Micro-switches will be used to detect the floor contact of the foot support.

Furthermore, the cosmetic of the prototype is important and sit-to-stand automation system will be the next development of this project. The sharp edges of prototype have to be removed or the prototype have to reconstruct by machine rather than manually made would secure the safety of the user. The right leg of the prototype has to be fabricated in order to achieve a fully automated walking system. Thus, stability in statics and dynamics of the system has to be developed. The running and stair climbing system of the pneumatic based power-assisted knee orthosis will be the final stage of the development.

A locking mechanism or clamping mechanism can be applied to reduce the complexity and improve the safety of the user. Besides that, the clamping mechanism can ease the height adjustment of the prototype. The Velcro straps can be replaced by a belt mechanism to improve the comfort of user.

REFERENCES

- Dollar, A. M., & Herr, H. (2007). Active Orthoses for the Lower-Limbs: Challenges and State of the Art. *2007 IEEE 10th International Conference on Rehabilitation Robotics, 1(c)*, 968-977. Ieee. doi:10.1109/ICORR.2007.4428541
- ADXL 335 sensor (2011). Retrieved April 14, 2012 from <http://www.smashingrobots.com/accelerometer-sensors-for-robots/adxl335-sensor/>
- Beyl, P., Naudet, J., Van Ham, R., & Lefeber, D. (2007). Mechanical Design of an Active Knee Orthosis for Gait Rehabilitation. *2007 IEEE 10th International Conference on Rehabilitation Robotics, 00(c)*, 100-105. Ieee. doi:10.1109/ICORR.2007.4428413
- Beyl, P., Van Damme, M., Cherelle, P., & Lefeber, D. (2009). Safe and compliant guidance in robot-assisted gait rehabilitation using Proxy-based Sliding Mode Control. *2009 IEEE International Conference on Rehabilitation Robotics, 277-282*. Ieee. doi:10.1109/ICORR.2009.5209505
- Deaconescu, A., & Deaconescu, T. (2009). Performance of a Pneumatic Muscle Actuated Rotation Module, *II*.
- Font-llagunes, J. M., Pàmies-vilà R., Alonso, J., & Llugràs, U. (2011). Simulation and design of an active orthosis for an incomplete spinal cord injured subject, *2*, 68-81. doi:10.1016/j.piutam.2011.04.007
- Giorgos, L. (2009). Basic Transistor Circuits. Retrieved April 15, 2012 from http://pcbheaven.com/wikipages/Transistor_Circuits/
- Hall, S.J. (2007). *Basic Biomechanics*. (5th ed.). New York: McGraw-Hill Humanities/Social Sciences/Langua.
- Hirata, Y., Iwano, T., Tajika, M., & Kosuge, K. (2009). Motion Control of Wearable Walking Support System with Accelerometer Based on Human Model, (December).
- Introduction to Constructing Pneumatic Circuits. Retrieved April 15, 2012 from http://www.gearseds.com/curriculum/learn/lesson_print.php?id=101

- Kawamoto, H., Hayashi, T., Sakurai, T., Eguchi, K., & Sankai, Y. (2009). Development of Single Leg Version of HAL for Hemiplegia, 5038-5043.
- Matthias, H. (2007). *Humanoid Robot Human-like Machine*. Australia: Advanced Robotic Systems International and I-Tech Education and Publishing.
- Miro-polycast (2007). Retrieved April 14, 2012 from http://verbandstoffe.net/pdf/daten_pdf_eng/Bandages/CAST%20BANDAGES/polycast.pdf
- Moreno, J. C., Brunetti, F., Rocon, E., & Pons, J. L. (2008). Immediate effects of a controllable knee ankle foot orthosis for functional compensation of gait in patients with proximal leg weakness. *Medical & biological engineering & computing*, 46(1), 43-53. doi:10.1007/s11517-007-0267-x
- Muscato, G., & Spampinato, G. (2007). Kinematical model and control architecture for a human inspired five DOF robotic leg. *Mechatronics*, 17(1), 45-63. doi:10.1016/j.mechatronics.2006.05.003
- Muscle. (n.d.). Retrieved June 11, 2011, from <http://lucy.vub.ac.be/gendes/actuators/muscles.htm>.
- Sawicki, G. S., & Ferris, D. P. (2009). A pneumatically powered knee-ankle-foot orthosis (KAFO) with myoelectric activation and inhibition. *Journal of neuroengineering and rehabilitation*, 6, 23. doi:10.1186/1743-0003-6-23
- Schneider, R.T. (2002). It looks like a piece of hose, but it's a pneumatic. Retrieved april 17, 2012 from <http://hydraulicspneumatics.com/other-technologies/it-looks-piece-hose-its-pneumatic>
- Solenoid Valve. Retrieved April 14, 2012 from <http://www.bdkindia.com/others/pdfs/solenoid-valve.pdf>
- Takeda, R., Tadano, S., Natorigawa, A., Todoh, M., & Yoshinari, S. (2009). Gait posture estimation using wearable acceleration and gyro sensors. *Journal of biomechanics*, 42(15), 2486-94. Elsevier. doi:10.1016/j.jbiomech.2009.07.016
- Takuma, T. & Hosoda, K. (2006). Controlling the walking period of a pneumatic muscle walker. *International Journal of Robotics Research*. 25 (9). 861–866.
- Tongen, A., & Wunderlich, R. E. (n.d.). Biomechanics of Running and Walking, 1-12.
- Wetenschappen, F. T. (1999). Conception and Realization of Pleated Pneumatic Artificial Muscles and their Use as Compliant Actuation Elements Conception and Realization of Pleated Pneumatic Artificial Muscles and their Use as Compliant Actuation Elements.

- Yang, C.-j, Zhang, J.-f, Chen, Y., Dong, Y.-m, & Zhang, Y. (2008). Proceedings of the Institution of Mechanical Engineers , Part C : Journal of Mechanical Engineering Science A review of exoskeleton-type systems and their key technologies. doi:10.1243/09544062JMES936
- Yang, C.-C., & Hsu, Y.-L. (2010). A review of accelerometry-based wearable motion detectors for physical activity monitoring. *Sensors (Basel, Switzerland)*, 10(8), 7772-88. doi:10.3390/s100807772

APPENDIX B: Festo quotation

37028704 / 370305
CASH SALES AREA 305/306
PRISCILLA SOH
CENTRAL
UTAR

Ship-to party 37028704
CASH SALES AREA 305/306
PRISCILLA SOH
CENTRAL

FESTO

Attn: Purchasing department

Dear Sir / Madam

Thank you for your enquiry. We are glad to furnish herewith our quotation for your reference and further action.

ATTN: Tony
HP: 012 - 334 5228
Email: cm_teng89@hotmail.com

- RM20 Delivery charges will be imposed for invoice value below RM350.
- Goods sold are strictly not returnable
- Kindly fax over purchase order attached with bank in slip for order processing.
- Our PBB ACCT NO : 3120307808

Quotation
4937018556

Date
02.11.2011

No of pages
1 of 1

Order reviewed by
MYOSALES

Description	Part number	Price	Supply Qty.	Net Amount
		RM		RM
Item 0010 Fluidic muscle DMSP-40-400N-RM-RM estimated delivery date: 24.11.2011	541405	1,330.20	1	1,330.20
Net Total				1,330.20
TOTAL				1,330.20

Sales Engineer
Priscilla Soh Suad Eng

We hope that the above quotation is in order. Please contact us if you need further information.

This quotation is valid for 30 days from date of issue.
Please use the Quotation Number in all communications.

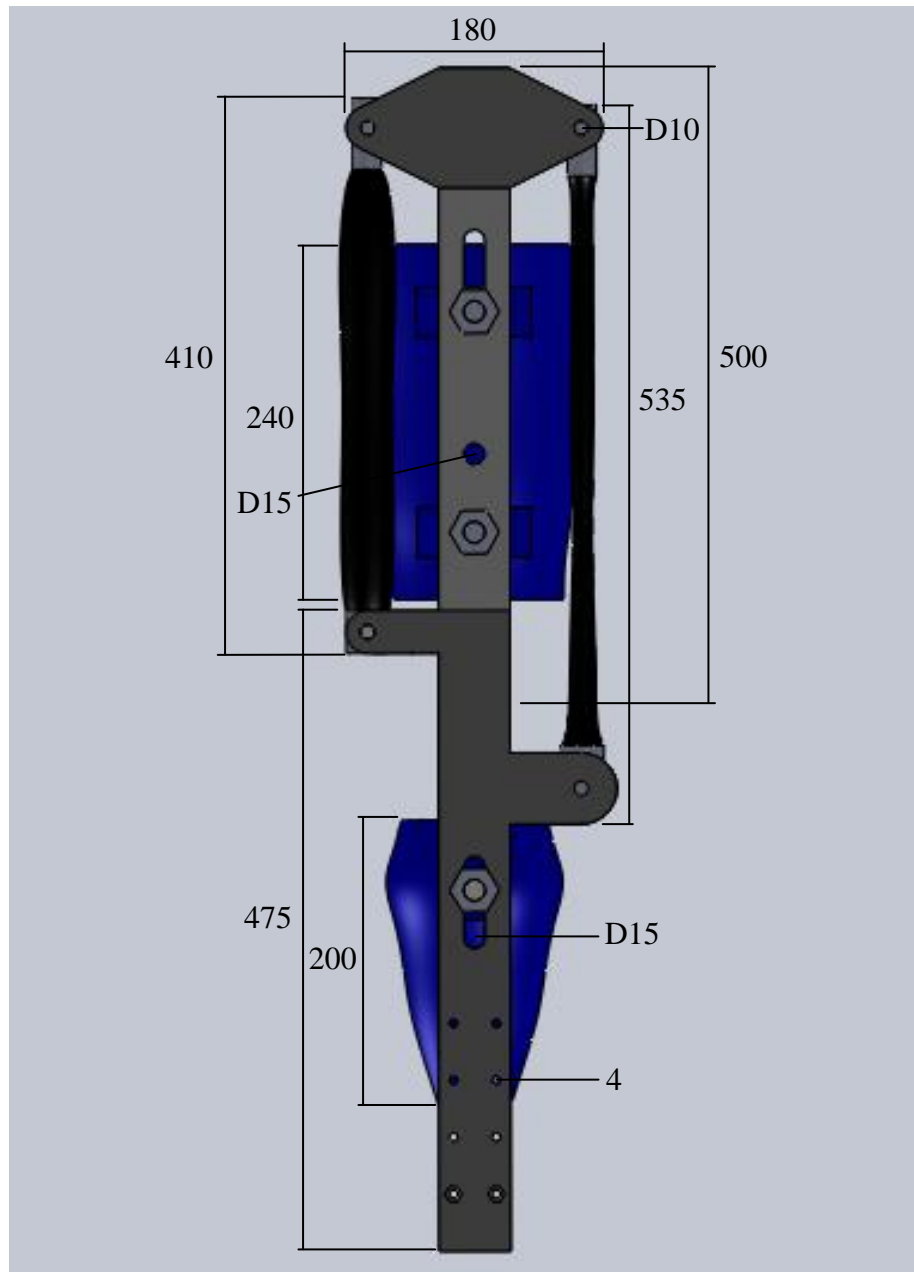
This is a computer generated quotation, thus no signature is required.

Penang branch:
Tel: +60(0)4 641 0918
Fax: +60(0)4 644 3634
Johor branch:
Tel: +60 (0)5 548 1002
Fax: +60 (0)5 547 1050
Melaka branch:
Tel: +60 (0)6 335 1038
Fax: +60 (0)6 335 1078
Johor Bahru branch:
Tel: +60 (0)7 352 3719
Fax: +60 (0)7 352 3726

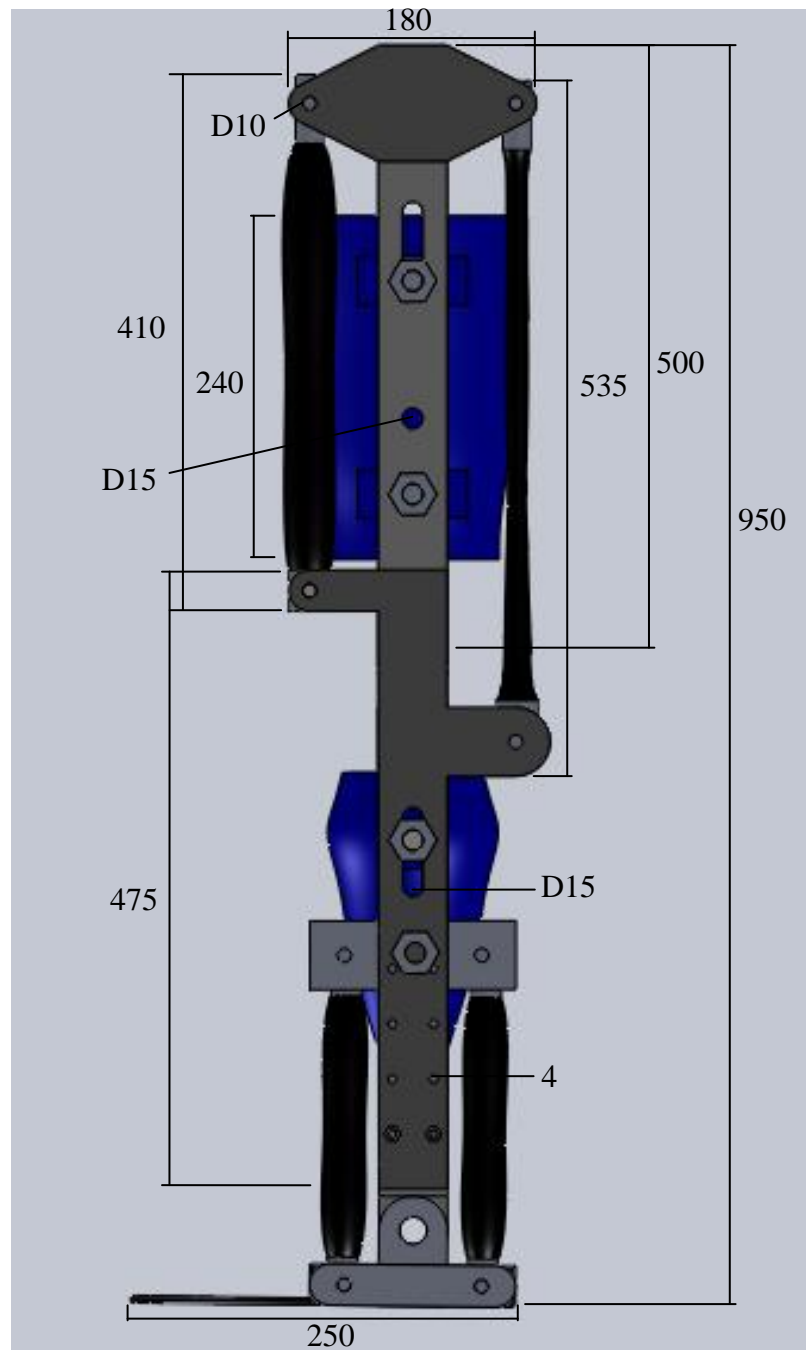
Festo Sdn. Berhad
(Company No.: 35696-D)

Head office
10 Persiaran Industri
Bandar Sri Damansara
52200 Kuala Lumpur
Malaysia
Tel: +60 (0)3 6286 8000 (Customer Service)
+60 (0)3 6286 8122 (General Line)
Fax: +60 (0)3 6275 6411
E-mail: csc_my@festo.com

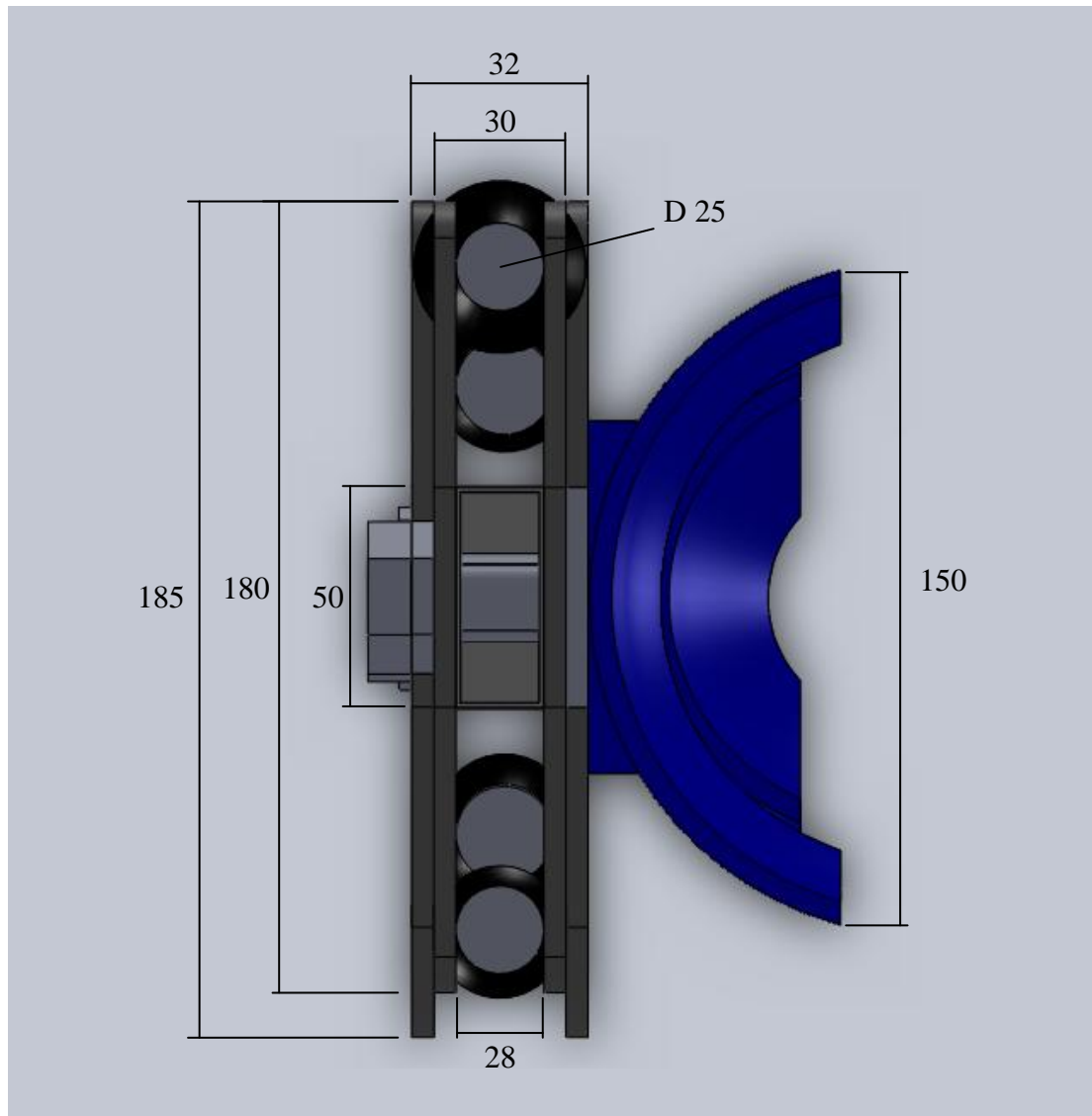
APPENDIX C: Solidworks Side View without Ankle Joint



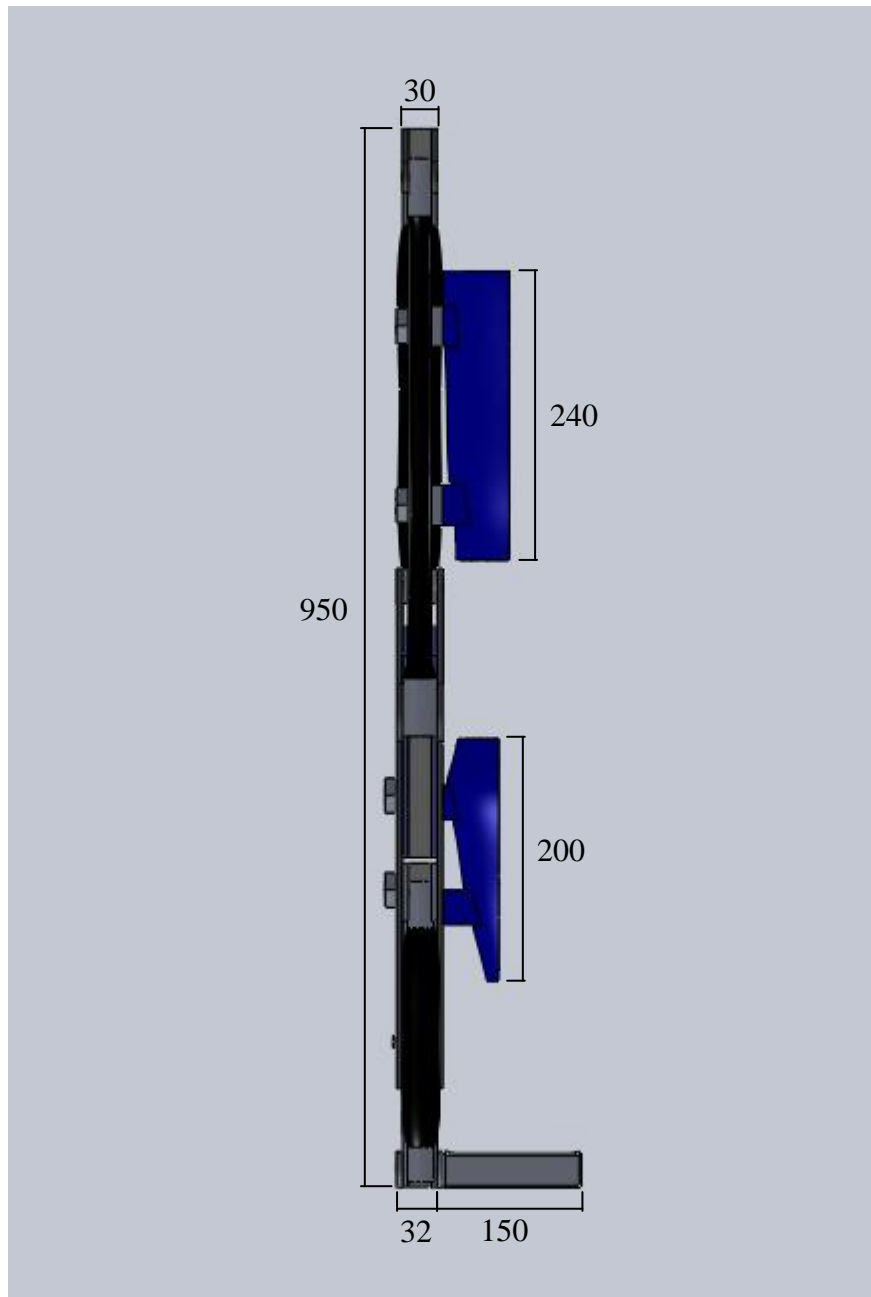
APPENDIX D: Solidworks 3D drawing Side View with Ankle Joint (in mm)



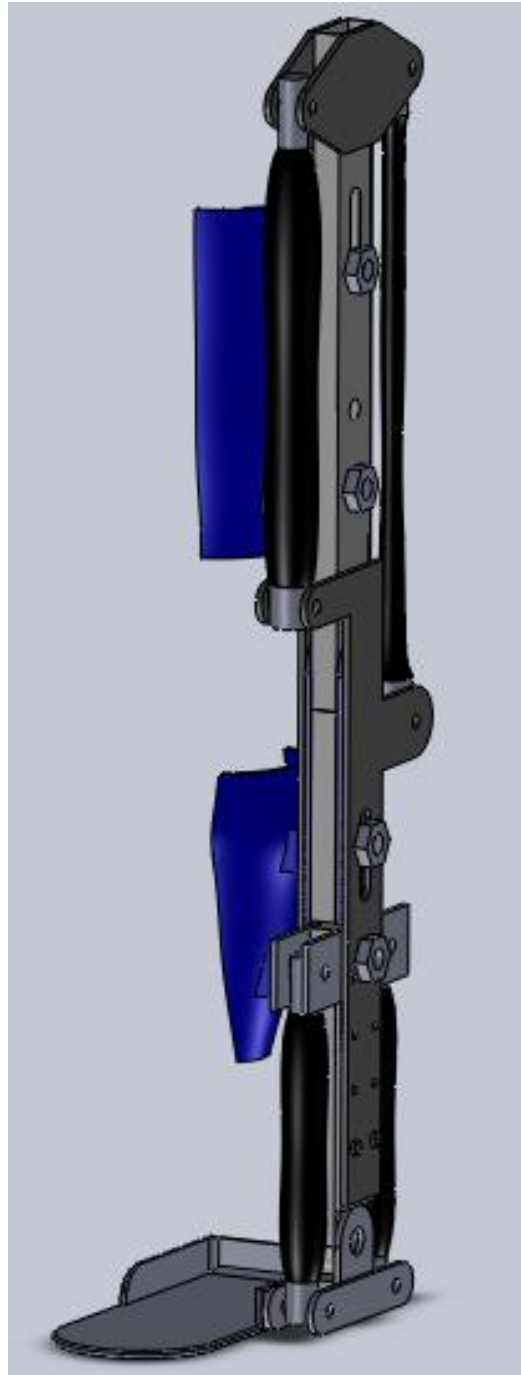
APPENDIX E: Solidworks 3D drawing Top View with Lower Leg MPAM (in mm)



APPENDIX F: Solidworks 3D drawing Front View with Ankle and Foot(in mm)



APPENDIX G: Solidworks 3D drawing without dimension



APPENDIX H: xlcd.c

```

#include <p18f4520.h>
#include "xlcd.h"

/*****
*
* Function Name: OpenXLCD
* Return Value: void
* Parameters: lcdtype: sets the type of LCD (lines)
* Description: This routine configures the LCD. Based on
*               the Hitachi HD44780 LCD controller. The
*               routine will configure the I/O pins of the
*               microcontroller, setup the LCD for 8-bit
*               mode and clear the display. The user must
*               provide the delay routines mentioned at the
*               beginning of "xlcd.h". The code is provided
*               at the end of this file.
*****/
void OpenXLCD(unsigned char lcdtype)
{
    DATA_PORT = 0;
    TRIS_DATA_PORT = 0xff;
    TRIS_RS = 0;
    TRIS_E = 0;
    RS_PIN = 0; // Register select pin made low
    E_PIN = 0; // Clock pin made low

    // Delay for 15ms to allow for LCD Power on reset
    Delay_1msX(15);

    // Setup interface to LCD
    TRIS_DATA_PORT = 0; // Data port output
    DATA_PORT = 0b00110000; // Function set cmd(8-bit interface)
    E_PIN = 1; // Clock the cmd in
    Delay_1msX(1);
    E_PIN = 0;

    // Delay for at least 4.1ms
    Delay_1msX(5);
}

```

```

// Setup interface to LCD
DATA_PORT = 0b00110000; // Function set cmd(8-bit interface)
  E_PIN = 1; // Clock the cmd in
Delay_1msX(1);
E_PIN = 0;

// Delay for at least 100us
Delay_1msX(1);

// Setup interface to LCD
DATA_PORT = 0b00110000; // Function set cmd(8-bit interface)
  E_PIN = 1; // Clock cmd in
Delay_1msX(1);
E_PIN = 0;

TRIS_DATA_PORT = 0xff; // Make data port input

// Set data interface width, # lines, font
WriteCmdXLCD(lcdtype); // Function set cmd

// Turn the display off then on
WriteCmdXLCD(DOFF&CURSOR_OFF&BLINK_OFF);
// Display OFF/Blink OFF
WriteCmdXLCD(DON&CURSOR_OFF&BLINK_OFF);
// Display ON/Blink ON

// Clear display
WriteCmdXLCD(0x01); // Clear display

// Set entry mode inc, no shift
WriteCmdXLCD(SHIFT_CUR_LEFT); // Entry Mode

// Set DD Ram address to 0
SetDDRamAddr(0); // Set Display data ram address to 0

return;
}

/*****
* Function Name: putsXLCD
* Return Value: void
* Parameters: buffer: pointer to string
* Description: This routine writes a string of bytes to the
* Hitachi HD44780 LCD controller. The user
* must check to see if the LCD controller is
* busy before calling this routine. The data
* is written to the character generator RAM or
* the display data RAM depending on what the
* previous SetxxRamAddr routine was called.
*****/

```

```

*****/

void putsXLCD(char *buffer)
{
    while(*buffer)          // Write data to LCD up to null
    {
        WriteDataXLCD(*buffer); // Write character to LCD
        buffer++;             // Increment buffer
    }
    return;
}

/*****
*   Function Name: putsXLCD
*   Return Value: void
*   Parameters:   buffer: pointer to string
*   Description:  This routine writes a string of bytes to the
*                 Hitachi HD44780 LCD controller. The user
*                 must check to see if the LCD controller is
*                 busy before calling this routine. The data
*                 is written to the character generator RAM or
*                 the display data RAM depending on what the
*                 previous SetxxRamAddr routine was called.
*****/

void putsXLCD(const rom char *buffer)
{
    while(*buffer)          // Write data to LCD up to null
    {
        WriteDataXLCD(*buffer); // Write character to LCD
        buffer++;             // Increment buffer
    }
    return;
}

/*****
*   Function Name: SetCGRamAddr
*   Return Value: void
*   Parameters:   CGaddr: character generator ram address
*   Description:  This routine sets the character generator
*                 address of the Hitachi HD44780 LCD
*                 controller. The user must check to see if
*                 the LCD controller is busy before calling
*                 this routine.
*****/

void SetCGRamAddr(unsigned char CGaddr)
{

```

```

    TRIS_DATA_PORT = 0;           // Make data port ouput
    DATA_PORT = CGaddr | 0b01000000; // Write cmd and address to port
    RS_PIN = 0;
    Delay_1msX(1);
    E_PIN = 1;                   // Clock cmd and address in
    Delay_1msX(1);
    E_PIN = 0;
    Delay_1msX(1);
    TRIS_DATA_PORT = 0xff;       // Make data port inputs

    return;
}

/*****
*   Function Name: SetDDRamAddr                                     *
*   Return Value: void                                           *
*   Parameters:   CGaddr: display data address                   *
*   Description:   This routine sets the display data address    *
*                  of the Hitachi HD44780 LCD controller. The    *
*                  user must check to see if the LCD controller  *
*                  is busy before calling this routine.         *
*****/

void SetDDRamAddr(unsigned char DDaddr)
{
    TRIS_DATA_PORT = 0;           // Make port output
    DATA_PORT = DDaddr | 0b10000000; // Write cmd and address to port
    RS_PIN = 0;
    Delay_1msX(1);
    E_PIN = 1;                   // Clock the cmd and address in
    Delay_1msX(1);
    E_PIN = 0;
    Delay_1msX(1);
    TRIS_DATA_PORT = 0xff;       // Make port input

    return;
}

/*****
*   Function Name: WriteCmdXLCD                                   *
*   Return Value: void                                           *
*   Parameters:   cmd: command to send to LCD                   *
*   Description:   This routine writes a command to the Hitachi *
*                  HD44780 LCD controller. The user must check  *
*                  to see if the LCD controller is busy before  *
*                  calling this routine.                         *
*****/

void WriteCmdXLCD(unsigned char cmd)

```

```

{
    TRIS_DATA_PORT = 0;           // Data port output
    DATA_PORT = cmd;           // Write command to data port
    RS_PIN = 0;                 // for sending a command
    Delay_1msX(1);
    E_PIN = 1;                  // Clock the command in
    Delay_1msX(1);
    E_PIN = 0;
    Delay_1msX(1);
    TRIS_DATA_PORT = 0xff;      // Data port input

    return;
}

```

```

/*****
*   Function Name: WriteDataXLCD                               *
*   Return Value:  void                                       *
*   Parameters:   data: data byte to be written to LCD       *
*   Description:  This routine writes a data byte to the     *
*                 Hitachi HD44780 LCD controller. The user   *
*                 must check to see if the LCD controller is *
*                 busy before calling this routine. The data  *
*                 is written to the character generator RAM or *
*                 the display data RAM depending on what the  *
*                 previous SetxxRamAddr routine was called.   *
*****/

```

```

void WriteDataXLCD(char data)
{
    TRIS_DATA_PORT = 0;           // Make port output
    DATA_PORT = data;           // Write data to port
    RS_PIN = 1;                 // Set control bits
    Delay_1msX(1);
    E_PIN = 1;                  // Clock data into LCD
    Delay_1msX(1);
    E_PIN = 0;
    RS_PIN = 0;                 // Reset control bits
    TRIS_DATA_PORT = 0xff;      // Make port input

    return;
}

```

```

/*****
*   Function Name: ClearXLCD                                   *
*   Return Value:  void                                       *
*   Parameters:   void                                         *
*   Description:  This routine clears the LCD display.       *
*****/
void ClearXLCD(void)

```

```

{
    WriteCmdXLCD(0x01);
}

/*****
*   Function Name: SetCurXLCD                               *
*   Return Value: void                                       *
*   Parameters:   data: data byte to be written to LCD      *
*   Description:  This routine set the location of the      *
*                 LCD(2X16) cursor.                          *
*                 If the given value is (0-15) the cursor    *
*                 will be at the upper line.                 *
*                 If the given value is (20-35) the cursor   *
*                 will be at the lower line.                 *
*                 -----                                     *
*                 |00|01|02|03|04|05|06|07|08|09|10|11|12|13|14|15| | *
*                 |20|21|22|23|24|25|26|27|28|29|30|31|32|33|34|35| | *
*                 -----                                     *
*****/

void SetCurXLCD(unsigned char data)
{
    if(data<16)
    {
        SetDDRamAddr(0x80+data);
    }
    else
    {
        data=data-20;
        SetDDRamAddr(0xc0+data);
    }
}

```

APPENDIX I: xlcd.h

```

#ifndef __XLCD_H
#define __XLCD_H

/* PIC18 XLCD peripheral routines.
 *
 * Notes:
 *- This file is modified from Microchip C18 "xlcd.h"
 *   to adapt to Cytron SK40C development board.
 *- These libraries routines are written to support the
 *   Hitachi HD44780 LCD controller.
 *- The user must define the following items:
 *- The LCD interface type (8-bits)
 *- The data port
 *- The tris register for data port
 *- The control signal ports and pins
 *- The control signal port tris and pins
 *- The user must provide this delay routine in program:
 *- Delay_1msX(unsigned int t) provides
 *   t milliseconds delay.
 *- User may copy the routine from "xlcd.c".
 */

/* DATA_PORT defines the port to which the LCD data lines are connected */
#define DATA_PORT      PORTD
#define TRIS_DATA_PORT TRISD

/* CTRL_PORT defines the port where the control lines are connected.
 * These are just samples, change to match your application.
 */
#define RW_PIN          /* PORT for RW; Connected to ground in SK40C */
#define TRIS_RW         /* TRIS for RW; Connected to ground in SK40C */
#define RS_PIN          LATBbits.LATB4 /* PORT for RS */
#define TRIS_RS         TRISBbits.TRISB4 /* TRIS for RS */
#define E_PIN           LATBbits.LATB5 /* PORT for D */
#define TRIS_E          TRISBbits.TRISB5 /* TRIS for E */

/* Display ON/OFF Control defines */
#define DON              0b00001111 /* Display on */
#define DOFF             0b00001011 /* Display off */
#define CURSOR_ON       0b00001111 /* Cursor on */

```

```

#define CURSOR_OFF      0b00001101  /* Cursor off */
#define BLINK_ON        0b00001111  /* Cursor Blink */
#define BLINK_OFF       0b00001110  /* Cursor No Blink */

/* Cursor or Display Shift defines */
#define SHIFT_CUR_LEFT  0b00010011  /* Cursor shifts to the left */
#define SHIFT_CUR_RIGHT 0b00010111  /* Cursor shifts to the right */
#define SHIFT_DISP_LEFT 0b00011011  /* Display shifts to the left */
#define SHIFT_DISP_RIGHT 0b00011111  /* Display shifts to the right */
#define INC_CUR         0b00000110  /* Increment cursor after each
byte written */

/* Function Set defines */
#define EIGHT_BIT       0b00111111  /* 8-bit Interface */
#define LINE_5X7        0b00110011  /* 5x7 characters, single line */
#define LINE_5X10       0b00110111  /* 5x10 characters */
#define LINES_5X7       0b00111011  /* 5x7 characters, multiple line
*/

#define PARAM_SCLASS    auto
#define MEM_MODEL       far          /* Change this to near for small
memory model */

/* OpenXLCD * Configures I/O pins for external LCD */
void OpenXLCD(PARAM_SCLASS unsigned char);

/* SetCGRamAddr * Sets the character generator address */
void SetCGRamAddr(PARAM_SCLASS unsigned char);

/* SetDDRamAddr * Sets the display data address*/
void SetDDRamAddr(PARAM_SCLASS unsigned char);

/* WriteCmdXLCD * Writes a command to the LCD */
void WriteCmdXLCD(PARAM_SCLASS unsigned char);

/* WriteDataXLCD * Writes a data byte to the LCD */
void WriteDataXLCD(PARAM_SCLASS char);

/* putcXLCD * A putc is a write */
#define putcXLCD WriteDataXLCD

/* putsXLCD * Writes a string of characters to the LCD */
void putsXLCD(PARAM_SCLASS char *);

/* putsXLCD * Writes a string of characters in ROM to the LCD */
void putsXLCD(const rom char *);

/* Delay_1msX * User defines these routines according to the oscillator frequency */
extern void Delay_1msX(unsigned int);

```

```
// Clear the display  
void ClearXLCD(void);  
  
//set the location of the lcd cursor  
void SetCurXLCD(unsigned char);  
  
#endif
```

APPENDIX J: Original Coding

```

////////////////////////////////////////////////////////////////////////////////////////////////////////////////////////////////
//Name      : Teng Chun Man      //
//Course    : Biomedical Engineering //
//Project Title : Pneumatic Power-Assisted Knee-Anke-Foot Orthosis //
//University : UTAR              //
////////////////////////////////////////////////////////////////////////////////////////////////////////////////////////////////

#include <p18f4520.h>
#include <adc.h>
#include "xlcd.h"
#include "delays.h"
#include <timers.h>           // Timer library functions
#include <math.h>            // C Library for math operations
#include <stdlib.h>          // C Library
#include <stdio.h>           // C Library
#include <string.h>          // C Library

#pragma config OSC = HS      // HS oscillator,
//#pragma config OSC = HSPLL //HS oscillator,PLL enable (4XFosc1)
#pragma config FCMEN = OFF   // Fail-Safe Clock Monitor disabled
#pragma config IESO = OFF    // Oscillator Switchover mode disabled
#pragma config PWRT = OFF    // PWRT disabled
// Brown-out Reset disabled in hardware and software
#pragma config BOREN = OFF
// WDT disabled (control is placed on the SWDTEN bit)
#pragma config WDT = OFF
// MCLR pin enabled; RE3 input pin disabled
#pragma config MCLRE = ON
// PORTB<4:0> pins are configured as digital I/O on Reset
#pragma config PBADEN = OFF
// CCP2 input/output is multiplexed with RC1
#pragma config CCP2MX = PORTBE
#pragma config LVP = OFF     // Single-Supply ICSP disabled
#pragma config XINST = OFF   // Extended Instruction Set

#define led1      LATBbits.LATB6
#define led2      LATBbits.LATB7
#define muscle1   LATEbits.LATE0
#define muscle2   LATEbits.LATE1

#define sw1       PORTBbits.RB0
#define sw2       PORTBbits.RB1

```

```

#define x_axis          PORTAbits.RA0
#define y_axis          PORTAbits.RA1

void Delay_1msX (unsigned int milliseconds);
void Delay_100msX (unsigned int msec);
int adc_readch0();
int   adc_readch1();

//-----
// VARIABLE
//-----
unsigned int i, j, t;
unsigned char dataString1[5];
unsigned char dataString2[5];
int readch0;
int readch1;
int e_ch0;
int e_ch1;
unsigned int

//temp buffer variable for ADC value for BCD conversion process
    bin = 0,
//buffer variable for showing direct ADC value on LCD
    binADC0 = 0,
    binADC1 = 0,
//BCD conversion variables
    ch0d0 = 0,
    ch0d1 = 0,
    ch0d2 = 0,
    ch1d0 = 0,
    ch1d1 = 0,
    ch1d2 = 0;

//-----
// BODY
//-----

void main()
{
    int resultch0;
    int resultch1;
    int resultled1;

    //set I/O input output
    TRISB = 0b00000011;    //Configure PORTB I/O direction
    TRISD = 0b00000000;    //Configure PORTD I/O direction
    TRISC = 0b11111100;    //Configure PORTB I/O direction
    TRISE = 0b00000000;
    PORTB = 0;
    PORTD = 0;

```

```

PORTC = 0;
PORTE = 0;
TRISA = 0b11111111;    //Configure PORTD I/O direction

```

```

// See ADC configuration on PIC18F4520's datasheet

```

```

OpenADC( ADC_FOSC_32
        & ADC_RIGHT_JUST
        & ADC_16_TAD,ADC_CH0
        & ADC_INT_OFF
        & ADC_VREFPLUS_VDD
        & ADC_VREFMINUS_VSS, 13 );

```

```

//-----
// Configure External LCD
//-----

```

```

OpenXLCD( EIGHT_BIT & LINES_5X7 );
ClearXLCD();          //Clear display

```

```

ClearXLCD();          //Clear display
//led1=1;
//Turn on led1

```

```

SetCurXLCD(0);
putcXLCD(33);
//Display standard 'A' using putcXLCD
putsXLCD("!!TEST!!");
//Display standard 'A' using putsXLCD
SetCurXLCD(20);
putsXLCD("Press sw2 to start");
//led1=0;

```

```

while(1)
{
if(!sw1)          //Test sw1 to change bar level
{
while(!sw1) led1=1; //Debounce sw1, Turn on led1
led1=0;          //Turn off led1
ClearXLCD();
Delay_100msX(2);
SetCurXLCD(0);
putsXLCD("Angle Detection");
SetCurXLCD(20);
putsXLCD("sw2 to begin");
Delay_100msX(1); //Delay 200ms
}
}

```

```

if(!sw2)          //Test sw2 to change cursor position
{
while(!sw2) led2=1;//Debounce sw2, Turn on led2
}
}

```

```

led2=0;           //Turn off led2
Delay_100msX(1); //Delay 100ms
ClearXLCD();
SetCurXLCD(0);
putsXLCD("X=");
SetCurXLCD(20);
putsXLCD("Y=");

while(1)
{
    adc_readch0();
    adc_readch1();

    e_ch0 = readch0;
    resultch0 = e_ch0;
    e_ch1 = readch1;
    resultch1 = e_ch1;

binADC0 = resultch0; //assigning ADC value to buffer variable

    //convert ADC value to BCD
    ch0d2 = binADC0 % 10;
    ch0d1 = (binADC0 / 10) % 10;
    ch0d0 = (binADC0 / 100) % 10;

    //convert BCD digit numbers to ASCII text characters for LCD
    ch0d0 += '0';
    ch0d1 += '0';
    ch0d2 += '0';

    SetCurXLCD(3);
    //print the ADC value on LCD
    putcXLCD(ch0d0);
    //Delay_1msX(1);
    putcXLCD(ch0d1);
    //Delay_1msX(1);
    putcXLCD(ch0d2);
    //Delay_1msX(1);

binADC1 = resultch1; //assigning ADC value to buffer variable

    //convert ADC value to BCD
    ch1d2 = binADC1 % 10;
    ch1d1 = (binADC1 / 10) % 10;
    ch1d0 = (binADC1 / 100) % 10;

    //convert BCD digit numbers to ASCII text characters for LCD
    ch1d0 += '0';
    ch1d1 += '0';
    ch1d2 += '0';

```

```

//SendLCD(0x80,0); //activate LCD line 1
    SetCurXLCD(23);
//print the ADC value on LCD
putcXLCD(ch1d0);
    Delay_1msX(10);
putcXLCD(ch1d1);
    Delay_1msX(10);
putcXLCD(ch1d2);
    Delay_1msX(10);

//-----
// OUTPUT TO RELAY
//-----

    resultled1 = resultch1;

    if (resultled1 < 350 | resultled1 > 360)
    {
        led1 = 1;
        led2 = 0;
        if (led1==1 | led2==0)
        {
            muscle2 = 0;
            muscle1 = 0;
            Delay_100msX(3);
            muscle2 = 1;
            muscle1 = 1;
            Delay_100msX(6);
        }
    }
    else
    {
        led2 = 1;

        if(led1==1)
        {
            muscle2 = 0;
            muscle1 = 0;
            Delay_100msX(3);
            muscle2 = 1;
            muscle1 = 1;
            Delay_100msX(6);
        }
    }

```

```

    }

    }//end while

    }//end if

} //end of while

    CloseADC();           // Disable A/D Converter

} //End of main

//-----
// FUNCTION
//-----

int adc_readch0()
{
    SetChanADC(ADC_CH0); // Set channel for adc ADC_CH0
    // Delay10KTCYx = Delay in multiples of 10,000 instruction cycles. unsigned char
    // (8 bit value) Delay for 500/4 milliseconds with 40 MHz clock
    //Delay_1msX(1);
    //Delay10TCYx(100);
    // Delay in multiple of 10.000 cycles time. Using a 40 MHz external oscillator, it
    // means 40 MHz / 4 --> 10^-7 = cycle time. Then in the PIC18F4520's datasheet page
    // 129 --> delay function duration (in second) = 10 * cycle time * value between the
    // brackets
    ConvertADC();           // Start Conversion
    while( BusyADC() );    // Wait for completion
    readch0 = ReadADC();   // Read result
    return(readch0);      // This function returns "adc_value" which is the adc result
}

int    adc_readch1()
{
    SetChanADC(ADC_CH1); // Set channel for adc ADC_CH1
    //Delay_1msX(1);
    //Delay10TCYx(100);
    // Delay in multiple of 10.000 cycles time. Using a 40 MHz external oscillator, it
    // means 40 MHz / 4 --> 10^-7 = cycle time. Then in the PIC18F4520's datasheet page
    // 129 --> delay function duration (in second) = 10 * cycle time * value between the
    // brackets -->

```

```

// Delay10KTCYx = Delay in multiples of 10,000 instruction cycles. unsigned char
(8 bit value) Delay for 500/4 milliseconds with 40 MHz clock
    ConvertADC();          // Start Conversion
    while( BusyADC() );    // Wait for completion
    readch1 = ReadADC();   // Read result
    return(readch1);      // This function returns "adc_value" which is the adc result
}

//-----
// DELAY
//-----
void Delay_1msX (unsigned int milliseconds)
{
    t=0;
    while(t<milliseconds)
    {
        Delay1KTCYx(11);
        Delay10TCYx(96);
        Nop();
        Nop();
        Nop();
        Nop();
        Nop();
        t++;
    }
} //End of Delay_1msX

void Delay_100msX (unsigned int msec)
{
    t=0;
    while(t<msec)
    {
        Delay10KTCYx(119);
        Delay1KTCYx(9);
        Delay10TCYx(96);
        t++;
    }
} //End of Delay_100msX

```

APPENDIX K: PCB board

